PREDICTIVE AND CORRECTIVE SCHEDULING IN ELECTRIC ENERGY SYSTEMS WITH VARIABLE RESOURCES

A Dissertation

by

YINGZHONG GU

Submitted to the Office of Graduate and Professional Studies of
Texas A&M University
in partial fulfillment of the requirements for the degree of

DOCTOR OF PHILOSOPHY

Chair of Committee,	Le Xie
Committee Members,	Mladen Kezunovic
	Steven Puller
	Shuguang Cui
Head of Department,	Chanan Singh

December 2014

Major Subject: Electrical Engineering

ABSTRACT

In the past decade, there has been sustained efforts around the globe in developing renewable energy-based generation in power systems. However, many renewables such as wind and solar are variable resources. They pose significant challenges to near real-time power system operations. This dissertation focuses on introducing and testing advanced scheduling algorithms for electric power systems with high penetration of variable resources. A novel predictive and optimal corrective look-ahead dispatch framework for real-time economic operation is proposed.

This dissertation has four key parts. First, the basic framework of look-ahead dispatch is introduced. Different from conventional static economic dispatch, look-ahead dispatch is the fundamental function for future power system scheduling. Taking the whole dispatch horizon into account, look-ahead dispatch has a better economic performance in scheduling the resources in power systems. The decision-making of look-ahead dispatch is cost-effective, especially when handling with high penetration of variable resources.

Second, we study the benefits of look-ahead dispatch in system security enhancement. An early detection algorithm is proposed to predict and identify potential security risks in the system. The proposed optimal corrective measures can be computed to prevent system insecurity at a minimized cost. Early awareness of such information is of vital importance to the system operators for taking timely actions with more flexible and cost-effective measures.

Third, novel statistical wind power forecast models are presented, as an effort to reduce the uncertainty of renewable forecast to support the look-ahead economic dispatch and security management. The forecast models can produce more accu-

rate forecast results by leveraging the spatio-temporal correlation in wind speed and direction data among geographically dispersed wind resources.

Fourth, we propose a stochastic look-ahead dispatch (LAED-S) module to handle the high uncertainty in renewable resources. Even with state-of-the-art forecast technology, the near-real-time operational uncertainty from renewable resources cannot be eliminated. Given the uncertainty level, a conventional deterministic approach is not always the best option. The proposed LAED-S is able to judge whether a stochastic approach is preferred. The innovative computation algorithm of LAED-S leverages the progressive hedging and L-shaped method to produce good stochastic decision-making in a more efficient manner.

Numerical experiments of a modified IEEE RTS system and a practical system are conducted to justify the proposed approaches in this dissertation. This framework can directly benefit the power system operation in moving from a static, passive real-time operation into a predictive and corrective paradigm.

DEDICATION

To my parents and beloved wife Bei.

ACKNOWLEDGEMENTS

First and foremost, I wish to express my deep respect and gratitude to my advisor Professor Le Xie. Working with him has been my greatest privilege, fortune, and one of the best periods of my life. Before he joined Texas A&M, I was simply an international student without any guidance. I didn't even know whether I had the opportunity to establish myself in this country. Meeting with him was a monumental turning point in my life, which thoroughly changed my fate. Being his first Ph.D. student and working with him at the beginning of his career, I was very fortunate to witness his hard work and passion initiating and developing this research program. I was touched and greatly influenced by his perseverance and drive for being a true educator and rigorous scholar. Very few Ph.D. students have such opportunities. I am so lucky to be one of them.

My advisor has been an extraordinary mentor for me in every aspect of my graduate school life. From critical thinking to professional presentation and writing skills, from project fund raising to social-networking and business etiquette, from American culture to international collaboration and long-term career development, I have learned far more than what a professor is required to teach in graduate school. I don't even know how to express my gratitude. My advisor has been a true inspiration for me.

Sincere thanks also go to Professors Mladen Kezunovic, Steven Puller, Shuguang Cui and Tie Liu for serving on my advisory committee. Prof. Kezunovic provided me essential support in various aspects and valuable advices especially regarding the implementation of my research in industries. Prof. Puller guided me through theories and methodologies of economy field and gave me the unique view of power

research from a non-engineering perspective. Prof. Cui offered me helpful advice regarding enhancing modeling and optimization. Prof. Liu and I engaged in insightful discussions about potential mathematical approaches and future directions for my research. I would like to thank them for all the valuable help, feedback, and support.

I would also like to thank Prof. Marc G. Genton at King Abdullah University of Science and Technology. He provided me with valuable guidance on research of spatial-temporal wind forecasts in power system operations.

It has been a wonderful experience to be with my colleagues: Fan Zhang, Anupam A. Thatte, Dae Hyun Choi, Omar A. Urquidez, Yang Chen, Chen (Nathan) Yang, Xinxin Zhu, Haiwang Zhong, James Carroll, Yun Zhang, Meichen Chen, Sean G. Chang, Meng Wu, Sadegh Modarresi, Xinbo Geng, Xiaowen Lai, Hao Ming, Yuanyuan Li, and Yang Bai. I will never forget the time we spent together - sweet and sour, such as preparing for the qualifying exam; rushing for paper deadlines; celebrating journal acceptances; attending conferences together; playing laser tags; visiting La Jolla beach; having barbecue parties, pool parties, Thanksgiving dinner, Halloween Festival; and others too numerous to name. I am grateful to them for making the seemingly stressful graduate life much more fun.

My special thanks also go to my family (my wife, my parents, my grandparents, my father-in-law, and my grandparents-in-law), for their selfless dedication in supporting me and encouraging me, for their pleasant company and understanding during some difficult moments.

I wish to express my gratitude especially to my dear wife, Bei, for her unconditional love and understanding. We have overcome so many challenges and shared so many exciting moments together-especially during the three years of a long-distance relationship across the Pacific Ocean. Overcoming the challenging times showed that we shared an invaluable bond between us. Her devotion is an impetus for me

to complete my Ph.D degree and carve out our future together.

TABLE OF CONTENTS

LIST OF FIGURES

FIGURE Page

LIST OF TABLES

TABLE Page

1. INTRODUCTION

1.1 Motivation and Overview

As efforts of reducing the reliance on conventional fossil fuel and mitigating the greenhouse gas emissions, many regions have set ambitious goals of achieving high penetration of renewable energy in the near future (as shown in Figure 1.1)[1, 2]. By the end of 2012, the global installed wind capacity has already reached the level of 283 GW (Figure 1.2) [3]. Intermittent resources such as wind and solar consist a large portion (up to 83% of the overall renewable capacity). The uncertainties and variability of these resources pose significant challenges to electric power system operations.

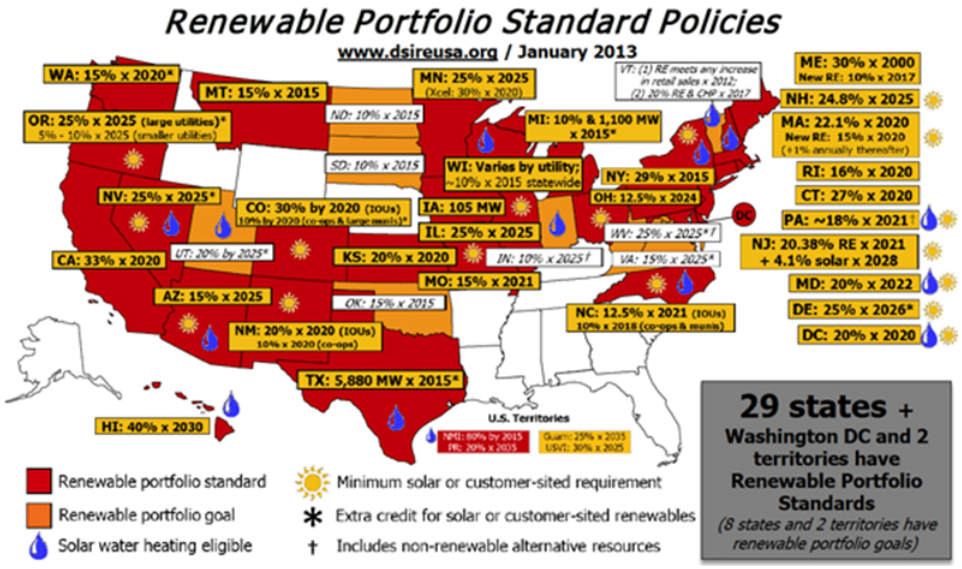

Figure 1.1: Renewable portfolio standard policies

This research is motivated by the need for more advanced scheduling (also known

as economic dispatch) algorithms with enhanced capability to manage the security risks due to the high variation and uncertainty introduced by intermittent resources and contingencies in electric power systems. In recent years, as an alternative to conventional static security constrained economic dispatch (SCED), look-ahead SCED has become a new industry standard in real-time energy market operations [4, 5]. In contrast with the single-stage optimization of static SCED, look-ahead SCED works out a scheduling plan for a future period (e.g., the next 2 hours). By (i) utilizing the accurate most recently updated load and intermittent generation forecasts (e.g., 10-minute ahead forecast) and (ii) incorporating the inter-temporal constraints (e.g., ramp rate), look-ahead SCED exhibits an improved economic performance over static SCED [6].

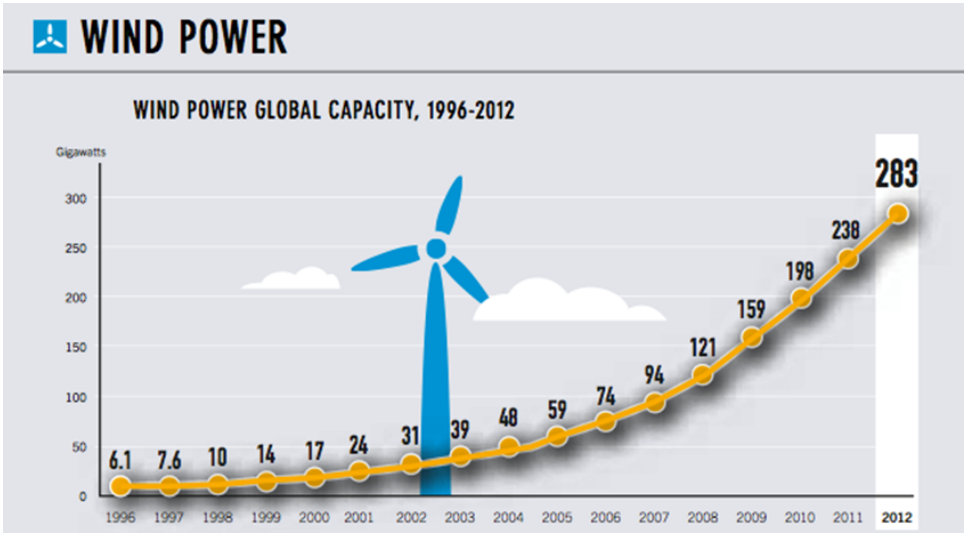

Figure 1.2: Wind power global capacity, 1996-2012

1.2 Literature Review

The concept of the look-ahead (dynamic) dispatch originated in the 1980s. Ross et. al. proposed a dynamic economic dispatch algorithm for generation units [7]. Carpentier et. al. discuss the coupling between short-term scheduling and dispatching [8]. Raithel et. al. study the improved allocation of generation through dynamic economic dispatch [9]. The major motivation behind conducting look-ahead (dynamic) economic dispatch was to incorporate the near-term variable load forecast and schedule the system resources cost-effectively. Recent work extends and justifies the joint benefits when taking into account the environmental impacts (emission costs, primarily), intermittent resources, and responsive demand resources. Xie et. al. use model predictive control based economic dispatch to co-optimize the economic and environmental concerns [10]. Later, they generalize the look-ahead model to integrate the price-responsive demand [11] and propose a novel look-ahead interactive dispatch internalizing inter-temporal constraints at the distributed energy resources level [12, 13]. Most of these research are focusing on the economic benefits of look-ahead dispatch, the potential added value of look-ahead dispatch in **system security enhancement** has not been well studied. This research aims at bridging this gap.

In supporting advanced look-ahead dynamic scheduling, accurate forecast method of renewable resources is essential. Therefore, many active efforts are devoted to this area [14]. One of the popular approaches are numerical weather prediction (NWP) approach which produces forecasts based on physical conditions such as terrain, obstacle, pressure, and temperature. Landberg proposes an NWP model from which the predictions are generated from the high-resolution limited area model (HIRLAM) of the Danish Meteorological Institute [15]. Negnevitsky et. al. suggest, with accurate

Digital Elevation Models (DEMs) and Model Output Statistics (MOS), specifically tuned NWP models performs well but are still unsuitable for short-term forecast [16]. Whereas NWP models play the key role in day-ahead to several hour-ahead wind forecasting, the computational burden and forecasting accuracy of NWP are still challenging in near-term forecasts (minutes-ahead to hour-ahead). As an alternative, data-driven statistical wind forecasting has gained increasing attention for near-term forecasts. Extensive research has been devoted to wind power forecasting problems [17, 18, 19, 20]. In short-term wind speed forecasting, statistical models that incorporate spatial information are the most competitive methods [20, 21]. A regime-switching space-time model [22] improves forecasts by 29% and 13% compared with persistence forecasts and autoregressive in terms of root mean squared error (RMSE). It is generalized by the TDD model [23] by treating wind direction as a circular variable and including it in the model. Regime-switching models based on wind direction and conditional parametric models with regime-switching substantially reduce variance in the forecast errors [24]. Adaptive Markov-switching autoregressive models [25] are developed for offshore wind power forecasting problems in which the regime sequence is not directly observable but follows a first-order Markov chain. For wind speed forecasting problems, more realistic metrics that have penalization on underestimates and forecasts for small true values are desired for model evaluation [20] instead of RMSE and mean absolute errors (MAE). Power curve error [23] is proposed as a loss function, which links prediction of wind speed to wind power by a power curve and evaluates the loss based on the wind power with penalty on underestimates. This research conducts critical assessment over different statistical forecast models and evaluates the benefits for power system operations.

In the domain of applying advanced optimization algorithms for power system scheduling, many valuable research efforts are devoted to handling the operational

uncertainty concerns. For example, Wang et. al. present a stochastic security-constrained unit commitment (SCUC) algorithm solved by Benders decomposition [26]. Meibom et. al. present a stochastic mixed integer scheduling model where the schedules are updated in a rolling manner as more up-to-date information become available [27]. Ruiz et. al. compare stochastic programming with existing reserve methods and evaluate the benefits of a combined approach for the efficient management of uncertainty in the unit commitment problem [28]. Papavasiliou et. al. justify that a stochastic programming unit commitment policy outperforms conventional reserve rules [29]. Hedman et. al. employ statistical clustering techniques to determine the reserve zones based on the power transfer distribution factors (PTDF) and electrical distances (ED) for uncertainty management [30]. Bertsimas et. al. propose a two-stage adaptive robust unit commitment model in the presence of nodal net injection uncertainty [31]. Wang et. al. formulates a chance-constrained two-stage (CCTS) stochastic unit commitment problem with uncertain wind power output [32]. Ryan et. al. propose a stochastic unit commitment algorithm focusing on the development of a decomposition scheme based on the progressive hedging algorithm [33]. Guan et. al. introduce an innovative min-max regret unit commitment model to minimize the maximum regret of the day-ahead decision from the actual realization of the uncertain real-time wind power generation [34]. Luh et. al. integrate the discrete Markov process based aggregated wind generation model into stochastic unit commitment problems [35]. This research leverages the advantages of the progressive hedging algorithm and L-shaped method to develop a parallel computation based stochastic look-ahead dispatch.

1.3 Major Contributions

The contributions of this research are from two-fold: electric power engineering and system sciences. The contributions with respect to electric power engineering are suggested as follow:

- Improved economic efficiency in scheduling large scale renewables.
- Early detection and optimal corrective measures for potential insecurities of power systems.
- Improved forecast of renewables via spatio-temporal statistics.
- Efficient stochastic look-ahead dispatch to handle uncertainties in power grid.

The contributions with respect to system sciences are suggested as follow:

- Enhanced dynamic programming for resource allocation in a temporally and spatially coupled complex system.
- Early detection and identification of potential infeasibilities.
- Improve resource prediction by leveraging spatial and temporal correlations over large data sets.
- Parallelizable stochastic programming algorithm to optimize systems under uncertainty.

1.4 Dissertation Outline

The rest of this dissertation is organized as follows.

Chapter 2 presents the look-ahead dynamic economic dispatch. The model of look-ahead economic dispatch is formulated. Market pricing in look-ahead dispatch

framework is discussed. Illustrative example of a simple system is provided to show the economic benefits of look-ahead dispatch. On the other hand, the impacts of uncertainties on look-ahead dispatch is discussed. Look-ahead dispatch suffers from the high uncertainty in net load. Numerical examples of a modified 24 bus system are conducted to justify the advantages of look-ahead dispatch.

Chapter 3 addresses the security management under a look-ahead dispatch framework. The mathematical model of security enhanced look-ahead economic dispatch is formulated. The concept of relaxing variables are introduced. The early detection and optimal corrective measures are presented. Numerical experiments of a modified 24 bus system as well as a 5889 bus practical system are conducted to justify the security benefits of a look-ahead dispatch framework.

Chapter 4 deals with the application of spatio-temporal wind forecast models. An overview of statistical wind forecast models are provided, followed by the introduction of the proposed spatio-temporal wind forecast models. We compare the performance of spatio-temporal wind forecasts using realistic wind farm data obtained from West Texas. For the critical assessment of the forecast models, a day-ahead reliability unit commitment model and a robust look-ahead economic dispatch formulation are presented. Numerical experiments are conducted to verify the benefits of incorporating spatio-temporal wind forecasts.

Chapter 5 explores the benefits and feasibility in applying a stochastic look-ahead economic dispatch algorithm for power system near-real-time operation. Based on the economic risk index, we propose an analytical criterion judging whether a stochastic approach is applicable to each dispatch interval. A stochastic look-ahead economic dispatch for near-real-time power system operation is formulated. A horizon division technique is applied to divide a look-ahead dispatch horizon into a deterministic portion and a stochastic portion. In order to implement an efficient

stochastic look-ahead dispatch for real-time operation, an innovative hybrid computing architecture is proposed which leverages the progressive hedging algorithm and L-shaped method. By advanced approach to reducing the problem size significantly, the algorithm can operate in a much efficient manner. Numerical experiments of a practical 5889 bus system are conducted to illustrate the effectiveness of the proposed approach.

Chapter 6 summarizes the conclusions of the research and discusses the directions of work that we wish to pursue in the future.

2. LOOK-AHEAD DYNAMIC ECONOMIC DISPATCH*

This chapter presents the look-ahead dynamic economic dispatch. Look-ahead dynamic economic dispatch is motivated by the need for better algorithms to manage the operation uncertainty and variability due to high penetration of variable renewable resources (e.g. wind and solar). With the fast development in renewable capacities, variable resources consist a large portion (up to 83% of the overall renewable capacity). The uncertainties and variability of these resources pose significant challenges to electric power system operations.

Recently, look-ahead dispatch has been proposed and studied as a mechanism to manage the increasing level of inter-temporal variation in electric energy supply portfolio [7, 36, 37, 38]. Several major Independent System Operators (ISO)/ Regional Transmission Organizations (RTO) are investigating and implementing various versions of look-ahead dispatch [5, 39, 4]. However, new issues arise in implementing look-ahead dispatch.

One issue of implementing look-ahead dispatch is the uncertainty in the forecast of renewable resources and system demand. Many studies are devoted to uncertainty handling in economic dispatch problems. In [40], a probabilistic method is applied to unit commitment in spinning reserve assessment. King, et al. use both deterministic and stochastic approaches to conduct dispatch [41]. Reliability index is introduced to test uncertainty under different formulations. Bouffard, et al. introduce a stochastic security framework into the market-clearing formulation and demonstrate its advan-

*This section is in part a reprint of the material in the papers: Y. Gu and L. Xie, "Look-ahead Dispatch with Forecast Uncertainty and Infeasibility Management," in *Power and Energy Society General Meeting, IEEE*, San Diego, 2012. Y. Gu and L. Xie, "Early Detection and Optimal Corrective Measures of Power System Insecurity in Enhanced Look-Ahead Dispatch," *IEEE Transactions on Power Systems*, vol. 28, pp. 1297-1307, 2013.

tage in higher penetration of wind power compared with worst-case deterministic approach [42].

The main objective of this chapter is introduce and justify the benefits of a look-ahead dispatch.

2.1 Look-ahead Security Constrained Economic Dispatch

Security constrained economic dispatch (SCED) is to maximize the total social welfare in power system operating when considering the operating security constraints such as generators capability limits, ramping limits, and transmission line capacity constraints.

Conventional SCED is conducted only one snapshot every 5 to 15 minutes [43]. Inter-temporal constraints such as generators' ramping constraints are incorporated by only considering the current generation outputs, which is not designed to handle the future variability of the variable resources.

Furthermore, in conventional static SCED, energy storage dynamic constraints can only be approximately represented in the capacity of charging and discharging for the immediate next time step. Without explicitly considering the inter-temporal energy dynamic constraints, the contribution of the energy system will be very limited.

The look-ahead dispatch is to expand single snapshot-based SCED problem into a multi-stage problem. The inter-temporal constraints (constraints terms) and inter-temporal benefits (objective terms) can be well taken in the optimization, which can improve the feasibility and optimality of the system.

2.1.1 Mathematical Formulation

The mathematical model of the look-ahead dispatch is presented in (2.1) to (2.8).

$$\max : f = \sum_{k=k_0}^{T} \sum_{i \in D} B_i(P_{D_i}^k) - \sum_{k=k_0}^{T} \sum_{i \in G} C_{G_i}(P_{G_i}^k) + \sum_{i \in S} E_i^T \hat{\lambda}_i^T \tag{2.1}$$

The objective function (2.1) is to maximize the total social welfare (total customer benefits minus system operating costs). In (2.1), G is the set of generators; D is the set of loads; S is the set of energy storage resources; $C_{G_i}(P_{G_i}^k$ is the generation cost of generator i; $B_i(P_{D_i}^k)$ is the benefit function of load i; $\hat{\lambda}_i^T$ is the unit value of stored energy, which is used to evaluate the energy value of storage resources at the final step in a look-ahead plan $\sum E_i^T \hat{\lambda}_i^T$;

This optimization is subject to various security constraints.

$$\sum_{i \in G} P_{G_i}^k = \sum_{i \in D} P_{D_i}^k, k = k_0, \ldots, T \tag{2.2}$$

The energy balancing equation (2.2) requires the steady state total supply equal to total demand from time to time, where $P_{G_i}^k$ is the output level of generator i at time step k;

$$E_i^{k-1} - E_i^k = \triangle t \cdot P_{G_i}^k, i \in S, k = k_0, \ldots, T \tag{2.3}$$

Energy dynamics of storage resources are given by (2.3), which characterize the relationship between the charging/discharging power and the energy level of the resources. E_i^k is the energy level of energy storage i at time step k.

$$-\mathbf{F}^{\max} \leqslant \mathbf{F}^k \leqslant \mathbf{F}^{\max}, k = k_0, \ldots, T \tag{2.4}$$

The branch power flow constraints are provided by (2.4), which can be implemented by two inequality constraints. $\mathbf{F}^k$ is the vector of branch flow at the time step k and $\mathbf{F}^{\max}$ is the vector of transmission constraints of branches.

$$-P_i^R \leqslant \Delta T(P_{G_i}^k - P_{G_i}^{k-1}) \leqslant P_i^R, i \in G, k = k_0, \ldots, T \tag{2.5}$$

The ramping rate constraints of generators are described by (2.5), where P_i^R is the ramping rate limit of generator i.

$$E_i^{\min} \leqslant E_i^k \leqslant E_i^{\max}, k = k_0, \ldots, T \tag{2.6}$$

In (2.6), the upper/lower bounds of energy level for storage resources are given, where $E_i^{\max}$ and $E_i^{\min}$ are the maximum and minimum energy capacity of the resources.

$$P_{G_i}^{\min} \leqslant P_{G_i}^k \leqslant P_{G_i}^{\max}, k = k_0, \ldots, T \tag{2.7}$$

In (2.7), the upper/lower bounds of the power levels of generators are provided, where $P_{G_i}^{\max}$ and $P_{G_i}^{\min}$ are the maximum and minimum power capacity of the resources.

$$P_{D_i}^{\min} \leqslant P_{D_i}^{k} \leqslant P_{D_i}^{\max}, k = k_0, \ldots, T \tag{2.8}$$

The upper and lower bounds of demand are described in (2.8).

2.1.2 Pricing in Look-ahead Dispatch Framework

In deregulated electricity market, the look-ahead dispatch could be implemented in two separate ways: 1) centralized look-ahead dispatch and 2) decentralized look-ahead dispatch [6]. In the decentralized look-ahead dispatch, optimization of multi-time scale horizons takes place at each market participant level (i.e. power plants and demands) and the optimization at system operator level is static [44].

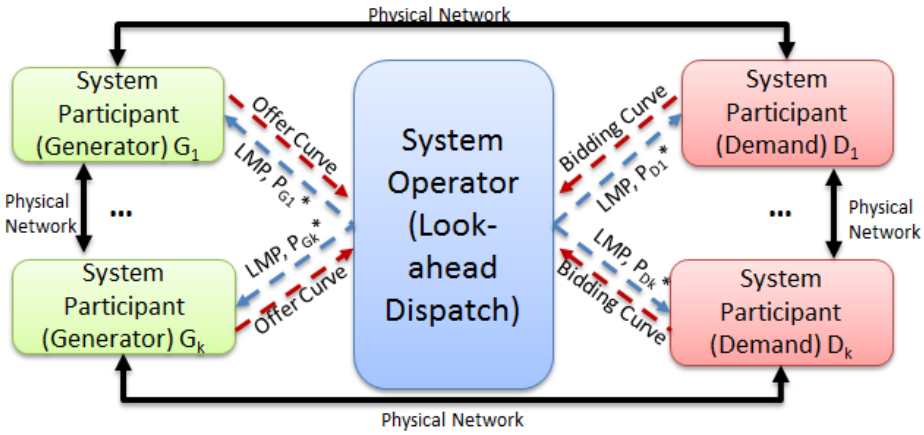

Figure 2.1: Information exchange for centralized look-ahead dispatch

The information exchanging in a centralized look-ahead dispatch is shown in Fig. 2.1. For each time step, market participants (i.e. power plants and demands) submit their offer / bidding curves for the future look-ahead period. The system

operator (ISO/RTO) collects those offer/ bidding curves and runs the look-ahead dispatch to clear the market. The price signals of the look-ahead period will be published. Only the dispatch results of the first step are executed.

In this section, clearing price λ^* in look-ahead framework is discussed. The relationships between the clearing price λ^* and various shadow prices are analyzed.

The locational marginal price (LMP) under static economic dispatch has been discussed in [45], which consists of incremental system costs due to incremental demand at the slack bus, incremental network losses, and transmission congestion terms.

We propose the definition of LMP in look-ahead SCED framework as the incremental generation cost over the entire look-ahead horizon due to incremental demand increase at bus i in the interval k.

$$LMP_i^k = \frac{\partial f}{\partial P_{D_i}^k} \tag{2.9}$$

The Lagrange function of the look-ahead SCED formulation from (2.1) to (2.8) can be written as

$$
\begin{aligned}
L = f &+ \sum_k \lambda_{el}^k (\sum_{i\in G} P_{G_i} - \sum_{i\in D} P_{D_i}) \\
&+ \sum_k \sum_{i\in S} \lambda_{E_i}^k (E_i^{k-1} - E_i^k - P_{G_i}^k) \\
&+ \sum_k \sum_{i\in G} \mu_{RU_i}^k (P_{G_i}^{k+1} - P_{G_i}^k - P_{G_i}^{RU}) \\
&+ \sum_k \sum_{i\in G} \mu_{RD_i}^k (P_{G_i}^{k+1} - P_{G_i}^k - P_{G_i}^{RD}) \\
&+ \sum_k \sum_{i\in G} \mu_{GU_i}^k (P_{G_i}^k - P_{G_i}^{\max}) \\
&+ \sum_k \sum_{i\in G} \mu_{GD_i}^k (P_{G_i}^k - P_{G_i}^{\min}) \\
&+ \sum_k \sum_{i\in L} \mu_{CU_i}^k (F_i^k - F_i^{\max}) \\
&+ \sum_k \sum_{i\in L} \mu_{CD_i}^k (F_i^k - F_i^{\min}) \\
&+ \sum_k \sum_{i\in S} \mu_{EU_i}^k (E_i^k - E_i^{\max}) \\
&+ \sum_k \sum_{i\in S} \mu_{ED_i}^k (E_i^k - E_i^{\min})
\end{aligned} \tag{2.10}
$$

In (2.10), λ_{el}^k is the dual variable of energy balance equation at interval k, $\lambda_{E_i}^k$ is the dual variable of energy dynamic equation of storage i, at interval k, $\mu_{RU_i}^k$ and $\mu_{RD_i}^k$ are the dual variables of ramping constraints of generator i at interval k, $\mu_{GU_i}^k$ and $\mu_{GD_i}^k$ are the dual variables of capacity constraints of generator i at interval k, $\mu_{CU_i}^k$ and $\mu_{CD_i}^k$ are the dual variables of transmission constraints of line i at interval k, $\mu_{EU_i}^k$ and $\mu_{ED_i}^k$ are the dual variables of energy upper and lower bound of storage i at interval k.

According to the Karush-Kuhn-Tucker (KKT) condition, at local optimality, the

gradients of L should equal to zeros, and thus yield (2.11) and (2.12).

$$\frac{\partial L}{\partial P_D} = \frac{\partial f}{\partial P_D} - \lambda_{el} - \mu_C^T \cdot H \tag{2.11}$$

$$\frac{\partial L}{\partial P_G} = \frac{\partial f}{\partial P_G} + \lambda_{el} + \mu_R + \mu_G + \mu_C^T \cdot H \tag{2.12}$$

Where, P_D is the vector of $P_{D_i}^k$, P_G is the vector of $P_{G_i}^k$, λ_{el} is the vector of λ_{el}^k, μ_C is the vector of the sum of $\mu_{CU_i}^k$ and $\mu_{CD_i}^k$, μ_R is the vector of the sum of $\mu_{RU_i}^k$ and $\mu_{RD_i}^k$, and μ_G is the vector of the sum of $\mu_{GU_i}^k$ and $\mu_{GD_i}^k$. H is the distribution factor matrix which characterizes the power flow in each branch when additional MWh of energy is transmitted from the corresponding bus to the slack bus.

(2.11) can be rearranged into (2.13) which is exactly the LMP in look-ahead SCED , consistent with the definition in (2.9).

$$\frac{\partial f}{\partial P_D} = \lambda_{el} + \mu_C^T \cdot H \tag{2.13}$$

Therefore, the LMP in look-ahead SCED framework at interval k can be calculated by the dual variable of energy balance equations and transmission constraints as well as the distribution factor matrix at interval k.

(2.12) indicates the relationship between the λ_{el} which is the price at slack bus and other dual variables including the ones corresponding to the inter-temporal ramping constraints.

Therefore, the inter-temporal ramping constraints will have impact on the LMP but this ramping component is naturally embedded into λ_{el} the dual variable of energy balance equation. The LMP in look-ahead SCED can be calculated by (2.13).

2.1.3 Advantages of Look-ahead Dispatch

In this subsection, we use simple system to illustrate the economic advantages of look-ahead dispatch.

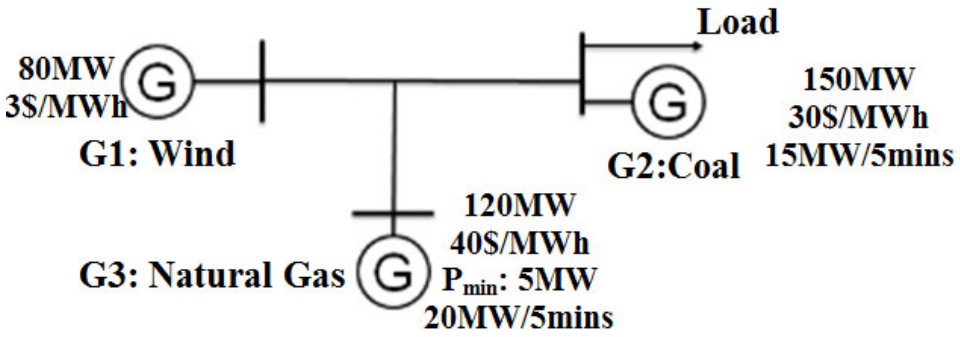

Figure 2.2: Illustrative example for economic performance improvement

Table 2.1: Illustrative Example: Static Dispatch

	0:00	0:05
Available Wind	65MW	80MW
G1	65MW	60MW
G2	40MW	25MW
G3	5MW	5MW
Load	110MW	90MW

The illustrative system is shown in Fig. 2.2. There are three generators the parameters of which are indicated. We apply both static dispatch and look-ahead dispatch to perform the scheduling for the system. The scheduling results are presented in Tab. 2.1 and Tab. 2.2. As we can see, the total generation cost in look-ahead dispatch ($198.75) is 12.5% lower than in static dispatch ($227.08). The static dispatch will

Table 2.2: Illustrative Example: Look-ahead Dispatch

	0:00	0:05
Available Wind	65MW	80MW
G1	65MW	80MW
G2	20MW	5MW
G3	25MW	5MW
Load	110MW	90MW

optimize every step separately. The lower marginal cost of coal generation enables its high output in the first step. However, due to the ramping rate limits, the higher output of coal power plant in the first step limits the reduction of coal generation in the second step and thus the more inexpensive wind generation cannot go up to 80MW but gets curtailed by 20 MW. The look-ahead dispatch will optimize the two steps together. In order to well-utilize wind generation, the expensive but fast ramp natural gas unit is scheduled at higher level in the first step, which enables fully utilization of wind generation at the second step. Therefore, the overall generation cost is lower than the cost in static dispatch.

2.2 Impacts of Uncertainties

Without presence of uncertainty, look-ahead SCED can produce more cost-effective dispatch results than static dispatch can. However, the look-ahead approach may suffer from uncertainties such as wind/solar forecast errors, load forecast errors, unexpected unit outages, etc. Under high level of uncertainty, the dispatch solutions of longer horizon look-ahead decision-making may not be as good as the ones of shorter horizon look-ahead dispatch.

It is illustrated in Fig. 2.3 that as the horizon goes longer, the operating uncertainty in future steps increases.

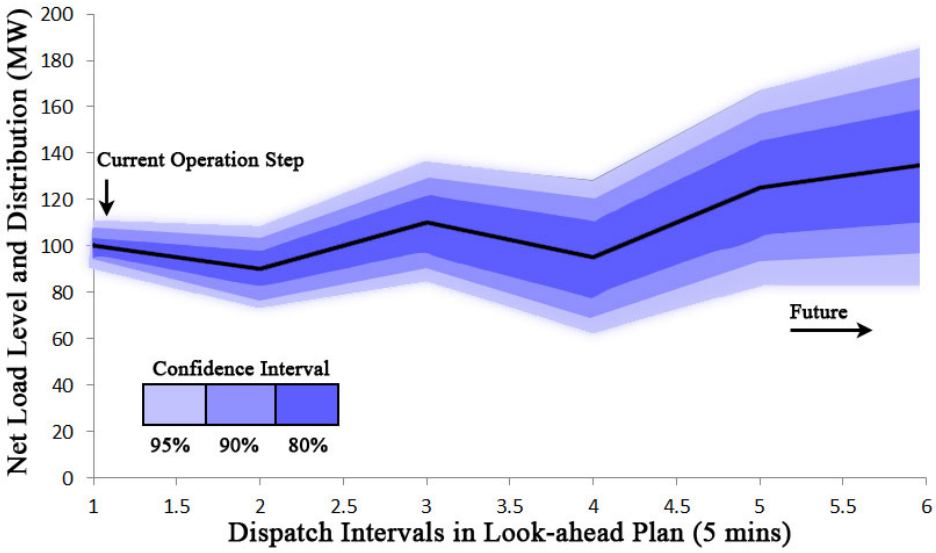

Figure 2.3: The operating uncertainty trend in a look-ahead horizon

2.3 Numerical Examples with Look-ahead Dispatch

In this section, we presented the numerical examples to illustrate the look-ahead dispatch. System setup details are provided in [46].

The total system operating cost of one day for different look-ahead horizon is presented in Fig. 2.4. The case with look-ahead horizon of one step is the static economic dispatch. It can be observed that in the look-ahead economic dispatch, the system operating cost could be reduced compared with using conventional static economic dispatch. With perfect system knowledge (no prediction errors), longer look-ahead horizon could lead to lower operating cost.

However, as discussed in Section 2.2, the performance of look-ahead dispatch may suffer from the uncertainties in future steps such as wind forecast errors. Given the high wind forecast errors (30% of actual value with increasing pattern), it can be observed in Fig. 2.5 that the longer look-ahead horizon may even lead to a poorer

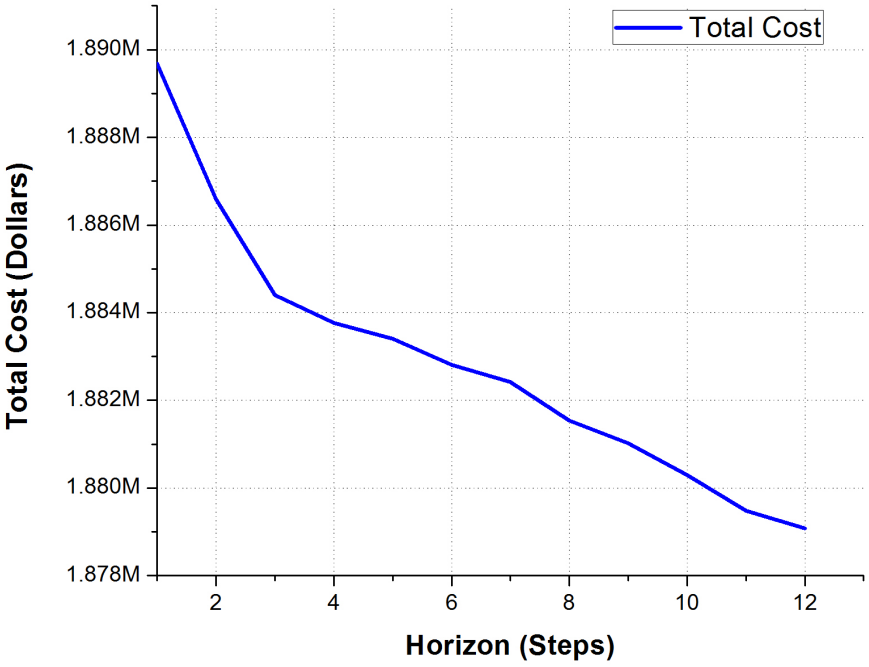

Figure 2.4: Total operating cost over different look-ahead horizon

performance in economic dispatch compared with the short look-ahead horizon. This is because the wind forecast errors in the long run are greater than the ones in the short run. The introduction of those errors could undermine the optimality of the solution. With the weighted predictive scheduling (WPS), as is shown in Tab. 2.3, the negative impacts from future uncertainties can be reduced and mitigated so the system operating cost can be lower than the one without WPS.

Therefore, as we discussed in this Chapter, look-ahead dispatch has economic advantages over the conventional static dispatch. However, under high uncertainty level, a look-ahead dispatch solution with longer horizon may suffers from the low quality of forecast and performs not as good as a solution with shorter horizon.

Table 2.3: Overall System Operating Cost under Forecast Uncertainty

T	Look-ahead	Look-ahead plus WPS	Difference
7	$2,281,167	$2,272,640	($8,527)
8	$2,282,643	$2,273,091	($9,552)
9	$2,284,102	$2,275,897	($8,206)
10	$2,285,253	$2,277,544	($7,709)
11	$2,285,230	$2,279,180	($6,050)
12	$2,286,851	$2,279,485	($7,367)

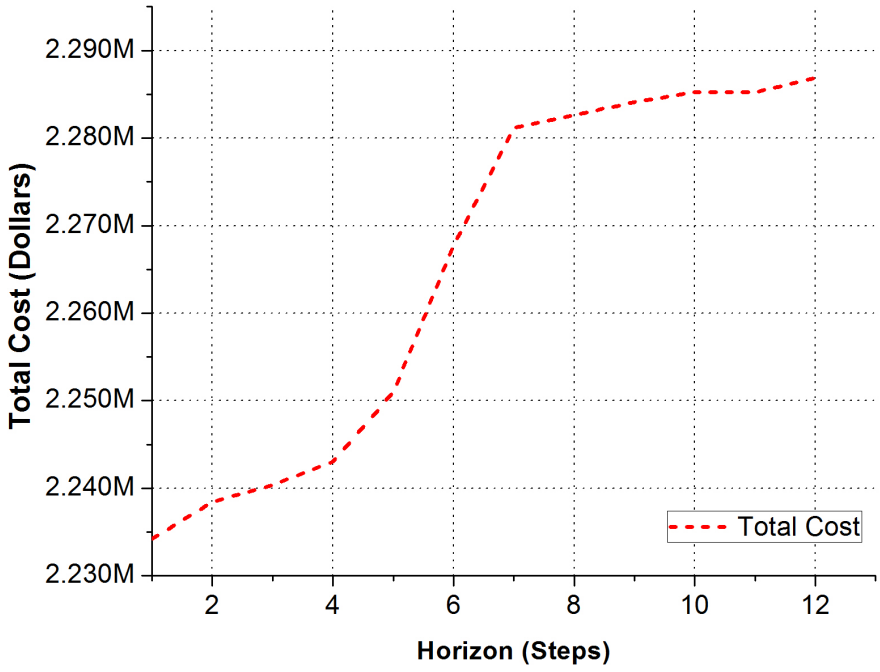

Figure 2.5: Total operating cost of high wind forecast uncertainty

3. EARLY DETECTION AND OPTIMAL CORRECTIVE MEASURES*

In Chapter 2, the economic benefits of look-ahead dispatch has been presented. This chapter discusses the security benefits of look-ahead dispatch. As the economic benefits have been well studied in academia and widely accepted in industry [7, 8, 9, 44], the potential added value of look-ahead dispatch in **system security enhancement** has not been well investigated. This research aims at bridging this gap.

3.1 Power System Security

Power system security refers to the capability of a system to withstand sudden disturbances or an unexpected loss of components [47]. In conventional power system operations, due to the limited time framework allowed for analyzing and responding to security problems, maintaining system security in real-time is a significant challenge [48]. Violations of system security constraints due to high variability in both demand and generation can cause severe consequences in real-time operations [49]. By taking advantage of the look-ahead SCED framework, the proposed look-ahead security management (LSM) can, at an earlier stage, *detect* and *identify* the violated security constraints which can cause potential security problems to the system. The violation of the constraints can furthermore be *quantified*. In addition, an optimal corrective plan can be worked out with minimal recovery costs for the system.† With LSM in the look-ahead SCED framework, it is possible to reduce the impacts of an

*This section is in part a reprint of the material in the papers: Y. Gu and L. Xie, "Look-ahead Dispatch with Forecast Uncertainty and Infeasibility Management," in *Power and Energy Society General Meeting, IEEE*, San Diego, 2012. Y. Gu and L. Xie, "Early Detection and Optimal Corrective Measures of Power System Insecurity in Enhanced Look-Ahead Dispatch," *IEEE Transactions on Power Systems*, vol. 28, pp. 1297-1307, 2013.

†Recovery cost is the cost of the deployed corrective measures to recover the system from infeasibility, namely, to protect the system against insecurity.

emergency ramp event[‡] (e.g., Feb. 26th, 2008 in the Electric Reliability Council of Texas (ERCOT)[§]) and enable a more robust and cost-effective system operation.

3.2 Security Enhanced Look-ahead Dispatch

Different from conventional static dispatch, look-ahead SCED expands the one-snapshot SCED into a multi-snapshot SCED. Inter-temporal constraints (constraint terms) and inter-temporal benefits (objective terms) can then be implemented in the optimization, which improves not only the optimality but also the feasibility of the dispatch problem.

3.2.1 Security Advantages: An Illustrative Example

In this section, illustrative example is used to demonstrate that besides the improvement in the economic benefits, another major advantage of look-ahead SCED is the improvement in feasibility to the dispatch problem, as shown in Fig. 3.1.

Figure 3.1: Illustrative example of look-ahead SCED feasibility improvement

There are two power sources in the illustrative example: a wind farm with 40 MW capacity and a coal power plant with 80 MW capacity and a 10 MW/15 mins ramping

[‡]A ramp event refers to the situation in which demands or intermittent generations (e.g., wind) increase/decrease in a short-term period, which poses difficulty for the system to balance the demand with the available generation resources.

[§]On Feb. 26, 2008, the wind generation dropped by about 1400 MW over ten minutes, while the demand increased by 4412 MW at the same time due to the weather conditions, which caused ERCOT to cut the demand by 1100 MW [50].

capability. In the illustrative example, both static SCED and look-ahead SCED are applied to the same scenario, as shown in Table 3.1 and Table 3.2, respectively.

Table 3.1: Static Dispatch (Infeasible)

	0:00	0:05
Available Wind	35MW	25MW
G1	60MW	70MW
G2	35MW	25MW
Total Generation	95MW	95MW
Load	95MW	105MW

With static dispatch, when the wind generation drops from 35 MW to 25 MW and demand increases from 95 MW to 105 MW, the coal power plant cannot ramp up in such a short period and therefore a loss of load of 10 MW occurs.

Table 3.2: Look-ahead Dispatch (Feasible)

	0:00	0:05
Available Wind	35MW	25MW
G1	70MW	80MW
G2	25MW	25MW
Total Generation	95MW	105MW
Load	95MW	105MW

With look-ahead SCED, this problem can be avoided. The change in wind resources and demand will be considered beforehand; although more coal capacity is used instead of inexpensive wind generation in the first interval, the demand can be satisfied by the total generation in the second interval. This example illustrates that,

due to the fact that multi-stage is considered within look-ahead SCED, the feasibility of the dispatch problem with look-ahead SCED improves upon the conventional dispatch approach.

3.2.2 Formulation of the Enhanced Look-ahead Dispatch

Extended from the model presented in Section 2, the security enhanced look-ahead SCED model presented in this paper incorporates contingency security constraints with the introduction of short-term dispatchable capacity (STDC).

The security enhanced look-ahead SCED is formulated as (3.1)-(3.11):

$$\min : f = \sum_{k=1}^{T} \sum_{i \in G} C_{G_i}(P_{G_i}^k) \tag{3.1}$$

Subject to

$$\sum_{i \in G_j} P_{G_i}^k - P_{D_j}^k = P_{N_j}^k(\theta), k = 1 \dots T, j \in N \tag{3.2}$$

$$\sum_{i \in G} P_{SU_i}^k \geqslant SU_D^k, k = 1 \dots T \tag{3.3}$$

$$\sum_{i \in G} P_{SD_i}^k \geqslant SD_D^k, k = 1 \dots T \tag{3.4}$$

$$-\mathbf{F}^{\max} \leqslant \mathbf{F}^k \leqslant \mathbf{F}^{\max}, k = 1 \dots T \tag{3.5}$$

$$-P_{Di}^R \leqslant \frac{1}{\Delta T}(P_{G_i}^k - P_{G_i}^{k-1}) \leqslant P_{Ui}^R, i \in G, k = 1 \dots T \tag{3.6}$$

$$P_{G_i}^k + P_{SU_i}^k \leqslant P_{G_i}^{\max}, i \in G, k = 1 \dots T \tag{3.7}$$

$$P_{G_i}^k - P_{SD_i}^k \geqslant P_{G_i}^{\min}, i \in G, k = 1 \dots T \tag{3.8}$$

$$P_{G_i}^{\min} \leqslant P_{G_i}^k \leqslant P_{G_i}^{\max}, k = 1 \dots T \tag{3.9}$$

$$0 \leqslant P_{SU_i}^k \leqslant P_{Ui}^R \Delta T, k = 1 \dots T \tag{3.10}$$

$$0 \leqslant P_{SD_i}^k \leqslant P_{Di}^D \Delta T, k = 1 \dots T \tag{3.11}$$

where, G is the set of all available generators; G_j is the set of generators in bus j, $C_{G_i}(P_{G_i})^k$ is the marginal generation cost of generator i; $P_{G_i}^k$ is the output level of generator i at time step k, with $P_{G_i}^{\max}$ and $P_{G_i}^{\min}$ as its upper and lower bounds; $P_{D_i}^k$ is the load level of bus i at time step k; $P_{N_j}^k(\theta)$ is the nodal power injection in bus j at time step k, $P_{SU_i}^k$ and $P_{SD_i}^k$ are the proposed short-term dispatchable capacity (STDC) of generator i at time step k; $\mathbf{F}^k$ is the vector of the branch flow at time step k and $\mathbf{F}^{\max}$ is the vector of the branches' capacity.

The objective function (3.1) is to minimize the total generation cost. Equality constraints (3.2) are the nodal energy balancing equations. Inequality constraints (3.3) and (3.4) are the constraints of upward/downward STDC requirement constraints. The inequality constraints from (3.5) to (3.11) are transmission capacity constraints, ramping capability constraints, mixed generator capacity constraints, and the upper and lower bounds of the decision variables.

By considering network losses, the nodal injection $P_{N_j}^k(\theta)$ is given by

$$P_{N_j}^k(\theta) = \sum_{j:(i,j)\in E} [0.5P_{loss}^k(\theta_i, \theta_j) - b_{ij}\sin(\theta_i - \theta_j)] \tag{3.12}$$

where E is the set of branches, θ_i is the voltage phase angle at bus i, and b_{ij} is the susceptance of branch (i, j). The nodal network loss $P_{loss}^k(\theta_i, \theta_j)$ can be approximated by its piecewise linear expression [51]. By using a second-order approximation of $\sin(\cdot)$, (3.12) can be formulated as (3.13) subject to constraints (3.14).

$$P_{N_j}^k(\theta) \approx \sum_{j:(i,j)\in E} [0.5g_{ij}\sum_{l\in L}\nu_{ij}^l\theta_{ij}^l - b_{ij}(\theta_i - \theta_j)] \tag{3.13}$$

where g_{ij} is the conductance of branch (i, j), ν_{ij}^l and θ_{ij}^l denote the slope and value

of the lth block of voltage phase angle.

$$0 \leqslant \theta_{ij}^{l} \leqslant \triangle\Theta, l = 1 \ldots L \tag{3.14}$$

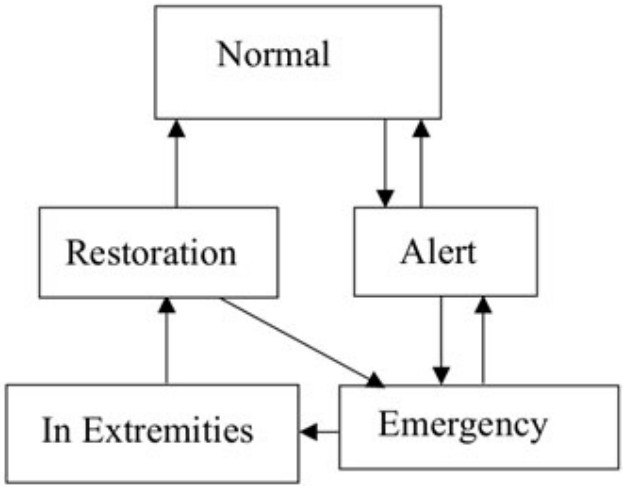

Figure 3.2: Power system security management diagram

Due to the operational uncertainties and potential contingencies in an electric power grid, only satisfying security constraints under current normal condition is not enough to ensure the system security. Therefore, power engineers introduce the concept of the "Alert" state, as shown in Fig. 3.2 [52]. An "Alert" state is defined that all the components of a system are working within their operating limits only under non-contingency scenario. The "Normal" state requires all components functioning well even under assumed contingencies(e.g., N-1). Therefore, in order to operate the system in the "normal" state, extra reserve capacity is required.

In many areas, determination of reserve capacity is within the day-ahead unit commitment decision-making layer. We introduce the concept of short-term

dispatchable capacity (STDC) which can handle the uncertainty and variations at the real-time economic dispatch layer. This can provide extra margin for the power system operational security, and work as indicators for inadequacy of spinning/nonspinning reserves.

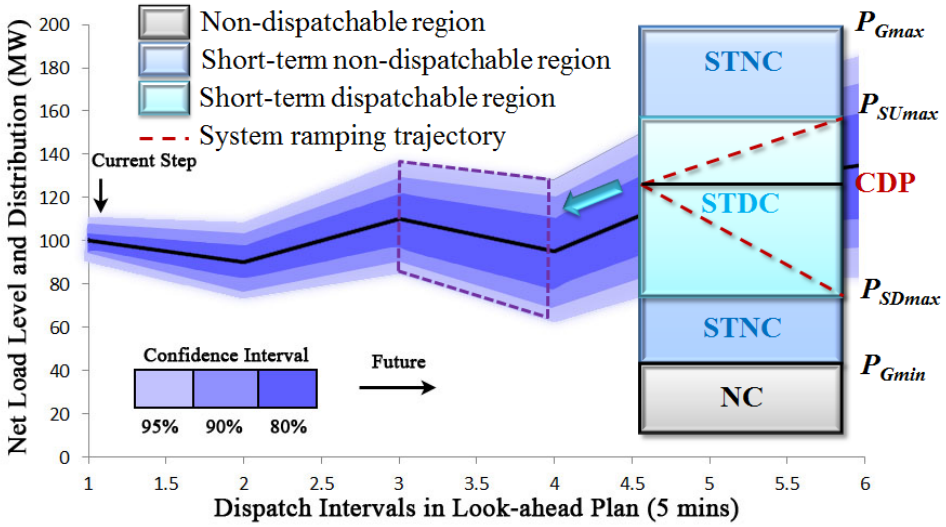

Figure 3.3: Illustrative diagram of short-term dispatchable capacity

The idea of STDC is illustrated in Fig. 3.3. Due to the uncertainty in demand, intermittent resources and the potential contingency of the units, sudden changes may lead to imbalances between the generation and the demand. The rest of the system units (not affected by the contingency) should respond in a short time and compensate for the system imbalances. Every generator has its dispatchable region, which is the distance from the current dispatch point (CDP) to its maximum output level. Due to the ramping constraint of each generator, the actual dispatchable capacity within a short period is generally less than the total capacity. We define the short-term dispatchable capacity (STDC) as *the maximum capacity which can be*

dispatched up (down) within one dispatch interval.

As shown in Fig. 3.3, given the ramping constraint, the dispatchable capacity within one dispatch interval is the STDC. The capacity required by minimum output constraint is the non-dispatchable capacity (NC). The capacity which is limited by the ramping constraint and cannot be dispatched within one dispatch interval is the short-term non-dispatchable capacity (STNC). STDC, NC, and STNC compose a complete portfolio of the installed capacity. The cumulative STDC indicates the overall ramping capability of the entire system to cope with variations in net load (demand - generation of intermittent resources) or generation inadequacy caused by a contingency.

We formulate (3.3) and (3.4) as short-term responsive N-1 contingency constraints. If (3.3) and (3.4) are satisfied, it can guarantee that the power system will have enough ramping capability to cope with the uncertainties and variations given the required confidence interval α (e.g., 95%).

We consider the following contingency events in evaluating the STDC requirements.

- The system doesn't have any generators failure while an unexpected change in intermittent resources and demand exceeds the total ramping capability of the system.
- The system has one generator failure, while an unexpected change in intermittent resources and demand exceeds the ramping capability of the rest system (unaffected by the contingency).

The requirements of upward/downward STDC can be evaluated by (3.15) and

(3.16), respectively.

$$P_{SA}^{U} = [\prod_{i \in G}(1 - P_{f_i})][1 - \phi(\frac{SU_D}{\sigma_{NL}})] + \sum_{i \in G} P_{f_i}[\prod_{\substack{j \in G \\ j \neq i}}(1 - P_{f_j})][1 - \phi(\frac{SU_D - P_{G_i}^{\max}}{\sigma_{NL}})] \tag{3.15}$$

$$P_{SA}^{D} = [\prod_{i \in G}(1 - P_{f_i})][1 - \phi(-\frac{SD_D}{\sigma_{NL}})] + \sum_{i \in G} P_{f_i}[\prod_{\substack{j \in G \\ j \neq i}}(1 - P_{f_j})][1 - \phi(\frac{-SD_D - P_{G_i}^{\max}}{\sigma_{NL}})] \tag{3.16}$$

In (3.15) and (3.16), $P_{SA}^{U(D)}$ are the probability of short-term dispatchable alert (upward/downward), which indicates whether the system-wide ramping capability is enough for handling the potential contingency scenarios , P_{f_i} is the probability of failure of the unit i, σ_{NL} is the variance of net load, and $\phi(\cdot)$ is the cumulative distribution function of a standard normal distribution. Given the confidence interval, the requirement of STDC can be determined by equation solver in the optimization toolbox of Matlab.

By incorporating the short-term responsive contingency constraints into the proposed look-ahead security management, it enables look-ahead dispatch predicting and quantifying not only the risks to the current status but also the risks under various potential contingency scenarios. By optimization, the utilization of the short-term dispatchable resources is maximized and the shortage of the ramping capability is minimized and reported to the system operator in advance. The valuable information provided could be used to check the adequacy of the system reserve or as a reference for further deployment of other resources.

3.3 Algorithm for Early Detection and Corrective Measures

A major advantage of look-ahead economic dispatch is to better utilize available resources to enable a larger feasibility region, as discussed in the previous section. However, due to the uncertainty of the renewable resources and potential contingencies, there is always the chance that a feasible dispatch plan which satisfies all security constraints does not exist. We define these situations as infeasibility in look-ahead SCED. The infeasibility is related with insecurity of system operation. It is possible to improve the robustness and security of scheduling operation by handle infeasibility issues appropriately.

For MPC-based optimization problems, there exist techniques to handle infeasibility issues. In [53, 54, 55, 56], a feasible MPC problem is recovered from infeasibility by dropping the violated constraints. Rawlings et al. propose and justify the minimal time approach, which removes the state constraints in the early stages of the infinite horizon problem to make it feasible [55, 56]. However, these approaches are not able to distinguish the relative importance of the various constraint violations. In power system operations, it is important to consider the priority level of different constraints. In [54, 57], Adersa et al. propose a method of recovering from infeasibilities that involves a prioritization of the constraints. The lowest prioritized constraints are dropped if the online optimization problem becomes infeasible. However, this method cannot quantify how much the constraint gets violated. Also, directly ignoring the infeasible constraints is sometimes unacceptable in practical power system operations. Another approach to solving infeasible MPC problems in which the constraints have different priorities is proposed by Tyler et al.[58]. In their approach, integer variables are introduced to handle the prioritization in an optimal problem. By solving a sequence of mixed-integer optimization problems, the size of

the violation of the constraints is minimized in terms of the prioritization. In [59], Vada et al. propose a method which utilizes a single-objective linear problem to handle infeasibility.

Starting from the previous work [60, 61] on handling the infeasibility of MPC problems, we propose a look-ahead security management (LSM) technique. With the proposed LSM technique, look-ahead economic dispatch not only improves the system feasibility but also predicts and identifies the infeasibility which may occur in the future. The violation of infeasible constraints, which is of great concern (or interest) to the system operators, can be quantified. Furthermore, the LSM technique can help in developing an optimal solution to recover the system from infeasibility with minimal recovery costs.

3.3.1 Relaxing Variables

Relaxing variables are introduced to handle infeasibilities. They are deployed to relax the constraints and make the problem feasible. High penalty terms associated with the relaxing variables are added in the objective function to eliminate the chances that the relaxing variables become alternatives to the original decision variables when the problem is feasible.

Fig. 3.4 illustrates the relaxing variables by distinguishing it with slack variables. A slack variable characterizes the distance from the current operating point to the boundary of the feasible region, which can ensure that the current operating point is within its feasible region. The relaxing variable r at optimality indicates the minimal distance from the current status to the status which gives a feasible solution.

3.3.2 Early Identification of Infeasibility

Infeasibility in economic dispatch is usually related to security problems in the physical power system, which refers to certain violations of the operating constraints

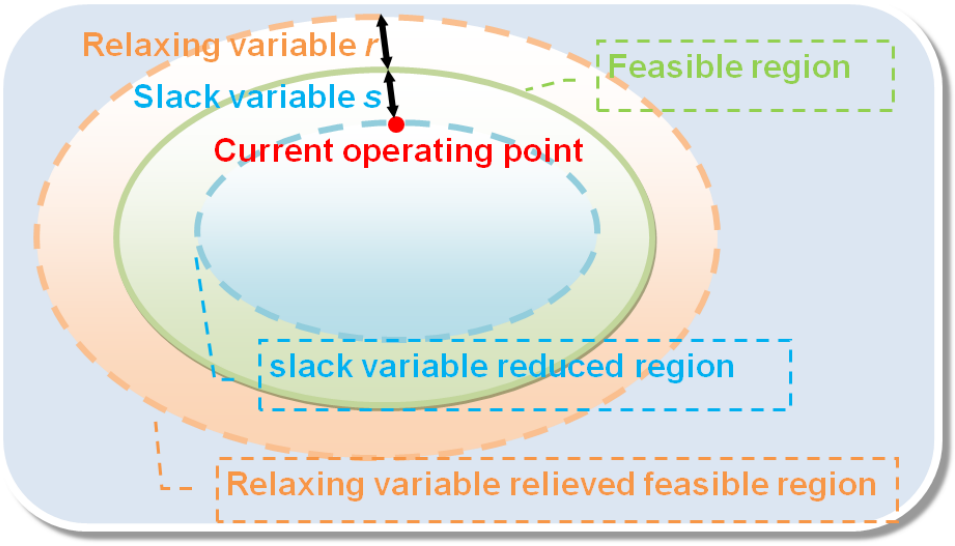

Figure 3.4: Conceptual illustration of relaxing variables

(e.g., the overloading of transmission lines, generators' ramping constraints and so on) or to regional or system-wide imbalances between the energy supply and demand. Any of these violations may cause contingencies or blackouts in the power system, and lead to severe consequences.

In power system real-time operations, it is very important to identify potential security problems in advance. The available measures for handling security problems depend on how much time remains for taking the measures. If the security issue is detected one to two hours ahead, a much broader set of corrective measures can be deployed. On the other hand, if the security violation is detected only 10-15 minutes prior to real-time, the number of corrective measures available are much fewer.

The proposed approach implemented in a look-ahead scheduling framework enables the scheduling framework to identify future security risks.

Relaxing variables can be introduced into security constraints (3.2), (3.5), (3.6), (3.9)-(3.11) and the problem can be formulated as follows:

$$\sum_{i \in G_j} P^k_{G_i} - P^k_{D_j} + r^k_{N_j} = P^k_{N_j}(\theta), k = 1 \dots T, j \in N \tag{3.17}$$

$$-\mathbf{F}^{max} - r^k_F \leqslant \mathbf{F}^k \leqslant \mathbf{F}^{max} + r^k_F, k = 1 \dots T \tag{3.18}$$

$$-P^R_i - r^k_{R_i} \leqslant \frac{P^k_{G_i} - P^{k-1}_{G_i}}{\Delta T} \leqslant P^R_i + r^k_{R_i}, i \in G \tag{3.19}$$

$$P^{min}_{G_i} - r^k_{G_i} \leqslant P^k_{G_i} \leqslant P^{max}_{G_i} + r^k_{G_i}, i \in G, k = 1 \dots T \tag{3.20}$$

$$0 \leqslant P^k_{SU_i} \leqslant P^R_{Ui} \Delta T + r^k_{SU_i}, i \in G, k = 1 \dots T \tag{3.21}$$

$$0 \leqslant P^k_{SD_i} \leqslant P^D_{Di} \Delta T + r^k_{SD_i}, i \in G, k = 1 \dots T \tag{3.22}$$

where $r^k_{N_j}$ are the relaxing variables of the nodal energy balance equations, r^k_F are the relaxing variables of the transmission constraints, $r^k_{R_i}$ are the relaxing variables of the ramping constraints, $r^k_{G_i}$ are the relaxing variables of the generator capacity constraints, and $r^k_{SU_i}$, $r^k_{SU_i}$ are the relaxing variables of the upward/downward short-term dispatchable capacity constraints, respectively.

By incorporating the relaxing variables, the objective function of the look-ahead SCED can be formulated as (21).

$$\min f = \sum_{k=k_0}^{T} \sum_{i \in G} C_{G_i}(P^k_{G_i})$$

$$+ I(r^k_{N_j}, r_F, r_{R_i}, r_{G_i}, r_{SU_i}, r_{SD_i}) \tag{3.23}$$

$I(.)$ is defined as the identification function of the violated constraints. $I(.)$ is suggested to be modeled as a linear or a quadratic function ¶. The coefficients of

¶If $I(.)$ is a linear function, the relaxing variables should be non-negative and then the relaxing variables of bidirectional constraints such as ramping constraints, capacity constraints can be split into two parts which indicate the violations of upward and downward constraints, respectively.

the relaxing variables in $I(.)$ indicate the sensitivity of the detection of constraints from various categories (e.g., ramping, transmission capacity). Because infeasibility may be caused by a violation of multiple constraints, the sensitivity of the different constraints must be specified according to the interest of detection. For example, if the system operator is more concerned with (or more interested in) the violation of the energy balance constraint than of the other constraints, the sensitivity $s_j, j \in C_i$ of the constraints in that category C_i should be higher than the sensitivity of the constraints in the other categories $C_l, l \neq i$.

$$\eta_j = \frac{\max_i(|\xi_i|)\chi}{s_j^{\gamma_j(k)}}, s_j \in (0,1), \chi \gg \max(|\xi_i|) \tag{3.24}$$

The coefficients of relaxing variable η_j are given by (3.24). In (3.24), $\gamma_j(k)$ is the discrimination degree among the constraints over different time steps. $\gamma_j(k)$ is the function of time step k, ξ_i is the coefficient of the ith decision variable in the original objective function, and χ is the parameter to differentiate the relaxing variable terms from the original decision variable terms. Therefore, χ is suggested to be a large number (e.g., 10^4).

For a conservative look-ahead strategy, it is preferred to identify the potential risks in an earlier rather than a later stage. The sensitivity of function $I(.)$ subject to constraints at different stages is suggested to be monotonically decreasing as time step k increases. This is implemented by the discrimination degree $\gamma_j(k)$, which is a function of time step k in a look-ahead plan, as described in (3.25). In addition, the choice of coefficient ς_j needs to obey (3.25) in order to guarantee the priority relationship of the various constraint categories at all time steps (e.g., ramping constraints versus transmission capacity constraints).

$$\gamma_j(k) = \frac{\varsigma_j}{k} + 1, \min_{j \in C_u}(s_j)^{\gamma_j(1)} \geqslant \max_{j \in C_v}(s_j), 0 < u < v \tag{3.25}$$

The linear form of $I(.)$ is presented in (3.26), where the relaxing variables and the corresponding coefficients are in vector form.

$$I(r) = \eta_{el}^T r_{el} + \eta_E^T r_E + \eta_F^T r_F + \eta_R^T r_R + \eta_G^T r_G \tag{3.26}$$

In look-ahead SCED real-time operations, if the whole plan is feasible, all the relaxing variables are equal to zero and the optimal solution is the same as for the look-ahead SCED in (3.1). However, if infeasibility exists, the corresponding relaxing variable becomes positive. The value of the relaxing variable indicates how much the violation of that constraint is. With the appropriate configuration of the relaxing variables in (3.26), the solution of the relaxed problem identifies and quantifies the potential insecurity in the system.

Due to the sophistication of power system operations, sometimes infeasibility can be caused by the violation of multiple constraints belonging to different categories (e.g., ramping rates v.s. transmission constraints). It is helpful to identify all of the potential factors causing the security issues and report the information by category in terms of system operators' prioritized concerns. We propose an enumeration tree approach in the LSM to accomplish this.

The sets of security constraint categories $C_j = \{$ constraints | belong to security constraint category j $\}$ are defined in terms of their priority to the operators' concerns (or interests): C_j has a higher priority to the system operator than C_i, where $0 < j < i$. The algorithm doing the enumeration is described as follows.

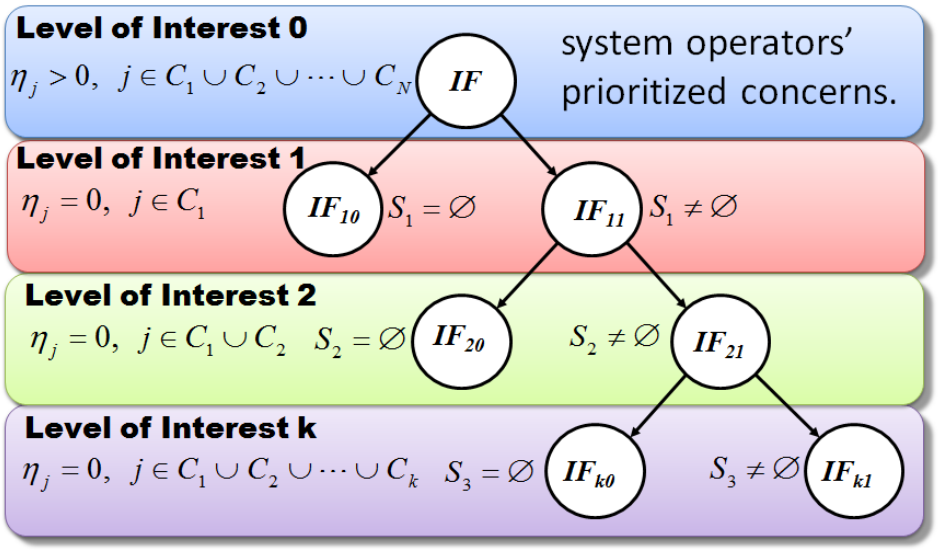

Figure 3.5: Enumeration tree approach to the identification of multiple factors

Step 1 (Initialization): Generate the initial full constraint set $C_T = C_1 \bigcup C_2 \bigcup ... \bigcup C_N$, configure the coefficients of relaxing variable η_i based on (3.24). Go to Step 2.

Step 2 (Optimization): Solve the infeasibility identification problem (3.23) subject to (3.17)-(3.22). Go to Step 3.

Step 3 (Termination test): If the feasibility region of the relaxed problem is empty, namely $S_k = \varnothing$, the identification process is terminated. It is reported that the constraints of the category at the current level of concern k do not cause the infeasibility and any constraints with lower priority $\{j|j > k\}$ do not cause the infeasibility either. End the program, otherwise go to Step 4.

Step 4 (Extension): If the feasibility region of the relaxed problem is not empty, namely $S_k \neq \varnothing$, however, all the non-zero relaxing variables do not belong to the category of the current level of concern k. The system operator is to be informed that the constraints of the category at the current level of concern

k do not cause the infeasibility and the infeasibility is caused by some lower prioritized constraints $\{j|j > k\}$. Go to Step 6, otherwise, go to Step 5.

Step 5 (Selection): The system operator is going to be reported the constraints with non-zero relaxing variables which are responsible to the infeasibility. Go to Step 6.

Step 6 (Configuration): Set the coefficients of all the constraints which belong to the category of the current level of concern k to zero, namely $\eta_j = 0, j \in C_k$. Move to the next level $k = k + 1$. Go back to Step 2.

The whole process is depicted in Fig 3.5. By means of this process, the system operators are informed of not only the factors about which they care the most but also of all the other potential factors causing this infeasibility, ranked in the order of their prioritized concerns.

3.3.3 Optimal Corrective Solution

With the concept of relaxing variable, the optimal corrective solution can be worked out at a minimal operating cost when system operations are infeasible.

$$R_M = \{r_{M_i}|\text{available measures for system recovery}\} \tag{3.27}$$

There are various corrective measures which can help the system recover from infeasibility (e.g., spinning reserve, non-spinning reserve, responsive demand, the fast-response unit, and tie-line support). Different corrective measures have different response speeds and operating costs. Generally, fast resources are more valuable (and expensive) than slow resources. Each corrective measure can be represented by

a relaxing variable r_{M_i}. The set of all the available measures for system recovery is represented by R_M in (3.27).

$$\min f_R = f + R(r_M) \tag{3.28}$$

The objective function of the optimal corrective solution can be modified from the original objective function (3.1) to the objective function of (3.28). $R(r)$ is the recovery cost function, which can be defined as a linear function of the relaxing variables r_M. Sometimes, there might be a non-linear relationship between the cost and capacity of the corrective measures. It is suggested to use a linear step-wise model to formulate this relationship for the sake of algorithm efficiency and simplicity. The coefficients of $R(r)$ are given by the marginal operating cost of the various corrective measures.

$$g(x) + r_M \geqslant 0, r, r_M \geqslant 0 \tag{3.29}$$

In the relaxed problem, the security constraints are formulated as (3.29). The original constraints $g(x)$ may be impacted by some corrective measures and thus get relaxed. r_M are the relaxing variables of the corrective measures. By solving this problem (3.28) to (3.29), an optimal corrective plan is worked out, which can recover the system from infeasibility at the lowest operating cost.

It should be noted that the mathematical model should be modified according to the practical circumstances of the power system. The introduction of relaxing variables is suggested to take into account the results of the infeasibility identification in terms of the time steps and areas impacted by the infeasibility as well as by the

degree of the violation. According to (3.28) and (3.29), a general formulation for an optimal corrective solution is provided in (3.30) - (3.38).

$$\min f_R = \sum_{k=k_0}^{T} \sum_{i \in G} C_{G_i}(P_{G_i}^k)$$

$$+R_M(r_{TIE}, r_{DR}, r_{SR}, r_{NR}, r_{LS}) \tag{3.30}$$

$$\sum_{i \in G} P_{G_i}^k + r_{TIE}^k + r_{DR}^k + r_{SR}^k + r_{NR}^k + r_{LS}^k = \sum_{i \in D} P_{D_i}^k \tag{3.31}$$

$$-\mathbf{F}^{max} \leqslant \mathbf{F_R}^k \leqslant \mathbf{F}^{max} \tag{3.32}$$

$$-P_i^R \Delta T \leqslant P_{G_i}^k - P_{G_i}^{k-1} \leqslant P_i^R \Delta T, i \in G \tag{3.33}$$

$$P_{G_i}^{min} \leqslant P_{G_i}^k \leqslant P_{G_i}^{max} \tag{3.34}$$

$$P_{G_i}^k + P_{SU_i}^k \leqslant P_{G_i}^{\max}, i \in G, k = 1 \ldots T \tag{3.35}$$

$$P_{G_i}^k - P_{SD_i}^k \geqslant P_{G_i}^{\min}, i \in G, k = 1 \ldots T \tag{3.36}$$

$$0 \leqslant P_{SU_i}^k \leqslant P_{Ui}^R \Delta T, k = 1 \ldots T \tag{3.37}$$

$$0 \leqslant P_{SD_i}^k \leqslant P_{Di}^D \Delta T, k = 1 \ldots T \tag{3.38}$$

The objective function (3.30) is to minimize the total operating cost, which includes the ordinary cost of maintaining energy balancing in the system and the additional cost of corrective measures to recover the system from infeasibility. r_{TIE}^k represents the capacity of tie-line support. r_{DR}^k represents the amount of responsive demand to be used. r_{SR}^k represents the capacity of spinning reserve to be used. r_{NR}^k represents the capacity of non-spinning reserve to be used. r_{LS}^k, as the last resort, is the amount of load which has to be cut to ensure the system security. The corrective

measures discussed here mainly help to relieve the energy balancing constraint by providing additional capacity or by reducing the demand level (3.31). The additional corrective capacity may also affect the branch flow. Therefore, the transmission capacity constraints are updated to (3.32), where the vector of branch flow $\mathbf{F_R}^k$ is calculated by the distribution factor matrix and the nodal injections of both the original injections and also the additional corrective injections. The corrective measures in this example do not impact the generators' capacity and ramping constraints. Hence, (3.33) - (3.34) remain the same.

3.4 Numerical Examples with Security Enhanced Look-ahead Dispatch

The proposed early detection and optimal corrective measures are tested in a 24-bus system and a practical 5889-bus system. Details of the system setup of the 24 bus system are presented in Section 3.4.1, and the results and analysis are provided in Section 3.4.2. The system description and simulation results of the practical system are given in Section 3.4.3. The simulations for the two systems are conducted on a Intel i7-990X 3.47GHz desktop computer with Matlab 2011a, IBM ILOG CPLEX v12.2, and Windows 7 operating system.

3.4.1 Simulation Platform Setup of 24 Bus System

The numerical example is modified from the IEEE Reliability Test System (RTS-24) [62]. The simulation duration is 24 hours with 5 minute intervals. The look-ahead horizon ranges from 5 minutes to 4 hours (4 hours by default). Load and wind profiles for 48 hours are collected from ERCOT [63]. Wind generation forecast errors are introduced with a linearly-increasing pattern from 1% to 15% of the actual wind generation potential. Loads are scaled and factored out according to the portions of the different buses [64].

The generator parameters are modified according to [62]. TABLE 3.3 provides

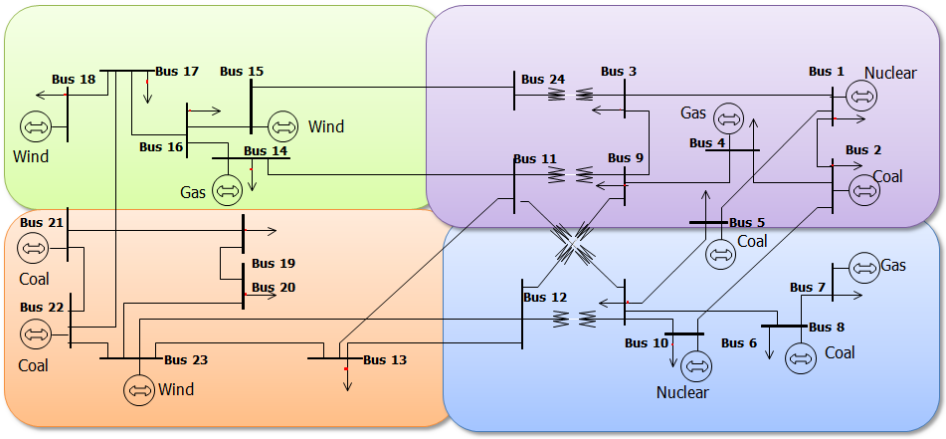

Figure 3.6: IEEE RTS-24 system (modified)

the generators' configuration information. The response features and costs of various corrective measures under the contingency scenario are, as presented in TABLE 3.4, configured according to [65, 66, 63].

3.4.2 Results and Analysis of 24 Bus System

This subsection provides a discussion of the simulation results for look-ahead economic dispatch with the proposed look-ahead security management.

For the system security experiment, a ramping emergency event[‖] is assumed as shown in Fig. 3.7. At time step 63 (about 5:15 am), the system demand increases by 16% (about 321 MW) and the overall wind generation drops by 55% (about 274 MW).

Simulations are conducted for both static SCED and look-ahead SCED with LSM. Under static SCED, the emergency situation is detected at 5:10 am, 5 minutes before real-time operation. Due to the large capacity mismatch and the limited response time, all the available STDC are out of use, resulting in a loss of load of 547.76 MW,

[‖]The wind generation curve and the demand curve in Fig. 3.7 are shown in the per unit system, namely, the ratio of the actual amount to the peak level.

Table 3.3: Generation Resources Parameters

Bus	Type	Cap.	Cost	RAMP	MTTF	MTTR
		MW	$/MWh	MW/min	hours	hours
1	Nuclear	140	15	1.1	1100	150
2	Coal	540	20	10.8	1960	40
4	Gas	300	40	15.0	2940	60
5	Coal	510	27	7.7	450	50
6	Nuclear	150	14	1.4	1100	150
7	Gas	490	49	34.3	450	50
8	Coal	165	23	3.1	1960	40
14	Gas	170	48	15.3	950	50
15	Wind	200	4	18.0	1035	90
18	Wind	240	6	24.0	950	60
21	Coal	300	21	5.4	1960	40
22	Coal	725	26	8.0	2940	60
23	Wind	70	5	7.7	400	50

Table 3.4: Corrective Measures under Contingency

Measures	Response	Cost ($/MW)
Load Shedding	Instantaneous	1038
Responsive Demand	10-30 minutes	300
Responsive Reserve	30 minutes	60
Non-spinning Reserve	1-2 hours	4.35

which causes economic loss of $568,570.38. However, under look-ahead SCED with LSM, the insecurity is detected at about 1:30 am, almost 4 hours before the real-time operation. The violation of energy balancing is quantified. Non-spinning reserve of 26.90 MW at 4.35 $/MW is deployed in advance to solve this security problem. The total recovery cost is $2806.56, which illustrates the advantage of LSM in the look-ahead SCED framework.

The aggregated generation profiles (classified by fuel type) in response to the ramping emergency are shown in Fig. 3.8 (static SCED) and Fig. 3.9 (look-ahead

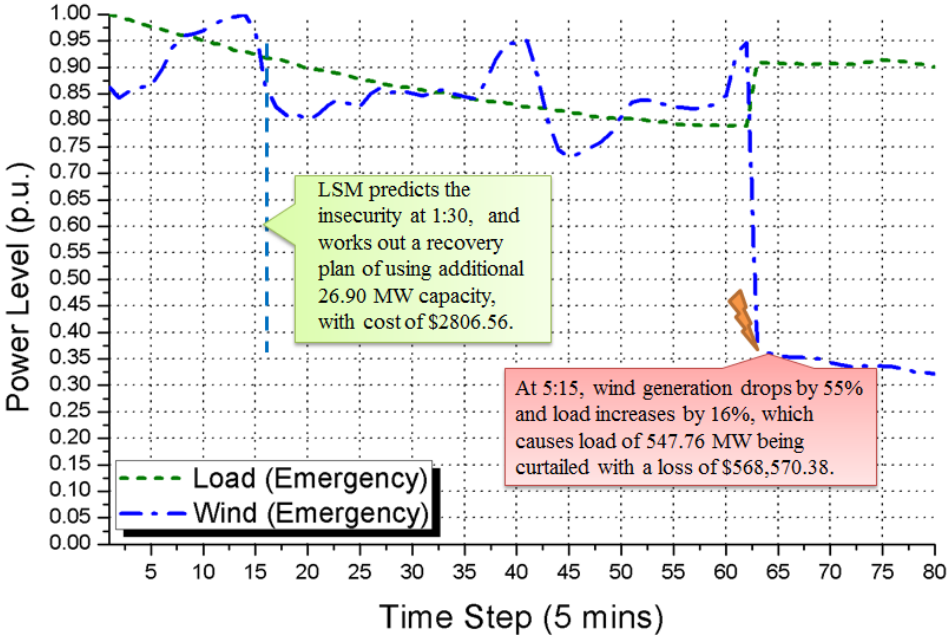

Figure 3.7: The contingency scenario for infeasibility study

SCED). In Fig. 3.8 the pink curve represents the loss of load capacity. Due to the low marginal cost, the wind generation keeps at the maximum level before the ramp event begins. During the ramp event, due to the low short-term dispatchable capacity of other generators (especially, the low ramp rate coal units), the overall energy supply cannot follow the net load increase and thus leads to the loss of load.

In contrast, under look-ahead SCED, depicted in Fig. 3.9, the wind generation reduces its output about 1 hour before the ramp event happens. This can pre-reserve the room for other high capacity but slow units (e.g., coal units) to ramp up in advance in order to cope with the coming ramp event. By gradually increase the generation output of those units, energy imbalance results from the ramp event is mitigated. With the deployment of non-spinning reserve ahead of time, loss of load can be avoided. The pink curve in Fig. 3.9 depicts the additional reserve capacity required to avoid any load shedding. In the optimal recovery plan generated by

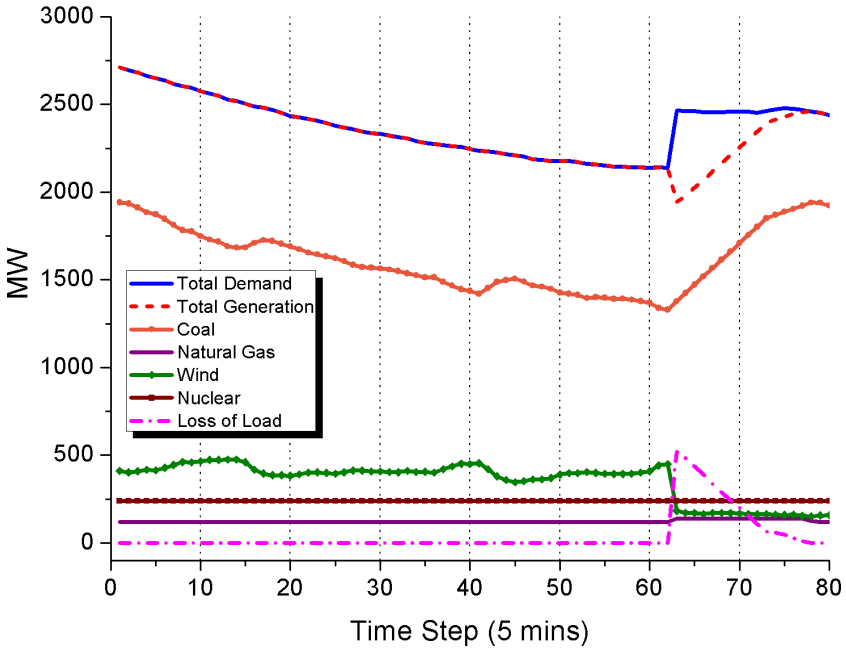

Figure 3.8: Operation of different types of generation (static SCED)

LSM, the capacity required to avoid a loss of load is significantly lower (by 95%) than without LSM.

The relaxing variables for the energy balancing constraints are presented in Fig. 3.10. At each time step, a scheduling plan over 48 intervals is solved. Each relaxing variable, depicted along the depth axis is associated with the energy balancing equation at that interval. The vertical axis indicates the values of relaxing variables, namely, the violation of energy balancing equations. As we can see, the first non-zero relaxing variable is located at the 47th interval at the scheduling plan of time step 16. This indicates that the infeasibility at time step 63 (5:15 am) is detected at time step 16 (1:30 am). Therefore, the alerts of the ramping emergency reaches the system operators almost 4 hours in advance. Due to the wind generation forecast errors, the violation of the energy balancing equation varies around the true

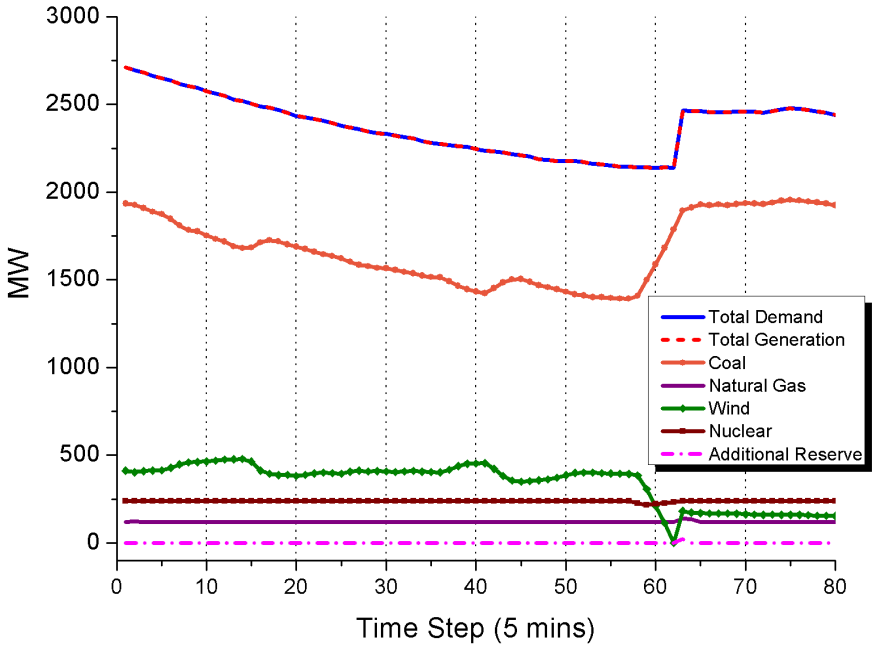

Figure 3.9: Operation of different types of generation (look-ahead SCED)

values.

As we discussed in Section 3.3.2, infeasibility may be caused by multiple factors. Using the enumeration tree approach, the violation of security constraints can be further identified. In Fig. 3.11, the relaxing variables for the ramping constraints of unit 8 are presented. Starting from step 16, the relaxing variables for the ramping constraints of generator 8 at step 63 are positive until the real-time operation of step 63. This indicates that, given the ramp event, the ramping capability is not enough to ensure energy balance in the system. If a certain number of ramping constraints could be relaxed, the issue could be solved. As we can see, the violation of the ramping constraints has a very similar pattern as the violation of the energy balancing equation in Fig. 3.10.

The performance of look-ahead SCED with LSM is further studied in terms of

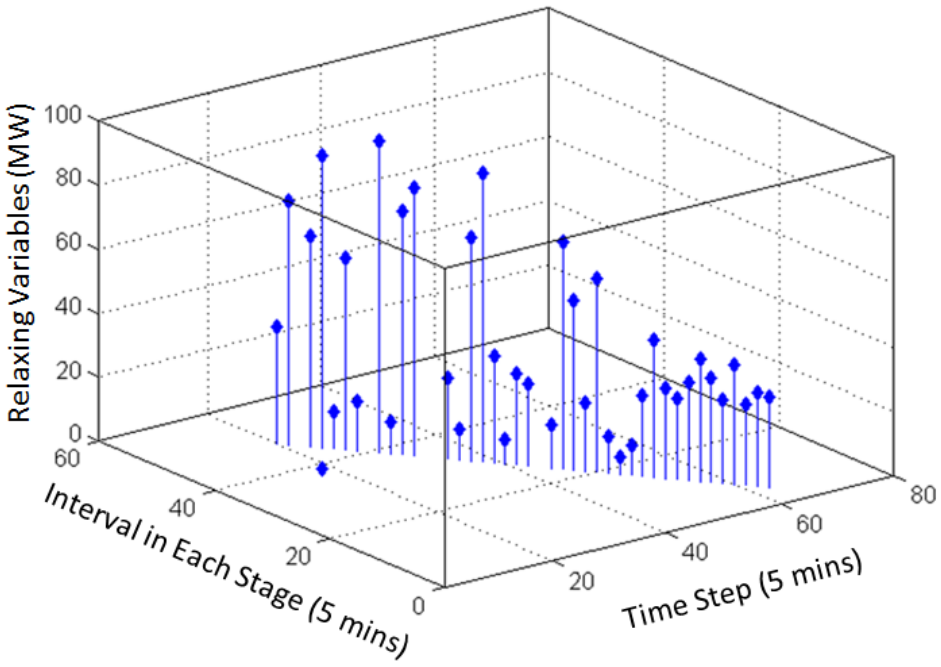

Figure 3.10: Relaxing variables to energy balancing constraints

the performance responses over different levels of look-ahead horizons.

In Fig. 3.12, the required capacity for system recovery under the ramp event is presented. As the look-ahead horizon increases, the required reserve capacity decreases significantly. It saturates at the level of 26.90 MW, which is 95% lower than with static SCED (when the horizon is equal to 1). Saturation indicates that the look-ahead horizon is long enough and that no further improvements to the infeasibility can be achieved.

The corresponding recovery costs over various look-ahead horizons are shown in Fig. 3.13. The vertical axis indicates the cost of system recovery, using a logarithmic scale with a base of 10. Note that for the first data point of 1-step look-ahead, the only corrective measure available to the system operator when the ramping emergency

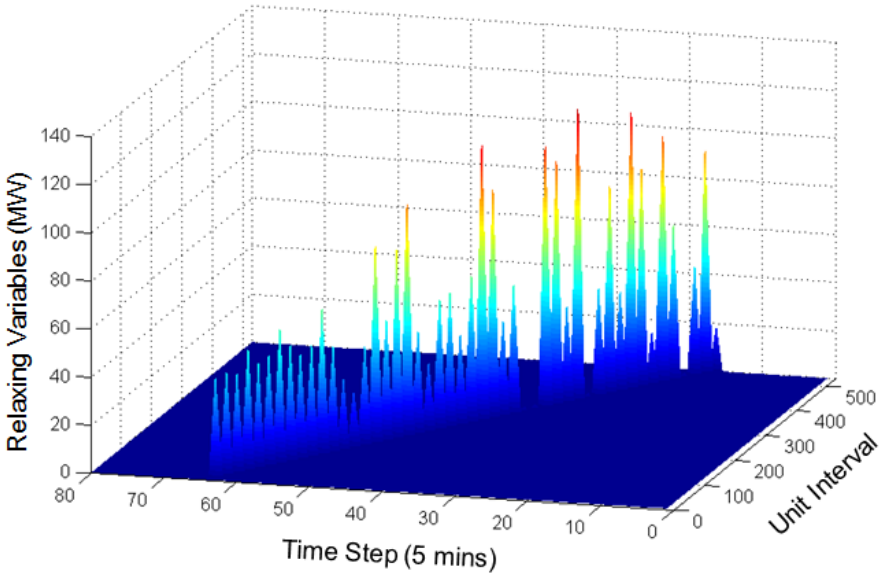

Figure 3.11: Relaxing variables to ramping constraints

occurs is load shedding. Therefore, the first data point reflects the cost of the load shedding (or loss of load). As the available response time decreases, the available measures for system recovery become fewer and more costly. Hence, to detect security risks in advance is of vital importance. With the LSM in look-ahead SCED, the total system recovery cost for the ramp event can be reduced by 99.51% compared with the static SCED.

3.4.3 5889-Bus System

The proposed look-ahead dispatch with security management is applied to a practical power system. The typology of the system is an equivalent typology of the ERCOT system, which covers about 85% of the Texas demand [64]. In that system, there are 5889 buses, 7220 transmission lines, and 523 power plants (including 76 aggregated wind farms with a total installed wind capacity of 9710.4 MW).

In the simulation, the demand and wind production potential are configured

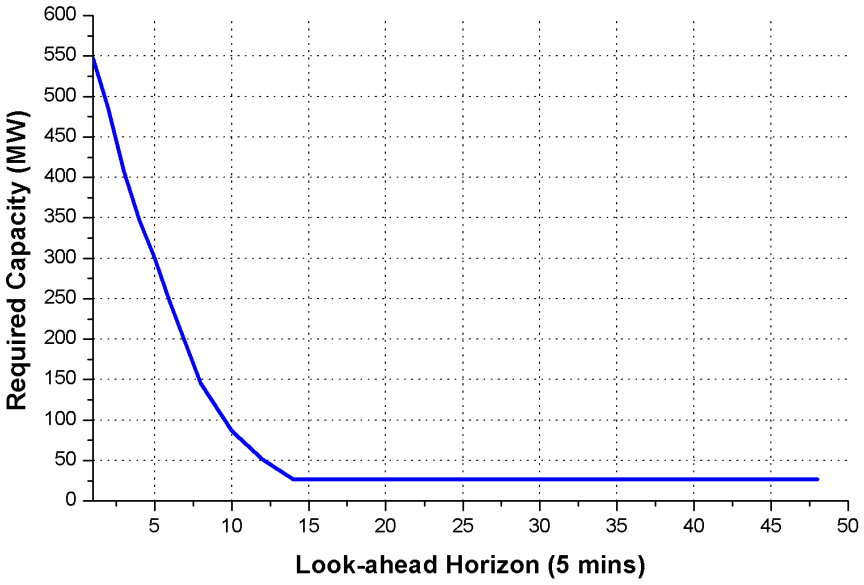

Figure 3.12: Required capacity over look-ahead horizons

according to the historical data of July 11th, 2009. We intentionally introduce a net-load ramp event into that day. Starting from 1 am, the available wind generation suddenly drops by 25%. On the other hand, the system demand increases by 15% from 1 am to 2 am. The proposed look-ahead dispatch with security management is tested under this scenario.

The average computation time and the optimal recovery cost in the practical test system over different look-ahead horizons is shown in Fig. 3.14. As we can see, the average computation time taken to perform look-ahead dispatch at one interval increases as the look-ahead horizon increases. This is because the size of the optimization problem is enlarged by considering more snapshots. Using the same simulation platform, it takes about 1 second to run a static dispatch and about 1 minute to run a 12 step look-ahead dispatch. Although the computation time

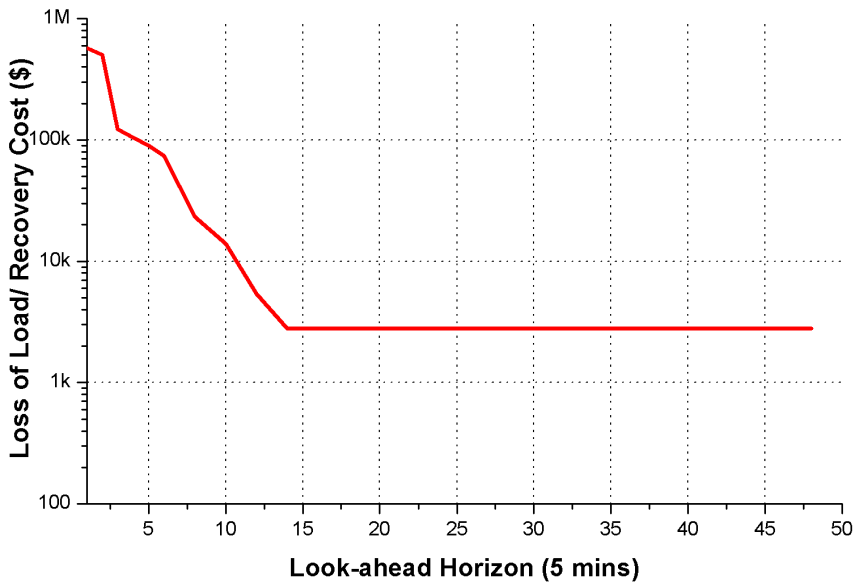

Figure 3.13: Recovery cost over look-ahead horizons

increases as the length of the horizon extends further, the absolute computation time is still less than 20% of the dispatch interval by using a desktop PC.

We believe this computational performance is acceptable and can be improved greatly in practical implementation with popular fast-MPC techniques [67]. The benefit of the proposed look-ahead dispatch is also attractive. By running the static dispatch, the system has to curtail the load of 3797.29 MW at 1 am to cope with the ramp event and the total loss of load is up to $ 3.94 million. By running 12 step look-ahead dispatch, the contingency is detected at 12 am (1 hour ago), and the insecurity is identified as the violation of the energy balancing equation at time step 12 (1 am). The generated optimal corrective solution suggests deploying non-spinning reserve of 1186.15 MW at 1 am with a total recovery cost of $12.38 thousand, a total security cost savings of up to 96.86%. Considering performance in terms of computation

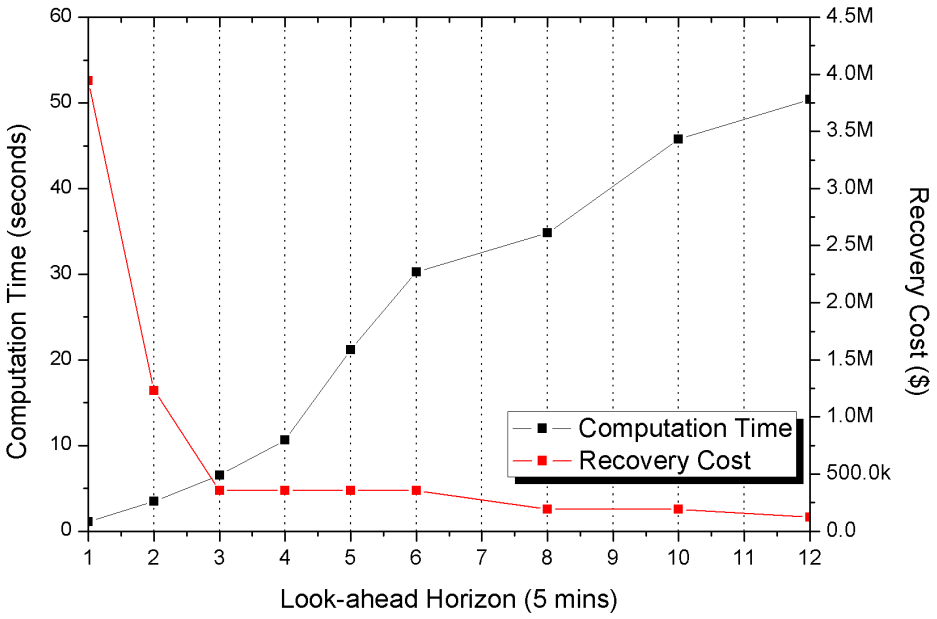

Figure 3.14: Computation time and recovery cost in the practical system test

time and recovery cost, we believe the proposed approach is implementable in a practical system and has attractive system security value, especially in preventing and handling unexpected ramp or contingency events.

3.5 Summary

In this Chapter, a look-ahead security constrained economic dispatch for enhanced security management is presented. By introducing the STDC and the contingency constraints, the proposed algorithm can consider circumstances under both normal operational conditions and contingency conditions. The proposed LSM can assist system operators to identify and quantify violations of the security constraints and work out an optimal recovery plan at a minimized recovery cost. The proposed enumeration tree approach can help to identify all of the potential factors that can cause system insecurity. The simulation is conducted on a modified IEEE RTS 24

bus system and on a practical 5889 bus system. The numerical performance suggests that the proposed approach is implementable in practical systems and has very attractive economic and operational value for enhancing power system security.

4. SPATIO-TEMPORAL WIND FORECASTS*

Look-ahead dynamic programming based approaches depend on information of systems' future circumstances. In power system domain, such information is the forecasts of load and variable generation resources. In this chapter, we present the advanced spatio-temporal wind forecast models.

4.1 Background

Uncertainties and variabilities in renewable generation, such as wind energy, pose significant operational challenges to power system operators [6, 68, 69, 70, 71]. While conventional wisdom suggests that more spatially dispersed wind farms could be aggregated and "smooth out" total wind generation at any given time, the reality is that wind generation tends to be strongly correlated in many geographical regions [72, 73]. As many regions/states are moving toward renewable portfolio standards (RPS) in the coming decade, the role of *accurate wind prediction* is becoming increasingly important for many regional transmission organizations (RTOs) [2].

The major uncertainty in conventional power grid operation comes from the demand side [74, 75, 76]. Nowadays, in power systems with high presence of intermittent generation, the main source of uncertainty comes from both demand and supply sides [6]. State-of-the-art load forecasts could achieve high accuracy in the day-ahead stage [77]. Compared with load forecasting, accurate forecast of wind generation still remains an open challenge. There exists a large body of literature on wind power forecasting, and state-of-the-art day-ahead wind forecast based on

*This section is in part a reprint of the material in the papers: L. Xie, Y. Gu, X. Zhu, and M. G. Genton, "Power system economic dispatch with spatio-temporal wind forecasts," in *Energytech*, 2011 IEEE, 2011, pp. 1-6. L. Xie, Y. Gu, X. Zhu, and G. M. G., "Short-Term Spatio-Temporal Wind Power Forecast in Robust Look-ahead Power System Dispatch," *IEEE Transactions on Smart Grid*, vol. 5, pp. 511-520, 2014.

numerical weather prediction (NWP) models has enabled relatively accurate wind forecast with approximately 15%-20% of wind speed forecast mean absolute error (MAE) [78, 79, 80, 81]. As the operating time moves closer to the near term (e.g., hour-ahead or 15 minute-ahead), at a high spatial resolution, the computation complexity (in terms of simulation time and memory requirements) often renders NWP models intractable [81].

In sharp contrast, data-driven statistical model is thought to be the most competitive method for near-term wind forecasting problems being able to capture the rapidly changing dynamics of the atmosphere and with nice model interpretation [21]. Statistical forecasting models could potentially provide *accurate and efficient* wind forecasts with MAE reduced to the range of around 5% or less [78]. A good set of references can be found in [20]. Our proposed spatio-temporal wind forecast model is directly targeted at *computationally efficient near-term* wind forecasts.

Starting from our preliminary work [82, 83], the main objective of this paper is to exploit a novel short-term spatio-temporal wind forecast model and quantify the dispatch benefits from improved short-term wind forecast. Wind generation is driven by wind patterns, which tend to follow certain geographical spatial correlations. For large-region wind farms, the wind generation forecast of the wind could significantly benefit from upstream wind power generation. Enabled by technological advances in sensing, communication, and computation, spatially correlated wind data could be leveraged for accurate system-wide short-term wind forecasts. This is potentially applicable to large-scale wind farms. The performance of such wind forecast model is critically assessed.

4.1.1 Wind Data Source in West Texas

The wind data we use here are the 5-minute averages of 3-second measurements of wind speed and direction collected by monitors placed at 10 meters above the ground from four sites in West Texas labeled ROAR, SPUR, PICT, and JAYT. Their locations are indicated by the red crosses in Figure 4.1, and more specific geographic information is listed in Table 4.1. The period of the wind data covers three years from January 1, 2008 to December 31, 2010.

Table 4.1: Site Information

ID	Location	Area	Latitude	Longitude
ROAR	3N Roaring Springs	Roaring S./Motley County	$N33°56'10.86"$	$W100°50'43.38"$
SPUR	1W Spur	Spur/Dickens County	$N33°28'51.05"$	$W100°52'34.90"$
JAYT	1SSE Jayton	Jayton (Kent Co. Airport)	$N33°13'56.69"$	$W100°34'03.99"$
PITC	10WSW Guthrie	Guthrie/King County	$N33°34'01.30"$	$W100°28'50.20"$

Winds in this area are mainly from the south or north as shown by the wind roses in Figure 4.2, where the petals are the frequencies of wind blowing from a particular direction, and the colored bands are the ranges of wind speed. Given the flatness in this area, the spatial correlation in wind can be captured when a southerly wind is blowing: wind at ROAR will mostly be just a shift from wind at SPUR. This means that to forecast the future wind speed at ROAR, it is definitely helpful to use the current and just past wind information at SPUR. Similarly, when the wind is blowing from the south or southeast, wind information at JAYT and PICT help in predicting the wind speed at ROAR. A good forecasting model should take into account both spatial and temporal correlations in wind.

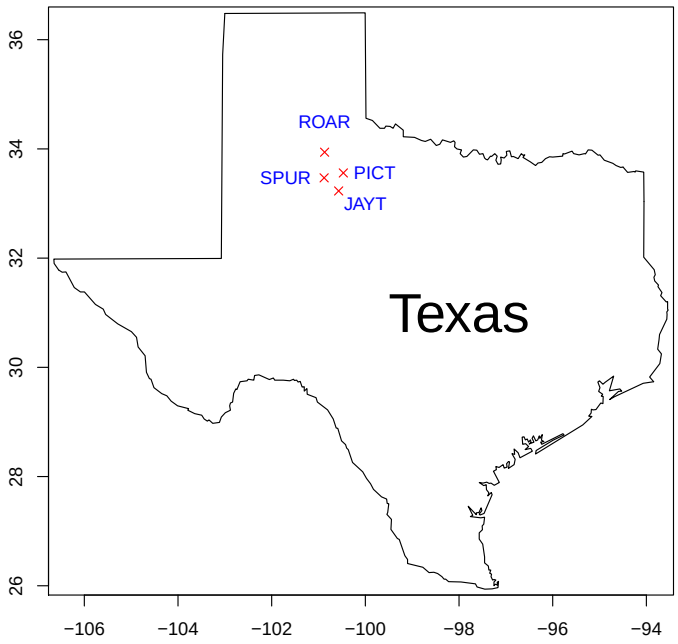

Figure 4.1: Map of the four locations in West Texas

4.1.2 Space-time Statistical Forecasting Models

We used four statistical models, PSS, AR, TDD and TDDGW, to forecast short-term wind speed at each of the four sites. In the first two models, only the temporal correlation in wind is considered, while the TDD and TDDGW models utilize wind information from the other three locations so that both spatial and temporal correlations in wind are taken into account. Moreover, the TDDGW model incorporates geostrophic information into the TDD model.

To make it simple, we describe the four models in the setting of forecasting wind speed at ROAR. Let $y_{R,t}$, $y_{S,t}$, $y_{J,t}$, and $y_{P,t}$ denote the wind speed at time t at ROAR, SPUR,JAYT, and PICT, respectively, and $\theta_{R,t}$, $\theta_{S,t}$, $\theta_{J,t}$, and $\theta_{P,t}$ denote the

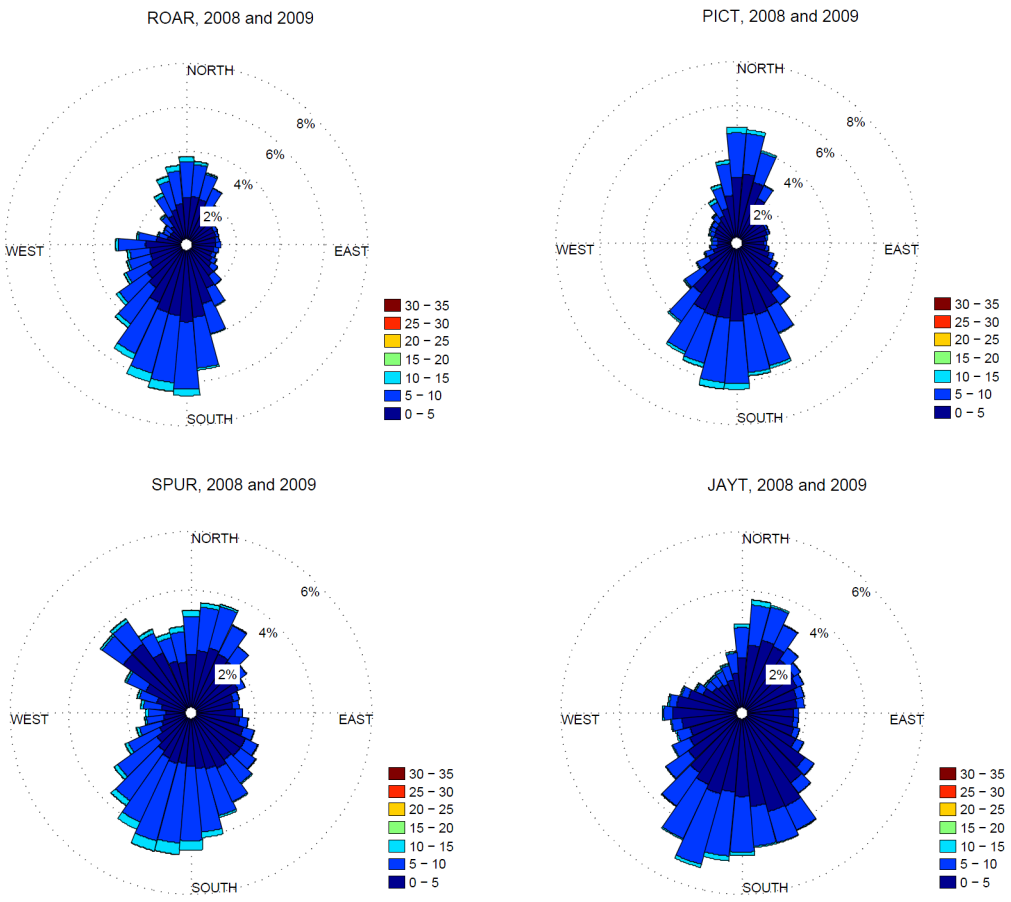

Figure 4.2: Wind roses of the four locations in West Texas

wind direction at time$t$. The goal is to estimate $y_{R,t+k}$, or the k-step-ahead wind speed at ROAR, denoted as $\hat{y}_{R,t+k}$, where each step is 5 minutes.

4.1.2.1 Persistent Forecasting

In the PSS model, it is assumed that the future wind speed is the same as the current one. For example, if $y_{R,t}$ is the wind speed at time t at ROAR, then the k-step future wind speed is predicted as $y_{R,t}$, or $\hat{y}_{R,t+k} = y_{R,t}$. PSS works very well for very short-term forecasting, such as 10-minute-ahead. The PSS model is usually treated as a reference and an advanced forecasting model is thought to be good if it

outperforms PSS.

4.1.2.2 Autoregressive Models

AR models predict the future wind speed as a linear combination of past wind speeds. In our case, we apply AR to model the center parameter, $\mu_{R,t+k}$, in equation (4.2) (defined in the next part) as follows:

$$\mu^r_{R,t+k} = \alpha_0 + \sum_{i=0}^{p} \alpha_{i+1} \mu^r_{R,t-i}. \tag{4.1}$$

The AR model assumes that future wind speed is related to historical wind information only at the same location, without considering the spatial correlation. Bayesian Information Criteria is used to selectee the order p.

4.1.2.3 Spatio-temporal Trigonometric Direction Diurnal Model

The TDD model is an advanced space-time statistical forecasting model. It generalizes the Regime-Switching Space-Time model [22] by including wind direction in the model. As a probabilistic forecasting model, the TDD model estimates a predictive distribution for wind speed at time $t + k$, thus providing more information about the uncertainty in wind. More recently, the TDDGW model, which incorporates geostrophic wind information into the TDD model, was proposed [84] and more accurate forecasts are obtained than from the TDD model.

In the TDD model, it is assumed that $y_{R,t+k}$ follows a truncated normal distribution on the nonnegative real domain, that is, $y_{R,t+k} \sim N^+(\mu_{R,t+k}, \sigma^2_{R,t+k})$ (this can be detected by the density plots in Figure 4.3), with center parameter $\mu_{R,t+k}$ and scale parameter $\sigma_{R,t+k}$. The key to achieve accurate forecasts lies in modeling these two parameters appropriately.

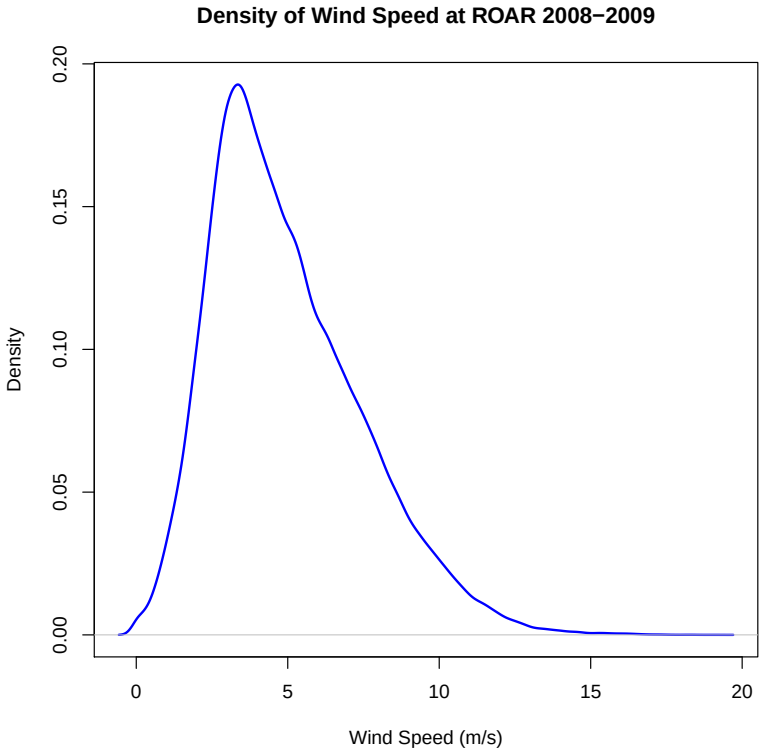

Figure 4.3: Wind speed density at ROAR 2008-2009

The center parameter, $\mu_{R,t+k}$, is modeled as

$$\mu_{R,t+k} = D_{R,h+k} + \mu^r_{R,t+k},$$

where $D_{R,h+k}$ is made of trigonometric functions to fit the diurnal pattern of the wind speed. Specifically,

$$D_{R,h} = d_0 + \sum_{j=1}^{2} \left\{ d_{2j-1} \sin\left(\frac{2\pi jh}{24}\right) + d_{2j} \cos\left(\frac{2\pi jh}{24}\right) \right\},$$

where $h = 1, 2, \ldots, 24$; see Figure 4.4. Figure 4.4 is the functional boxplot [85] of daily wind speed from 2008-2009 with the solid white line as the mean wind speed

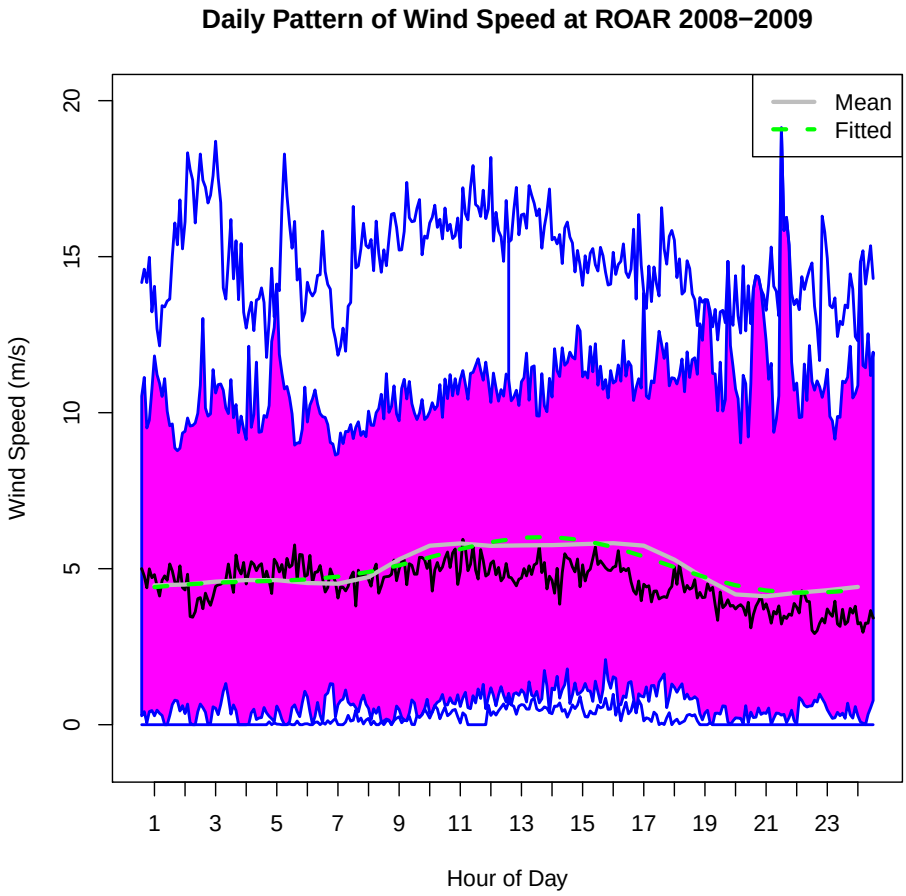

Figure 4.4: Functional boxplot of daily wind speed at ROAR 2008-2009

over 24 hours, the solid black line as the median, and the dashed green line as the fitted daily pattern.

The residual series after removing the diurnal pattern, $\mu^r_{R,t+k}$, is modeled as a linear function of current and past (up to time lag p) wind speed residuals and trigonometric functions of wind direction residuals at ROAR, as well as SPUR, JAYT, and PICT as follows:

$$\mu^r_{R,t+k} = \alpha_0 + \sum_{s\in\{R,S,J,P\}} \sum_{i=0}^{p} \alpha_{i+1}\mu^r_{s,t-i} + \sum_{s\in\{R,S,J,P\}} \sum_{j=0}^{p} \left[\beta_{j+1}\sin(\theta^r_{s,t-j}) + \gamma_{j+1}\cos(\theta^r_{s,t-j})\right]. \quad (4.2)$$

The scale parameter, $\sigma_{R,t+k}$, is modeled as

$$\sigma_{R,t+k} = b_0 + b_1 v_t, \quad (4.3)$$

where b_0, $b_1 > 0$ and v_t is the volatility value:

$$v_t = \left[\frac{1}{8}\sum_{s\in\{R,S,J,P\}} \sum_{i=0}^{1} (\mu^r_{s,t-i} - \mu^r_{s,t-i-1})^2\right]^{1/2}.$$

The coefficients in equation (4.2) along with b_0, b_1 in equation (4.3) are estimated by the continuous ranked probability score method (see [86] for more details). Predictors in (4.2) are selected with the Bayesian Information Criteria (see [23]).

4.1.2.4 Incorporate Geostrophic Wind information into the TDD Model

As we know, pressure and temperature also have significant effects on wind speed. If this information could be taken into account in wind forecasting problems, more accurate forecasts would be expected. However, it was found that adding surface pressure and temperature directly into the center parameter model in (4.2) brings no improvement to the forecasting accuracy. This is the motivation of the TDDG-W model. It takes geostrophic wind, which extracts information on pressure and

temperature, into the TDD model as a predictor.

Geostrophic wind is the theoretical wind that results from an exact balance between the pressure gradient force (horizontal components) and the Coriolis force if there were no friction above the friction layer, and this balance is called the geostrophic balance. It is parallel to straight isobars. Figure 5 illustrates the difference between geostrophic wind (left) and real wind or surface wind (right). The approximation of

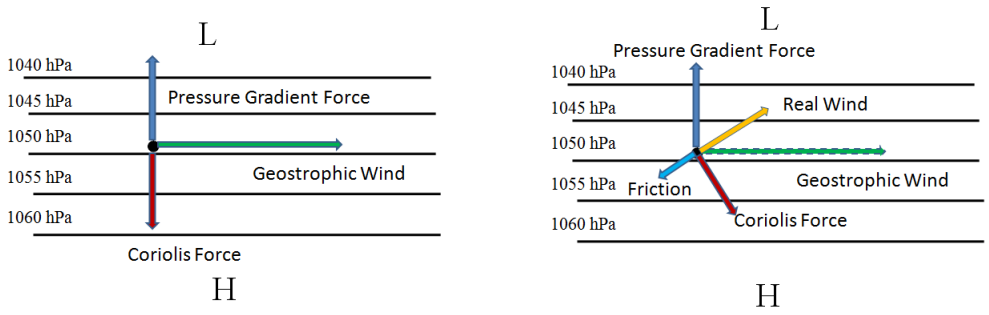

Figure 4.5: The pressure gradient, Coriolis, and friction forces influence the movement of air parcels. Geostrophic wind (left) and real wind (right)

geostrophic wind is based on Newton's Second Law. It involves calculation of geopotential heights by referring to 850 hPa based on pressure, temperature and elevation, and fitting a plan of the geopotential height gradient in the region. Due to the space limitation, we refer readers to [84] for more detailed information.

The TDDGW model incorporates geostrophic wind into the TDD model, as shown in (4.4). This model not only includes important information on pressure and temperature, but it also has a clear and meaningful physical interpretation. Moreover, the TDDGW model keeps the advantage of the TDD model, namely to account for the spatio-temporal correlation in wind:

$$\mu^r_{R,t+k} = \alpha_0 + \sum_{s\in\{R,S,J,P\}} \sum_{i=0}^{p} \alpha_{i+1}\mu^r_{s,t-i} + \sum_{k=0}^{p} c_{k+1} gw^r_{R,t-i} + \sum_{s\in\{R,S,J,P\}} \sum_{j=0}^{p} \left[\beta_{j+1}\sin(\theta^r_{s,t-j}) + \gamma_{j+1}\cos(\theta^r_{s,t-j})\right], \quad (4.4)$$

where $gw^r_{R,t-i}$s are the residuals of the geostrophic wind after removing the diurnal pattern and the c_{k+1}s are the coefficients. Since geostrophic wind is above the friction layer, it covers a large area. That means locations within the small area of our interests have very similar geostrophic values. We therefore use the geostrophic wind variable as a common predictor as shown in (4.4). The median of the truncated normal distribution is used as a point forecast:

$$z^+_{1/2} = \mu_{t+1} + \sigma_{t+1} \cdot \Phi^{-1}[1/2 + (1/2)\Phi(-\mu_{t+1})/\sigma_{t+1}],$$

where $\Phi(\cdot)$ is the cumulative distribution function of a standard normal distribution.

4.2 Forecasting Results and Comparison

In this section, the aforementioned four forecasting models are implemented to forecast 10-minute-ahead, 20-minute-ahead and up to 1-hour-ahead wind speed at the four locations in West Texas on one day each month except May 2010 (the days are chosen randomly).In the AR, TDD and TDDGW models, a 45-day sliding window of observations prior to the forecast is used to estimate coefficients in the models in which the variables are selected using the data from 2008 and 2009. For the diurnal pattern, the averages of 45 days' hourly wind speeds are used.

To evaluate the performance of the four forecasting models, mean absolute errors (MAE), defined below, are calculated from the forecasts on the 11 days and listed in

Table 4.2:

$$MAE = \frac{1}{T}\sum_{t=1}^{T} |y_{R,t+k} - \hat{y}_{R,t+k}|,$$

where $T = 3168$ for 11 days.

Table 4.2: MAE Values of Different Forecast Models

Location	Model	10 min	20 min	30 min	40 min	50 min	60 min
PICT	PSS	0.56	0.72	0.84	0.92	1.00	1.08
	AR	0.55	0.70	0.80	0.87	0.94	1.00
	TDD	**0.54**	**0.68**	**0.77**	0.84	0.90	0.95
	TDDGW	**0.54**	**0.68**	**0.77**	**0.83**	**0.89**	**0.94**
JAYT	PSS	0.50	0.63	0.71	0.78	0.83	0.89
	AR	0.48	0.60	0.68	0.75	0.8	0.86
	TDD	**0.47**	**0.57**	**0.64**	0.69	0.73	0.78
	TDDGW	**0.47**	**0.57**	**0.64**	**0.68**	**0.71**	**0.75**
SPUR	PSS	0.51	0.64	0.73	0.81	0.86	0.92
	AR	0.49	0.61	0.69	0.76	0.80	0.86
	TDD	**0.48**	**0.59**	**0.67**	0.72	0.76	0.81
	TDDGW	0.49	**0.59**	**0.67**	**0.71**	**0.75**	**0.79**
ROAR	PSS	0.55	0.71	0.82	0.92	0.98	1.02
	AR	**0.54**	0.68	0.78	0.86	0.92	0.96
	TDD	**0.54**	**0.67**	0.77	0.85	0.90	0.93
	TDDGW	**0.54**	**0.67**	**0.76**	**0.82**	**0.87**	**0.90**

From Table 4.2, we can see that MAE values increase by column, which means that the forecast accuracy reduces when the forecasting horizon, k, gets larger. Among the four models, the AR, TDD, and TDDGW models have smaller MAE values than the PSS and the space-time models, TDD and TDDGW, are more advanced than the PSS and AR models with smaller MAE values. As expected, by incorporating the geostrophic wind information, the TDDGW model increases its predictive accuracy. Its MAE values are reduced further compared with the TDD model, especially for 40-min-ahead or longer time lead forecasting. Relative to

the MAE value of PSS, the TDDGW model obtains 15.7% reduction at JAYT for 1-hour-ahead forecasting, while it is 12.4% for the TDD model. This means that, by incorporating geostrophic wind information into the TDD model, we can further reduce the forecasting error up to 3.3%, based on the relative MAE value to PSS. The computational time for hour-ahead forecast using a laptop PC for one step of the TDDGW model is approximately 1.5 minutes, and the computational time for one step of TDD is approximately 1 minute. In contrast, recent literature suggests that it is currently impossible to compute the NWP models for hour-ahead scheduling purposes [81]. Therefore, data-driven statistical wind forecast models provide computationally feasible solutions for near-term operations for system operators. In the next two sections, the economic benefits of improved forecast are quantified in look-ahead dispatch models.

4.3 Scheduling Models for Critical Assessment

With the spatio-temporal wind forecast models, we present in this section a critical assessment of the economic performance for power system operations. The power system scheduling framework formulated is designed with two layers: 1) Day-ahead reliability unit commitment (RUC)[87, 88] and 2) robust look-ahead real-time (every 5 minutes) scheduling.

4.3.1 Day-ahead Reliability Unit Commitment

The structure of the two-layer dispatch model is described in Fig. 4.6. The models of day-ahead reliability unit commitment (RUC) and real-time scheduling are presented below.

The day-ahead reliability unit commitment ensures the reliability of the physical power system after clearing the day-ahead market. It takes place 24 hours prior to the real-time operation, as shown in Fig. 4.6. Energy balancing and ancillary services

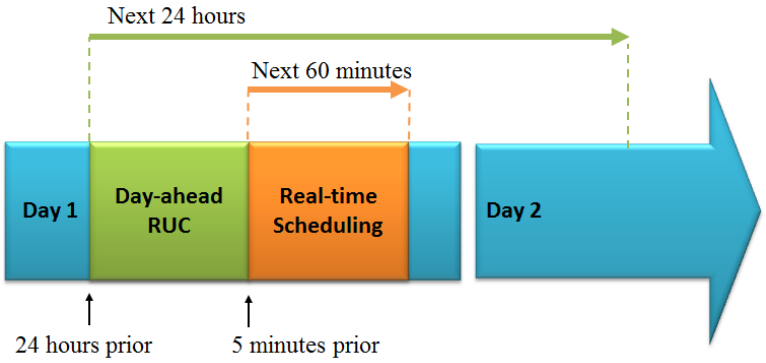

Figure 4.6: Two-layer dispatch model

(reserve services) are co-optimized with start-up/shut-down decisions. The model is formalized as follows:

$$\min_{P^k_{G_i}, P^k_{W_i}, P^k_{Rs_i}, x^k_i} : \sum_{k=k_0}^{T} [\sum_{i \in G} C_{G_i}(P^k_{G_i}) + \sum_{i \in W} C_{W_i}(P^k_{W_i}) + \sum_{i \in G} C_{Rs_i}(P^k_{Rs_i}) + \sum_{i \in F} C_{U_i}(x^k_{U_i}) + \sum_{i \in F} C_{D_i}(x^k_{D_i})] \tag{4.5}$$

s.t.

$$\sum_{i \in G} P^k_{G_i} + \sum_{i \in W} P^k_{W_i} = \sum_{i \in D} P^k_{D_i}, \ k = k_0, \ldots, T \tag{4.6}$$

$$\sum_{i \in G} P_{Rs_i}^k \geq Rs^k,\ k = k_0, \ldots, T \tag{4.7}$$

$$|\mathbf{F}^k| \leqslant \mathbf{F}^{max},\ k = k_0, \ldots, T \tag{4.8}$$

$$|P_{G_i}^k - P_{G_i}^{k-1}| \leqslant P_i^R \Delta T, i \in G,\ k = k_0, \ldots, T \tag{4.9}$$

$$x_i^k P_{G_i}^{\min} \leqslant P_{G_i}^k \leqslant x_i^k P_{G_i}^{\max}, i \in G, k = k_0, \ldots, T \tag{4.10}$$

$$P_{G_i}^k + P_{RS_i}^k \leqslant x_i^k P_{G_i}^{\max}, i \in G, k = k_0, \ldots, T \tag{4.11}$$

$$x_i^k - x_i^{k-1} \leqslant x_{U_i}^k, i \in G, k = k_0, \ldots, T \tag{4.12}$$

$$x_i^{k-1} - x_i^k \leqslant x_{D_i}^k, i \in G, k = k_0, \ldots, T \tag{4.13}$$

$$P_{W_i}^{min} \leqslant P_{W_i}^k \leqslant P_{W_i}^{max},\ i \in W, k = k_0, \ldots, T \tag{4.14}$$

$$P_{W_i}^k \leqslant \hat{P}_{W_i}^k = f(\tilde{\mathbf{P}}_W),\ i \in W, k = k_0, \ldots, T \tag{4.15}$$

$$x_i^k, x_{U_i}^k, x_{D_i}^k \in Binary, i \in G, k = k_0, \ldots, T. \tag{4.16}$$

In the proposed formulation, the objective function (4.5) is to minimize the power system operating costs including generation cost, reserve cost and start-up/shut-down cost of units. This scheduling problem is subject to various security constraints. (4.6) is the energy balancing equation. (4.7) is the system reserve requirement, which is often assessed according to system reliability requirement. (4.8) is the transmission capacity constraints. (4.9) are the ramping constraints of all generation units. (4.10) are the generators' capacity limits for generator units. (4.11) are the combined capacity constraints of generator units for providing energy and reserve services. (4.12) and (4.13) are start-up/shut-down indicator constraints. (4.14) is the capacity limit of wind farms. In this research, wind resources are assumed not to participate into ancillary services market providing reserve services. (4.15) is the wind forecast for each wind farm at time k, the details of which are explained in Section 4.1. (4.16) gives the binary constraints to integer decision variables.

4.3.2 Robust Look-ahead Economic Dispatch

Following the day-ahead scheduling from the previous subsection, we assume that system operators conduct a real-time dispatch every 5 minutes. We formulate this dispatch model as a multi-stage robust look-ahead economic dispatch to utilize the information of advanced spatio-temporal forecast. The robust look-ahead dispatch minimizes system operation cost over a horizon of multiple steps (e.g., one hour) for worst cases under predefined uncertainty set. As other look-ahead economic dispatch, only the dispatch decisions of the first step are executed. The updated information, such as wind forecast, load forecast and system conditions will be fed into the dispatch model for future decision-making. The robust look-ahead economic dispatch is formulated as

$$\max_{\mathbf{u}\in\mathbb{U}} \min_{P^k_{G_i},P^k_{W_i},P^k_{SU_i},P^k_{SD_i}} : \sum_{k=k_0}^{T}[\sum_{i\in G} C_{G_i}(P^k_{G_i}) + \sum_{i\in W} C_{W_i}(P^k_{W_i})] \tag{4.17}$$

s.t.

$$\sum_{i\in G} P^k_{G_i} + \sum_{i\in W} P^k_{W_i} = \sum_{i\in D} \hat{P}^k_{D_i},\ k = k_0,\dots,T \tag{4.18}$$

$$|\mathbf{F}^k| \leqslant \mathbf{F}^{max},\ k = k_0, \ldots, T \tag{4.19}$$

$$|P_{G_i}^k - P_{G_i}^{k-1}| \leqslant P_i^R \Delta T, i \in G \cup W,\ k = k_0, \ldots, T \tag{4.20}$$

$$\sum_{i \in G} P_{SU_i}^k \geqslant SU_D^k(\mathbf{u}), k = k_0, \ldots, T \tag{4.21}$$

$$\sum_{i \in G} P_{SD_i}^k \geqslant SD_D^k(\mathbf{u}), k = k_0, \ldots, T \tag{4.22}$$

$$P_{G_i}^k + P_{SU_i}^k \leqslant P_{G_i}^{\max}, i \in G, k = k_0, \ldots, T \tag{4.23}$$

$$P_{G_i}^k - P_{SD_i}^k \geqslant P_{G_i}^{\min}, i \in G, k = k_0, \ldots, T \tag{4.24}$$

$$P_{G_i}^{min} \leqslant P_{G_i}^k \leqslant P_{G_i}^{max},\ k = k_0, \ldots, T \tag{4.25}$$

$$P_{W_i}^{min} \leqslant P_{W_i}^k \leqslant P_{W_i}^{max},\ k = k_0, \ldots, T \tag{4.26}$$

$$P_{W_i}^k \leqslant \hat{P}_{W_i}^k,\ k = k_0, \ldots, T \tag{4.27}$$

$$0 \leqslant P_{SU_i}^k \leqslant P_{Ui}^R \Delta T, k = k_0, \ldots, T \tag{4.28}$$

$$0 \leqslant P_{SD_i}^k \leqslant P_{Di}^D \Delta T, k = k_0, \ldots, T. \tag{4.29}$$

The objective function (4.17) is to minimize the total operating cost for energy balancing. In real-time scheduling, various security constraints are considered. Energy balancing constraints are provided in (4.18). Transmission capacity constraints are given in (4.19). Ramping constraints of generators are presented in (4.20). We introduce short-term dispatchable (STDC) capacity to make sure the system has enough ramping capability to handle the uncertainty [89]. (4.21) and (4.22) are the upward/downward STDC balancing equations. The STDC are constrained by the ramping capability of each unit as presented in (4.28) and (4.29). Capacity constraints of conventional generators and wind farms are described in (4.25) and (4.26), respectively. (4.23) and (4.24) are combined capacity constraints between generation capacity and STDC. The dispatch points of wind generation should be no larger than the forecasted wind production potentials, as is shown in (4.27).

The uncertainty set $\mathbb{U}$ is given by (4.30).

$$\begin{aligned}\mathbb{U}(\hat{\mathbf{P}}_W^k, \bar{\mathbf{P}}_W^k, \hat{\mathbf{P}}_D^k, \bar{\mathbf{P}}_D^k, \overline{\Pi}_W^k, \underline{\Pi}_W^k, \overline{\Pi}_D^k, \underline{\Pi}_D^k, \bar{u}_W^k, \underline{u}_W^k, \bar{u}_D^k, \underline{u}_D^k) := \\ \{\hat{\mathbf{P}}_W^k \in \mathbb{R}^{|\mathbf{W}|}, \hat{\mathbf{P}}_D^k \in \mathbb{R}^{|\mathbf{D}|} : \sum_{i \in \mathbf{W}} \frac{\hat{P}_{W_i}^k - \bar{P}_{W_i}^k}{\bar{u}_{W_i}^k - \bar{P}_{W_i}^k} \leqslant \overline{\Pi}_W^k, \\ \sum_{i \in \mathbf{W}} \frac{\bar{P}_{W_i}^k - \hat{P}_{W_i}^k}{\bar{P}_{W_i}^k - \underline{u}_{W_i}^k} \leqslant \underline{\Pi}_W^k, \sum_{i \in \mathbf{D}} \frac{\hat{P}_{D_i}^k - \bar{P}_{D_i}^k}{\bar{u}_{D_i}^k - \bar{P}_{D_i}^k} \leqslant \overline{\Pi}_D^k, \\ \sum_{i \in \mathbf{D}} \frac{\bar{P}_{D_i}^k - \hat{P}_{D_i}^k}{\bar{P}_{D_i}^k - \underline{u}_{D_i}^k} \leqslant \underline{\Pi}_D^k, \hat{P}_{W_i}^k \in [\underline{u}_{W_i}^k, \bar{u}_{W_i}^k], \forall i \in \mathbf{W}, \\ \hat{P}_{D_j}^k \in [\underline{u}_{D_j}^k, \bar{u}_{D_j}^k], \forall j \in \mathbf{D}\} \end{aligned} \tag{4.30}$$

Here $\hat{\mathbf{P}}_W^k$ is the vector of wind production potential forecasts fed into the dispatch model as presented in (4.27). $\bar{\mathbf{P}}_W^k$ is the vector of expectations of wind forecast for each location at each time step. $\bar{u}_W^k$ and $\underline{u}_W^k$ defines the upper bounds and lower bounds of wind forecast deviation from the expectation. $\overline{\Pi}_W^k$ is defined as the budget of uncertainty for wind forecast, which takes the value between 0 and $|\mathbf{W}|$, where $|\mathbf{W}|$ is the number of wind sources modeled in the system. If the budget is set to be 0, the problem formulation turns out to be deterministic. As $\overline{\Pi}_W^k$ grows, the uncertainty set $\mathbb{U}$ enlarges, which indicates the system operation is toward more risk-averse, and the system is protected against higher degree of uncertain conditions.

Similarly, for the load forecast uncertainty, $\hat{\mathbf{P}}_D^k$ is the vector of load forecasts fed into the dispatch model. $\bar{\mathbf{P}}_D^k$ is the vector of expectations of load forecast for each bus at each time step. $\bar{u}_D^k$ and $\underline{u}_D^k$ defines the upper bounds and lower bounds of load forecast deviation from the expectation. $\overline{\Pi}_D^k$ is defined as the budget of uncertainty for load forecast, which takes the value between 0 and $|\mathbf{D}|$.

4.4 Numerical Examples with Spatio-temporal Forecasts

In this section, we conduct a numerical experiment on a 24-bus system to critically assess the *operational economic benefits* from improved short-term forecasts. The system setup details are provided in [90]

4.4.1 Results and Analysis

In this section, the simulation results of the numerical experiments are presented. The distribution of the forecast errors of the wind generation reveals the accuracy of

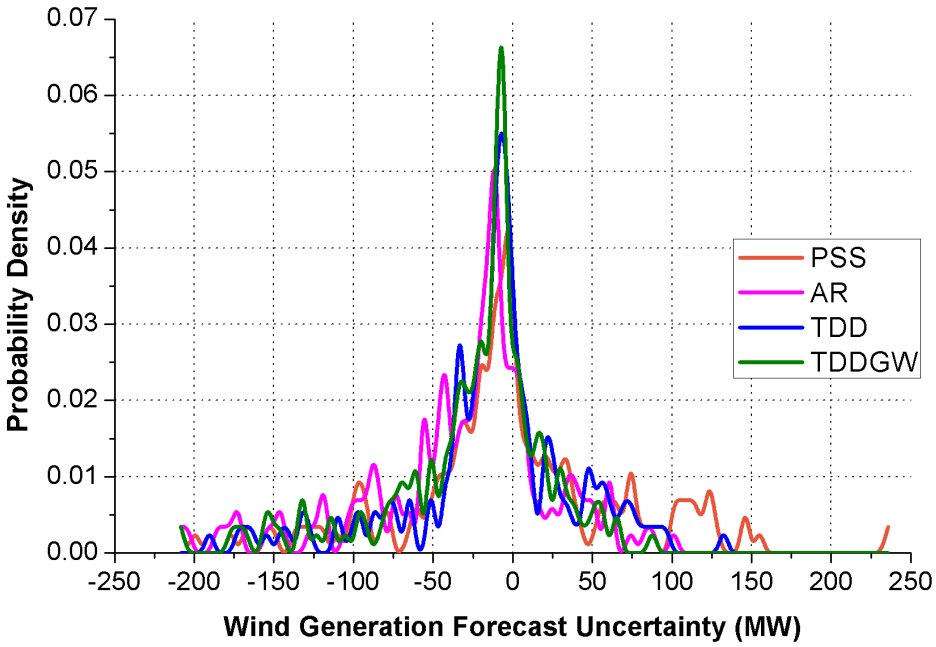

Figure 4.7: Distribution of forecast errors under different forecast models

the forecast approach. The distribution of its errors for the perfect forecast (PF) with 100% accuracy is a concentrated spike at the zero origin of the x-axis. The better the forecast accuracy the closer the distribution pattern is to the central spike. A

forecast model with poor accuracy has its errors distributed widely. The probability density distributions of the wind generation forecast errors (for a 200 MW wind farm) using the PSS, AR, TDD and TDDGW models under various simulation days are presented in Fig. 4.7. As we can observe, the distribution of the forecast errors of the PSS model is relatively spread out. The distribution of forecast errors of the TDD model is concentrated and has a higher central spike than do the AR and PSS models. The central spike of the TDDGW is higher than that of any other models. The shape of the forecast error distribution of the TDDGW model is closest to that of the perfect forecast. This is also verified by the wind speed forecast MAE presented in TABLE 4.2.

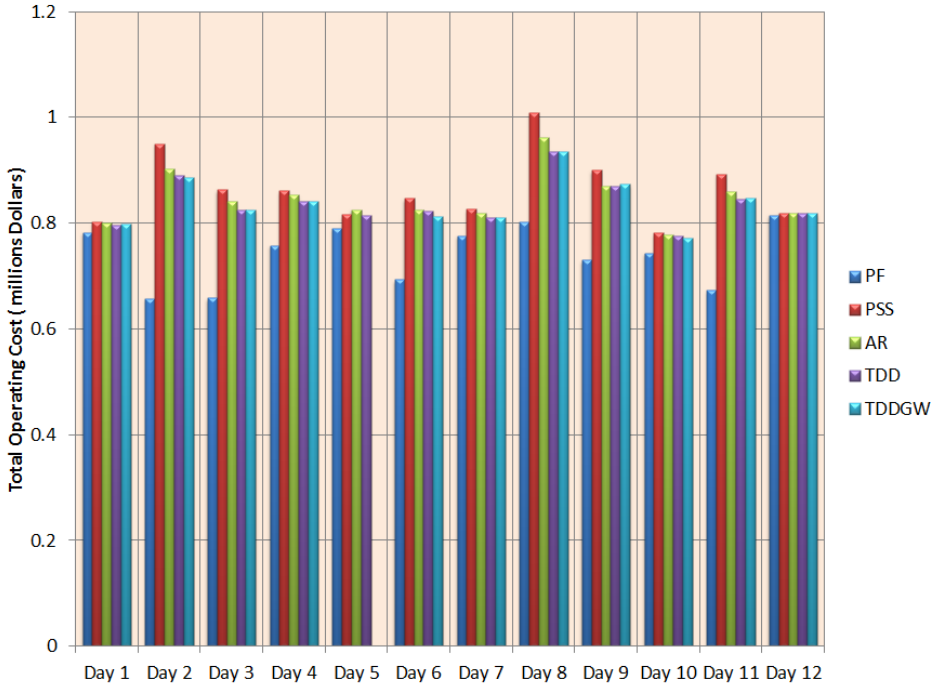

Figure 4.8: Total operating cost using different forecast models

By incorporating different forecast models into the power system economic dis-

patch, the economic performance differs. The economic performance results of Case A are presented in Fig. 4.8, which includes the total operating cost of each simulation day. The costs of the perfect forecast, PSS, AR TDD and TDDGW models are represented by the blue bar, the red bar, the green bar, the purple bar and the cyan bar, respectively. As we can see, for most of the cases, the spatio-temporal forecasts (TDD and TDDGW) have lower operating costs than do the PSS and AR models.

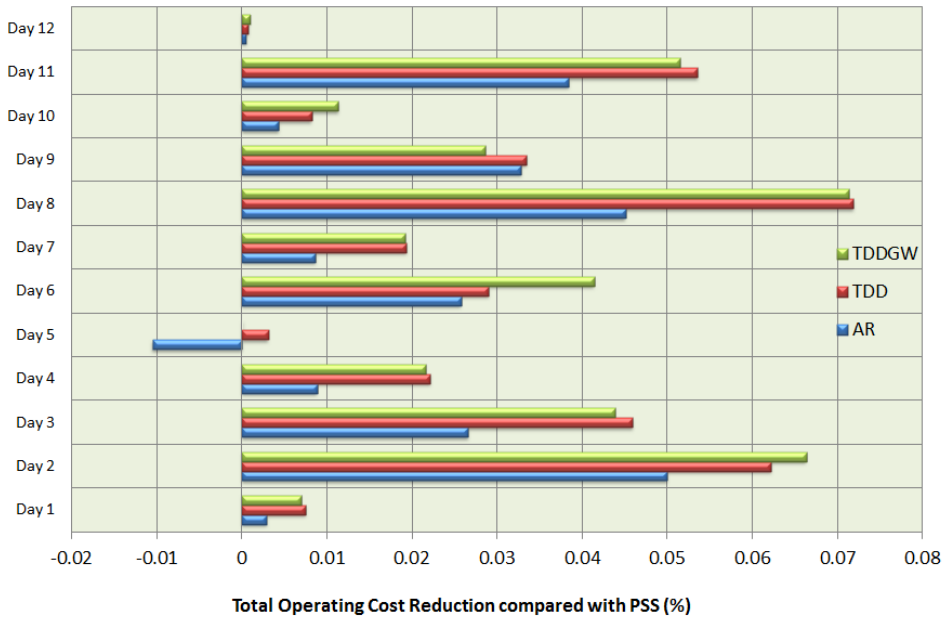

Figure 4.9: Operating cost reduction using different forecast models

Taking the PSS model as a benchmark, the reduction in operating cost by percentage using various forecast models is presented in Fig. 4.9. As we can see, the TDD and TDDGW models, which consider spatio-temporal wind correlation, outperform the AR model and the PSS model in most of the cases. By incorporating the effect of geostrophic wind, the TDDGW model can have a lower system operating

cost than the TDD model. For most of the days, the AR model performs better than the PSS model. However, it is observed that for some days (Day 5), the AR model does not produce as good a forecast as does the PSS model. That is the limitation of wind forecast based on purely historical data. In contrast, by incorporating spatial correlations, the TDD model can produce more accurate forecasts than can the PSS model and enable lower system operating costs.

4.5 Summary

Spatio-temporal wind forecast models (TDD and TDDGW models) are used and critically evaluated in this chapter. It is shown that by incorporating spatial correlations of neighboring wind farms, the forecast quality in the near-term (hours-ahead) could be improved. The TDD and TDDGW models are incorporated into a robust look-ahead economic dispatch and a day-ahead reliability unit commitment. Compared with conventional temporal-only statistical wind forecast models, such as the PSS models, the spatio-temporal models consider both the local and geographical wind correlations. By leveraging both temporal and spatial wind historical data, more accurate wind forecasts can be obtained. The potential economic benefits of advanced wind forecast are illustrated using a modified IEEE RTS 24 bus system. It is observed that the spatio-temporal model can increase wind resources utilization, and reduce system costs against uncertainty. Such data-driven statistical methods for short-term wind forecast are also applicable in other similar regions with high wind penetration.

5. STOCHASTIC LOOK-AHEAD SCHEDULING

As we discussed in Chapter 2, the look-ahead dispatch may suffer from the uncertainties in the system. Motivated by the increasing need of managing *near-real-time* operational uncertainty for the power grids, this chapter aims at applying advanced stochastic programming for look-ahead economic dispatch.

In the past decade, the global renewable capacity (wind, solar, etc.) has tremendously increased to 1470 GW [91]. The uncertainty caused by imperfect forecasts of renewables poses significant challenges to power grid operation [92]. In addition to renewable energy, another factor for power system operational uncertainty is power system contingency due to severe weather conditions. Weather-related power contingencies are estimated to have an annual cost ranging from $25 to $70 billion in the United States[93]. These two factors pose significant risks to power system operations.

While most of this research focuses on day-ahead power system scheduling, the uncertainty impacts on *near-real-time* (See Section 5.1.1 for details) is influential for system operations and should also be carefully investigated [90]. As an example, Fig. 5.1 (data collected from [94, 95]) shows a typical relationship between wind power forecast accuracy and wind forecast horizon. As the forecast horizon extends chronologically, the system operational uncertainty rises significantly(from less than 1% to more than 20%). Within near-real-time framework, wind forecast has two features: 1) the forecast is more accurate than a day-ahead forecast, and 2) uncertainty is still not negligible and requires being well handled, especially under "ramping events" or bad weather conditions. These features expose a great opportunity to adjust the dispatch plan by using the updated forecast. Taking advantage of this opportunity

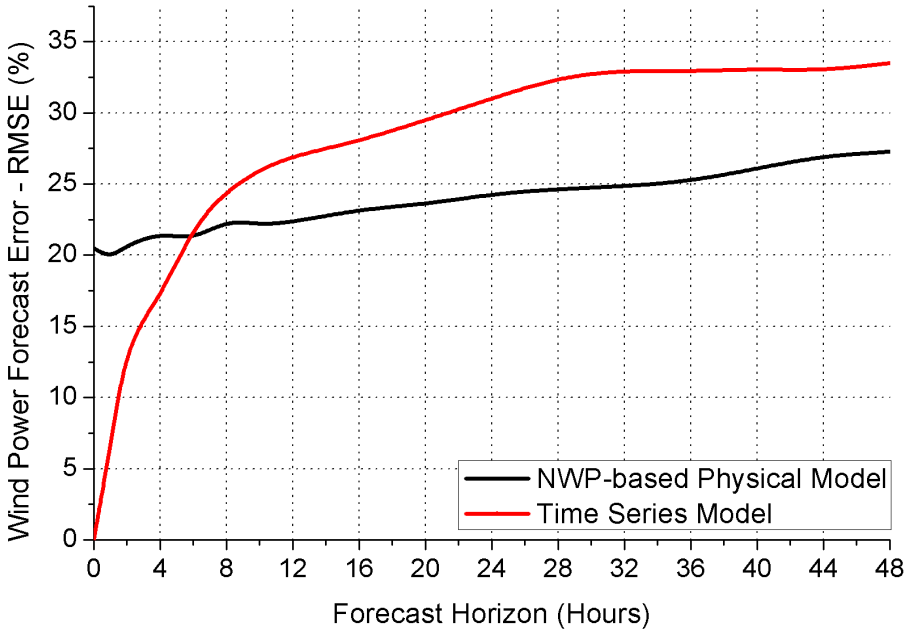

Figure 5.1: Wind power forecast accuracy versus forecast horizon

helps mitigate negative impacts of economic/technical risks at the day-ahead stage and improve the decision-making for power system scheduling.

More recently the community has begun to investigate into the issue of near-term operational uncertainties. Keshmiri et. al. formulate an optimized stochastic problem for power system economic dispatch [96]. Jabr presents an adjustable robust optimization approach based optimal power flow (OPF) [97]. Lee et. al. develop a two-stage stochastic convex programming based economic dispatch problem for operational decision-making under uncertainty [98]. Xie et. al. introduce the robust optimization into a spatial temporal wind forecast based look-ahead economic dispatch [90].

In this chapter, we investigate the potential benefits and applicability to implement a stochastic programming based look-ahead dispatch in power systems.

5.1 Stochastic Look-ahead Dispatch

The conventional scheduling for real-time operation is a deterministic economic dispatch that optimizes over single dispatch interval, also known as "static economic dispatch" or "ED-Static." ED-Static worked very well for decades, because the variability and uncertainty of net load were low at real-time operation. Due to the increased renewable penetration recently, a conventional ED-Static is not sufficient to handle the rising net-load variability. A deterministic look-ahead dispatch ("LAED-D") is established and favored by more and more industry practitioners [89].

Nevertheless, as a deterministic approach, LAED-D is not designed to make decisions against uncertainty. In this section, we explore the modeling and benefits of stochastic look-ahead dispatch (LAED-S), a stochastic approach.

5.1.1 Near-Real-Time Operation

The conventional "real-time" operation, by definition, only includes the next dispatch interval (e.g., 5 min). In contrast, we introduce the new concept of "near-real-time" operation: the operational window from 5 min-ahead to 4 hours-ahead *. Compared with the well-known real-time operation, near-real-time operation allows handling the risks over time.

Fig. 5.2 shows an illustrative example of typical operational uncertainties. Whereas day-ahead scheduling needs to use a lot of computation resources to manage the higher-level uncertainties and complexities, near-real-time scheduling allows the operators to make decisions with more accurate information. Whereas the real-time scheduling leaves limited room for corrective actions, near-real-time scheduling could leverage wider time-horizon, more controllability and flexibility of the system for

*The size of the near-real-time operation window can vary depending on the actual system circumstances (e.g., wind penetration, system topology, load conditions, etc.).

cost-effective and secure dispatch solutions [89]. Not just relieving the burden and complexity of decision-making at the day-ahead stage, sophisticated near-real-time scheduling offers unique benefits that could not have been achieved from day-ahead or real-time scheduling alone.

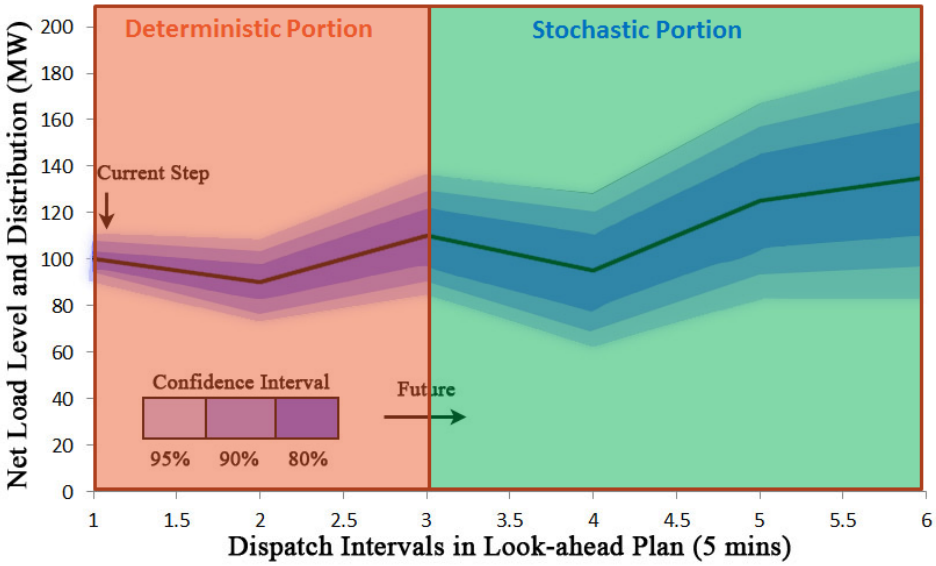

Figure 5.2: The horizon division of a stochastic look-ahead dispatch

5.1.2 Framework of Stochastic Look-ahead Dispatch

The framework of the proposed LAED-S is presented in Fig. 5.3. The LAED-S framework comprises different modules. The whole process starts with the system initialization module in which system models are established and market data are assimilated from the database. A core judgement module then triggers the analytical criterion that checks whether a stochastic approach applies to the current system circumstances or not. If not, LAED-D is activated to generate the dispatch results. If a stochastic approach is preferred, the horizon division module decomposes the

look-ahead horizon into a deterministic portion and a stochastic portion. A scenario generation module generates a group of representative scenarios that approximate the uncertainty distributions associated with the net load. With the generated scenarios, the core LAED-S algorithm then computes the optimal solutions. No matter via a deterministic approach or a stochastic approach, the solutions are fed to the post-processing modules to prepare the results for system operators.

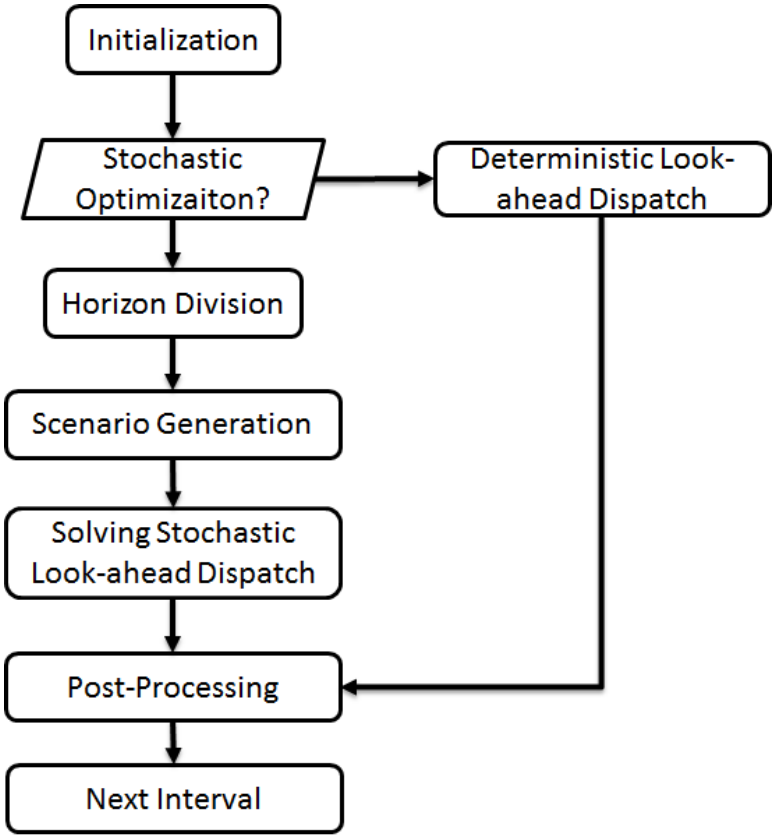

Figure 5.3: The general flowchart of a stochastic look-ahead dispatch

5.1.3 Mathematical Formulation

A LAED-S model can be formulated as (5.1) - (5.11):

$$\min : f = \sum_{k \in T_I} \sum_{i \in G} C_{G_{i,s_0}} P_{i,s_0}^k$$

$$+ \sum_{s \in S} \rho_s \sum_{k \in T_{II}} \sum_{i \in G} C_{G_{i,s}} P_{i,s}^k + R_s^k \tag{5.1}$$

Subject to

$$\sum_{i \in G} P_{i,s}^k = L_s^k, k \in T_I \cup T_{II}, s \in S \cup \{s_0\} \tag{5.2}$$

$$\sum_{i \in G} P_{SU_{i,s}}^k \geqslant SU_s^k, k \in T_I \cup T_{II}, s \in S \cup \{s_0\} \tag{5.3}$$

$$\sum_{i \in G} P_{SD_{i,s}}^k \geqslant SD_s^k, k \in T_I \cup T_{II}, s \in S \cup \{s_0\} \tag{5.4}$$

$$-\mathbf{F_s^k}^{\max} \leqslant \mathbf{F_s}^k \leqslant \mathbf{F_s^k}^{\max}, k \in T_I \cup T_{II}, s \in S \cup \{s_0\} \tag{5.5}$$

$$-P_{D_i}^R \leqslant \frac{(P_{i,s}^k - P_{i,s}^{k-1})}{\Delta T} \leqslant P_{U_i}^R,$$

$$i \in G, s \in S \cup \{s_0\}, k \in T_I \cup T_{II} \tag{5.6}$$

$$P_{i,s}^k + P_{SU_{i,s}}^k \leqslant P_{i,s}^{\max},$$

$$i \in G, s \in S \cup \{s_0\}, k \in T_I \cup T_{II} \tag{5.7}$$

$$P_{i,s}^k - P_{SD_{i,s}}^k \geqslant P_{i,s}^{\min},$$

$$i \in G, s \in S \cup \{s_0\}, k \in T_I \cup T_{II} \tag{5.8}$$

$$P_{i,s}^{\min} \leqslant P_{i,s}^k \leqslant P_{i,s}^{\max}, s \in S \cup \{s_0\}, k \in T_I \cup T_{II} \tag{5.9}$$

$$0 \leqslant P_{SU_{i,s}}^k \leqslant P_{Ui}^R \Delta T, s \in S \cup \{s_0\}, k \in T_I \cup T_{II} \tag{5.10}$$

$$0 \leqslant P_{SD_{i,s}}^k \leqslant P_{Di}^D \Delta T, s \in S \cup \{s_0\}, k \in T_I \cup T_{II} \tag{5.11}$$

The objective function (5.1) is to minimize the overall expected generation cost plus recourse cost if system emergency happens. Equality constraints (5.2) are

the energy balancing equations. Inequality constraints (5.3) and (5.4) are the upward/downward STDC requirement constraints. The inequality constraints from (5.5) to (5.11) are transmission capacity constraints, ramping capability constraints, mixed generator capacity constraints, and the upper and lower bounds of the decision variables, respectively.

5.2 Benefits Illustration for LAED-S

In this section, we present two simple examples to illustrate the benefits of LAED-S. The presented examples are 2 and 3 bus systems. ED-Static, LAED-D and LAED-S are tested under the assumed scenarios. For the look-ahead dispatch, the look-ahead horizon consists of 2 steps. For LAED-S, the first step is a deterministic step and the second step is a stochastic step.

5.2.1 Economic Benefits for Stochastic Look-ahead Dispatch

The first example illustrates the economic benefits for LAED-S. As shown in Fig. 5.4, there are a wind farm of 90 MW, a coal unit of 140 MW and a natural gas unit of 40 MW in the system. The generator parameters are provided in the figure.

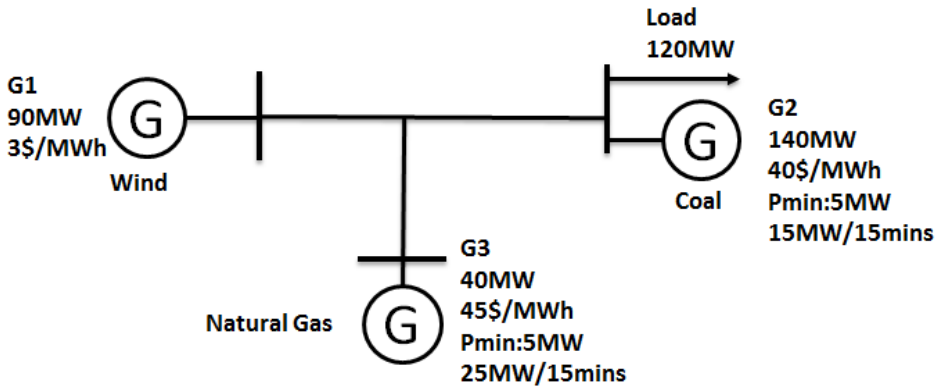

Figure 5.4: Illustrative example of economic benefits for a stochastic look-ahead dispatch

Table 5.1 provides the wind and load profiles under three assumed scenarios. Only the wind generation at the second interval is associated with uncertainty.

Table 5.1: Scenario Definition for Illustrative Example 1 (Unit: MW)

Time Interval	0:00		0:15		
	Wind	Load	Wind	Load	Probability
Scenario 1	65	120	90	100	0.4
Scenario 2	65	120	80	100	0.4
Scenario 3	65	120	60	100	0.2

Given the load and wind profiles, we conducted the three dispatch algorithms: ED-Static, LAED-D, and LAED-S. The dispatch decisions for time interval 1 are presented in Table 5.1. After time interval 1's realization, the decisions for time interval 2 are presented in Table 5.3. The economic dispatch minimizes the generation

Table 5.2: Dispatch Decisions for Time Interval 1 :Illustrative Example 1 (Unit: MW)

	G1	G2	G3
ED-Static	65	50	5
LAED-D	65	30	25
LAED-S	65	20	35

cost over the targeted time framework. Not considering future changes, ED-Static makes "short-sighted" decisions that only optimize the current interval. ED-Static schedules wind and coal capacity as much as possible at the first interval due to their low cost. At the second interval, when wind production potential (WPP) increases and load decreases, ED-Static could not fully utilize the "inexpensive" wind energy

but instead the most-expensive natural gas capacity because it is the only available resource given the ramping-down limit of the slow coal unit.

LAED-D performs differently. Owing to its capability of taking future into account, the look-ahead dispatch schedules some natural gas capacity at time interval one although it is more expensive. In return, the look-ahead dispatch is able to fully utilize the expected WPP at the second time interval. In this way, the generation cost of a look-ahead dispatch can be much lower than ED-Static.

If wind forecast uncertainty is considered, LAED-S reveals its advantage. Although LAED-D can fully utilize the expected WPP, it doesn't guarantee the realized WPP can be fully utilized. A decision made by LAED-D may suffer from underestimation scenario such as Scenario 1. LAED-S can overcome this shortage by taking all the scenarios into account to minimize the overall expected cost. Although the expected wind is 80 MW, given the consideration of 90 MW wind potential under scenario 1, LAED-S uses even more natural gas capacity at the first interval. In this way, the system has more ramp down capability when the wind potential is higher than the expected. As observed from Table 5.3, the overall expected cost by using the stochastic approach outperforms the deterministic look-ahead approach and static approach.

5.2.2 Security Benefits for Stochastic Look-ahead Dispatch

The second illustrative example (Fig. 5.5) presents the security advantage of LAED-S. In this example, we assume there are one wind farm and one coal power unit in the system. The parameters of the system are indicated in Fig. 5.5. The assumed load and wind profiles are listed in Table 5.4. We conduct three dispatch algorithms based on the given system and wind/load profiles. The dispatch decisions for time interval 1 are presented in Table 5.4. After time interval 1 is realized, the

Table 5.3: Dispatch Decisions for Time Interval 2: Illustrative Example 1 (Unit: MW)

ED-Static	G1	G2	G3	Wind Cur.	Cost ($)
Scenario 1	60	35	5	30	4225
Scenario 2	60	35	5	20	4225
Scenario 3	60	35	5	0	4225
Expected Cost ($)	4225				
LAED-D	G1	G2	G3		Cost
Scenario 1	80	15	5	10	3585
Scenario 2	80	15	5	0	3585
Scenario 3	60	35	5	0	4325
Expected Cost ($)	3733				
LAED-S	G1	G2	G3		Cost
Scenario 1	90	5	5	0	3265
Scenario 2	80	15	5	0	3635
Scenario 3	60	35	5	0	4375
Expected Cost ($)	3635				

decisions for time interval 2 are presented in Table 5.6. We assume the cost of loss of load is $ 1000 per MWh.

Figure 5.5: Illustrative example of security benefits for a stochastic look-ahead dispatch

In this example, the load increases in the second time interval and WPP decreases. As we can see from Table 5.6, ED-Static does not consider the future change in load

and wind profile. ED-Static uses wind as much as possible at the first time interval because wind is cheap. However, when the wind drops and load increases at the second time interval, the slow coal unit cannot ramp up to meet the increased load. As a result, the short-sighted decision leads to loss of load at 5 MW and 15 MW under Scenario 2 and Scenario 3, respectively.

Table 5.4: Scenario Definition for Illustrative Example 2 (Unit: MW)

Time Interval	0:00		0:15		
	Wind0	Load0	Wind	Load	Probability
Scenario 1	65	95	60	100	0.4
Scenario 2	65	95	50	100	0.5
Scenario 3	65	95	40	100	0.1

LAED-D performs better in this case. By taking future into consideration, LAED-D reserves some wind capacity at time interval 1 and use more expensive coal capacity. As a result, the system is able to satisfy the increased load at the second time interval, because wind can ramp up quickly. In this way, the loss of load can be reduced.

Table 5.5: Dispatch Decisions for Time Interval 1: Illustrative Example 2 (Unit: MW)

	G1	G2
ED-Static	65	30
LAED-D	63	32
LAED-S	50	45

Since LAED-D only considers the expected WPP, it doesn't consider the scenario

3 in which the drop in wind is 10% more than expected. Therefore, loss of load cannot be avoided. LAED-S can overcome this shortage. It takes all the scenarios into account and makes decisions to reserve wind capacity appropriately so that loss of load under all three scenarios can be avoided. Due to the advantage in avoiding loss of load, the expected cost for the stochastic dispatch is much lower than LAED-D and ED-Static.

Table 5.6: Dispatch Decisions for Time Interval 2: Illustrative Example 2 (Unit: MW)

ED-Static	G1	G2	LOL	Cost ($)	Probability
Scenario 1	60	40	0	3175	0.4
Scenario 2	50	45	5	8345	0.5
Scenario 3	40	45	15	18315	0.1
Expected Cost ($)	7274				
LAED-D	G1	G2	0		
Scenario 1	60	40	0	3249	0.4
Scenario 2	50	47	3	6499	0.5
Scenario 3	40	47	13	16469	0.1
Expected Cost ($)	6196				
LAED-S	G1	G2	0		
Scenario 1	60	40	0	3730	0.4
Scenario 2	50	50	0	4100	0.5
Scenario 3	40	60	0	4470	0.1
Expected Cost ($)	3989				

5.3 Power System Uncertainty Response

As illustrated in the examples in Section 5.2, a stochastic approach can be helpful for better system dispatch decisions. In this section, by introducing the concept of power system uncertainty response, we are going to address the core research question of when we need a stochastic dispatch.

5.3.1 Analytical Criterion for Stochastic Dispatch

Whether to conduct a stochastic programming to an application depends on the tradeoff between the achievable benefits and the affordable computation resources. For power system operation, given fixed computation resources and operation time-framework, the key gauge whether to conduct a stochastic programming is deeply associated with how much benefit can be accomplished.

Definition 1: Let $\delta^k_{W_{i,s}}$ and $\delta^k_{L_s}$ represent the forecast errors (MAE) associated with expected WPP $\hat{P}_{i,s}, i \in \mathbb{W}$ and expected load $\hat{L}^k_s$ at time step k. Let $\delta^k_{C_{i,s}}$ represents the potential capacity loss of the conventional online generation capacity $\delta^k_{C_{i,s}}$. The summation of $-\sum_{i\in\mathbb{W}} \hat{\delta}^k_{W_{i,s}}$, $-\sum_{i\in\mathbb{C}} \hat{\delta}^k_{C_{i,s}}$ and $\hat{\delta}^k_{L_s}$ is defined as a net load forecast error $L^k_{net_s}$. For $k = 1, 2, 3, T$, define an index for net load uncertainty:

$$\delta^{net}_{t,k} \triangleq \lim_{n\to+\infty} \frac{\zeta_N \sqrt{\sum_{s=1}^{n} \Pr(s) \|\tilde{L}^k_{net}\|}}{\|\mathbb{E}(\hat{L}^k_s - \sum_{i\in\mathbb{W}} \hat{P}_{i,s})\|}, \tag{5.12}$$

The net load uncertainty defined in (5.12) refers to the uncertainty associated with load and renewable generation's forecast errors, and potential capacity loss due to various contingencies etc.

Definition 2: Let cost function at time step k: $f_k \triangleq \min f(P^k_{i,s}, \delta^k_{W_{i,s}}, \delta^k_{L_s})$. For $k = 1, 2, 3, \cdots$, define a power system economic risk value:

$$R_{t,k} \triangleq \lim_{n\to+\infty} \frac{\zeta_R \sqrt{\sum_{s=1}^{n} \Pr(s) \|\tilde{f}_i - \mathbb{E}(\tilde{f})\|}}{\|\mathbb{E}(\tilde{f})\|}, \tag{5.13}$$

The power system economic risk defined in (5.13) essentially indicates the potential deviations in system operating and recourse costs if unexpected events occur.

Definition 3: Given the wind forecast errors $\delta^k_{W_{i,s}}$ and load forecast errors $\delta^k_{L_s}$

under scenario space $\mathbb{S}$, for time step $k = 1, 2, 3, \cdots$, a power system uncertainty response is defined as a function mapping the corresponding net load uncertainty $\delta_{t,k}^{net}$ to the power system economic risk $R_{t,k}$:

$$\dot{\mathcal{U}}_{t,k}(\delta_{t,k}^{net}) : \delta_{t,k}^{net} \rightarrow R_{t,k}, \tag{5.14}$$

Based on numerous historical data analyses of a practical power system, we draw a typical mapping relationship between the net load uncertainty $\delta_{t,k}^{net}$ and economic risks $R_{t,k}$, as depicted in Fig. 5.6.

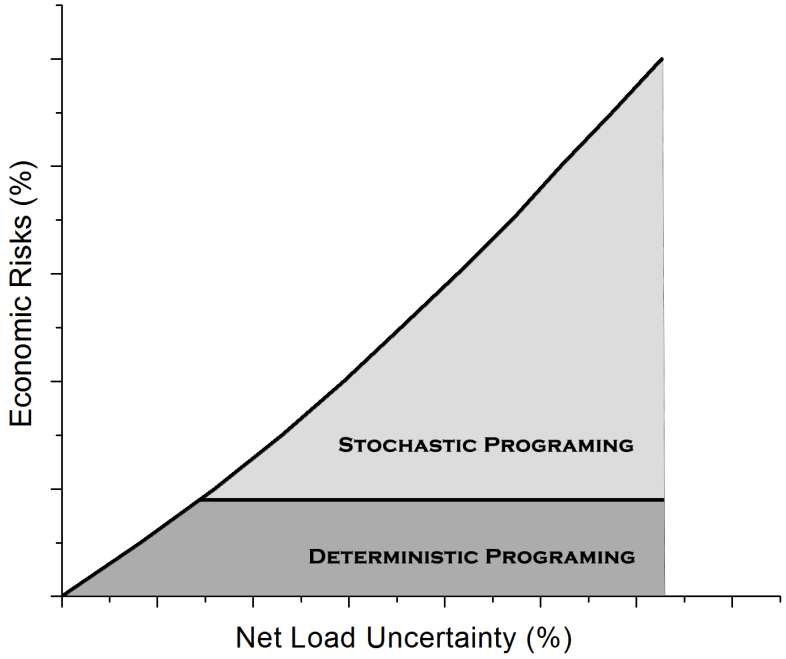

Figure 5.6: Typical uncertainty response to net load uncertainties in a power system

In Fig. 5.6, when the net load uncertainties increase, the potential system eco-

nomic risks go up as well. We assume the system operation has a security zone criterion (e.g., 2%). When the system operation exceeds this zone, the system is better handled by sophisticated risk-aware decision-making such as stochastic programming.

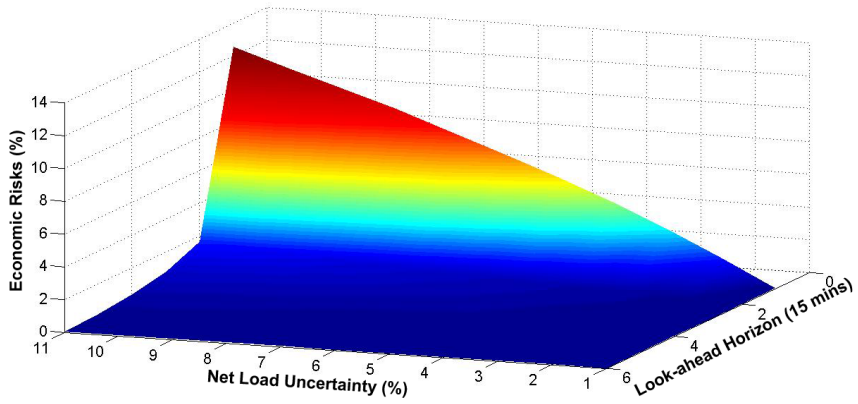

Figure 5.7: Typical uncertainty response to net load uncertainties over look-ahead horizon

However, practical power system operation is much more complicated. The impacts of uncertainties at different time steps project different levels of impacts on the economic risks of system operations as is illustrated in Fig. 5.7. It requires an approach taking into account uncertainty impacts of various time scales.

Definition 4: Given the wind forecast errors $\delta^k_{W_{i,s}}$ and load forecast errors $\delta^k_{L_s}$ under scenario space $\mathbb{S}$, for time step $k = 1, 2, 3, \cdots$, the power system uncertainty response over look-ahead horizon $t \in [1, T]$ is defined as a function mapping the net load uncertainty $\delta^{net}_{t,k}$ to the power system economic risk $\mathcal{R}_k$:

$$\mathcal{U}_k(\delta^{net}_{t,k}, t \in [1, T]) \triangleq \int_{\mathbb{T}} \dot{\mathcal{U}}_{t,k}[\delta^{net}_{t,k}(t)]dt \rightarrow \mathcal{R}_k, \tag{5.15}$$

Based on numerical studies, the multi-time-scale uncertainty responses can be discretized into snapshots at each dispatch interval, as is presented in Fig. 5.8. As we can observe from Fig. 5.8, the uncertainty affects the near-term operation more influentially than the long-term operation. In order to consider the uncertainty impacts under various time steps, (5.16) is adopted.

$$\mathcal{R}_k \approx \sum_{t}^{T} \beta_k R_{t,k}(\delta_{t,k}^{net}), \tag{5.16}$$

where R_{total} is the total economic risk given the impact of uncertainties at all time steps in a look-ahead horizon, R_k is the economic risk associated with the impact of uncertainties at time step k in a look-ahead horizon, R_k is a function of $\delta_{t,k}^{net}$ the net load uncertainty time step k, and β_k is the adjustment weighting factors.

Power systems have different operational patterns due to topology, load, renewables, seasons, weathers, geographical conditions etc. Under different power system operational patterns, the uncertainty responses are different. For generalization purposes, (5.16) can be updated as (5.17), where $R_k^{Pa_i}(.)$ represents the relationship between economic risks and uncertainties given the operational pattern Pa_i.

$$\mathcal{R}_k \approx \sum_{t}^{T} \beta_k R_{t,k}^{Pa_i}(\delta_{t,k}^{net}). \tag{5.17}$$

In practical implementation, uncertainty responses $\dot{\mathcal{U}}_{t,k}(\delta_{t,k}^{net})$ of a system are computed via historical data and numerical experiments in an off-line process. After pattern recognition and data analysis, the continuous uncertainty response functions can be discretized into (5.17) in a piece-wise linear form. Given the assessment of

net-load uncertainty from forecast providers, the economic risks $\mathcal{R}_k$ are calculated online before LAED-S takes place.

5.3.2 Horizon Division

In this subsection, we further utilize the uncertainty response presented in the previous section to develop a quantitative approach to decomposing the stochastic look-ahead horizon.

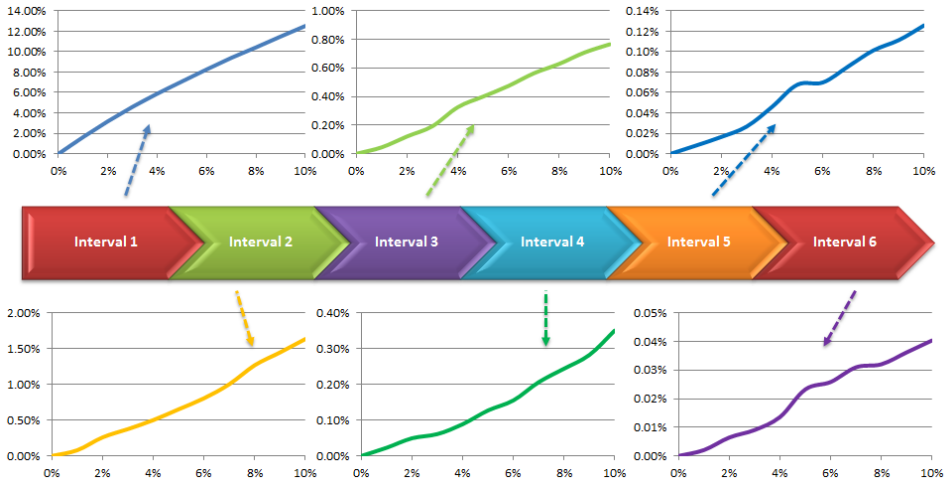

Figure 5.8: Multi-time-scale uncertainty response under a deterministic look-ahead dispatch

As presented in Fig. 5.2, the look ahead horizon can be decomposed into a deterministic portion and a stochastic portion. The deterministic portion represents those time steps which have relatively low economic risks. The stochastic portion are the time steps associated with various realizations of high economic risks. These realizations, if considered, can improve the current dispatch decisions and lead to better scheduling performance in future steps.

$$Tp_{st} := \{Tp_{st_j} | \sum_{t=j}^{T} \beta_k R_{t,k}^{Pa_i}(\delta_{t,k}^{net}) \geqslant \xi_{st_k}^{Pa_i}\}, \tag{5.18}$$

$$Tp_{det} := \{Tp_{det_j} | \sum_{t=j}^{T} \beta_k R_{t,k}^{Pa_i}(\delta_{t,k}^{net}) < \xi_{det_k}^{Pa_i}\}, \tag{5.19}$$

For horizon division, two types of sets are defined: stochastic time-period sets and deterministic time-period sets, as shown in (5.18) and (5.19), respectively. Tp_{st} is the set of all stochastic time periods, $\xi_{st_k}^{Pa_i}$ is the economic risk criterion for stochastic portion at time step k under pattern Pa_i, Tp_{det} is the set of all deterministic time periods, $\xi_{det_k}^{Pa_i}$ is the economic risk criterion for deterministic portion at time step k under pattern Pa_i. (5.18) and (5.19) provide analytical criterion to conduct horizon division into a stochastic portion and a deterministic portion.

5.4 Scenario Generation

Scenario generation is an important process in stochastic programming, especially for a large scale LAED-S problem. An effective stochastic scenario generation mechanism establishes the sampling space that represents the full distribution of the uncertainty in the problem.

Thanks to the research efforts in advanced power system forecast [81, 90, 99, 100], the probability distribution of load and renewable generation resources are available. Large number of scenarios are generated through Monte Carlo simulation so as to mimic the potential realization of the net load uncertainty [101].

A sample space consisting of many scenarios (e.g. 1000) is generated by Monte Carlo simulation, as is shown in Fig. 5.9. For practical power system operation, due to the inertia of renewable generation and load, the *persistence* of net load should not be neglected, namely, the future realization of net load level is correlated with

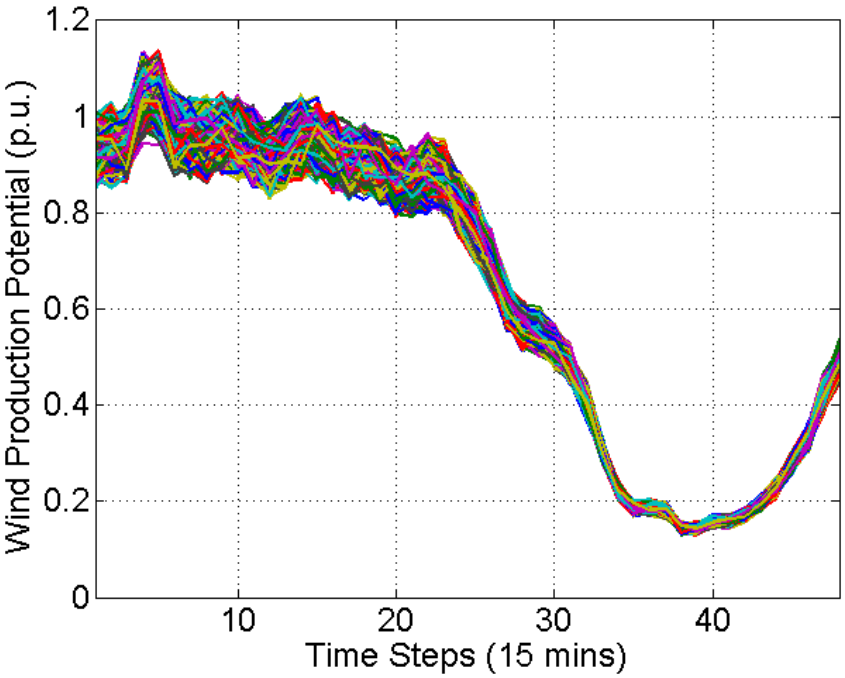

Figure 5.9: Wind production potential (per unit) under 1000 scenarios generated by Monte Carlo simulation

its past realization.

$$P_L^k = \beta_{LF} P_L^{k-1} \cdot p_L^k + (1 - \beta_{LF}) p_L^k, \beta_{LF} \in [0, 1] \tag{5.20}$$

We consider the net load persistence in (5.20), where P_L^k is the realization of net load at time step k, $\beta_{LF} \in [0, 1]$ is the persistence factor (PF) which indicates the correlation of the net demand realization at next step to current one, and p_L^k is the net load forecast at time step $k + 1$.

In Fig. 5.9 and Fig. 5.10, the scenario sample spaces of (PF $= 0.3$) and (PF $= 0.7$) are shown, respectively. Considering persistence correlations, net demand pattern is smoother and the distribution of scenarios turns out more diverse in the long

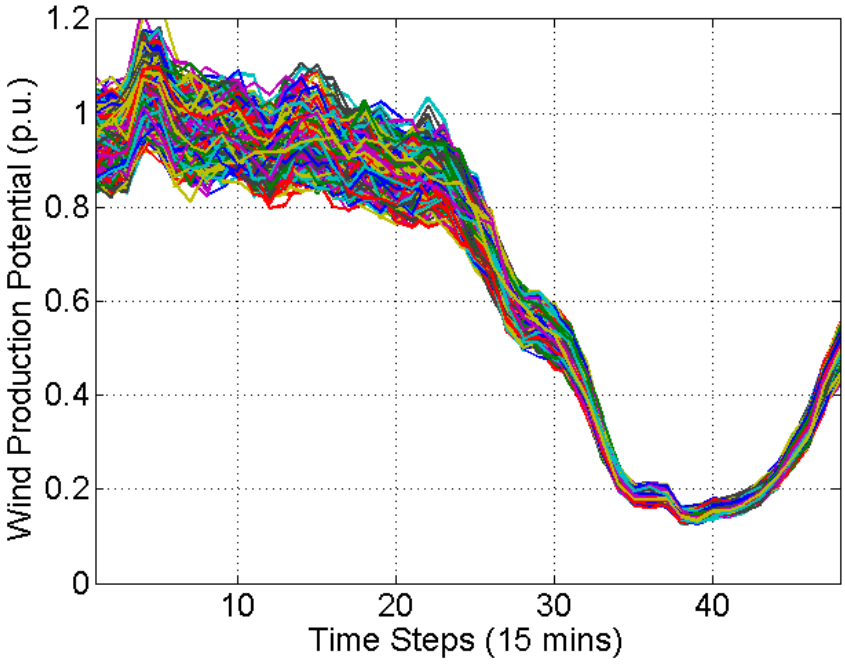

Figure 5.10: Wind production potential (per unit) under 1000 scenarios with persistence factor PF = 0.7

run. However, if the persistence considered is too strong, the temporal correlations become dominant against the net demand forecast.

A scenario reduction process is conducted to find out a reduced sample space with representative scenarios. It has been justified that, satisfying reasonable conditions, a good decision-making can be obtained through reduced scenario sets as long as the reduced scenario sets are sufficiently close to the original scenario set [102]. A commonly used metric measuring the probability distance between scenario sets is the Kantorovich distance [103].

$$D_K(Q, Q') = \inf_{\eta} \{ \int_{S \times S} d(s, s') \eta(ds, ds') : \int_S \eta(\cdot, ds') = Q, \int_S \eta(ds, \cdot) = Q' \}. \tag{5.21}$$

As is presented in (5.21), this formulation is named as Monge-Kantorovich transportation problem. More details of this formulation are available in [104]. In this paper, the distance between two scenarios is defined by the norm of the difference between their net load pairs (5.22).

$$d(s, s') = \| P^s_{\text{net}} - P^{s'}_{\text{net}} \|, \tag{5.22}$$

where $d(s, s')$ is the distance between scenario s and s', and P^s_{net} is the vector of net load of scenario s during the target operation horizon. As discussed in [102, 105, 103], if the uncertainties only associated with right-hand sides and the reduced scenarios' set S_R is a subset of the original scenarios' set S_0,(5.21) can be equivalently expressed as (5.23).

$$D_K(Q, Q') = \sum_{s \in S_0 \setminus S_R} \rho_s \min_{s' \in S_R} d(s, s'). \tag{5.23}$$

We employ the forward selection algorithm [103] iteratively to generate a reduced scenario set which is close to the original scenario set. The reduced sample space of 20 selected scenarios are shown in Fig. 5.11.

The scenario generation and reduction mechanism presented above can prepare

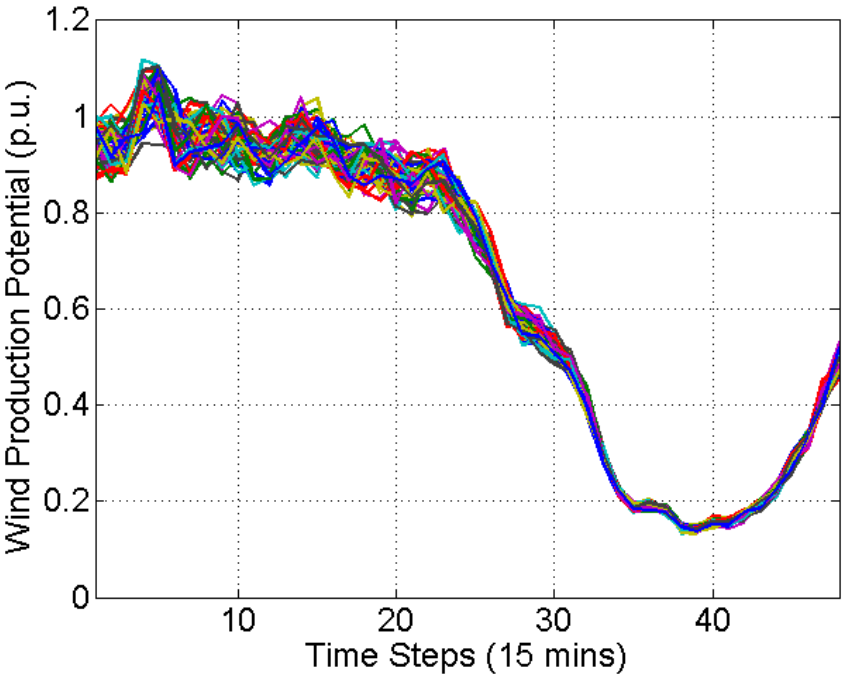

Figure 5.11: Wind production potential (per unit) under 50 representative scenarios after scenario reduction process

a representative scenario set for LAED-S.

5.5 Hybrid Computation Framework

At near real-time operations, since decisions have to be sent every 5-10 minutes, the computation time of any proposed dispatch has to observe this tight constraint. In addition, a practical algorithm needs to be robust against many circumstances.

To solve the proposed LAED-S problem, we use a hybrid computation framework consisting of a progressive hedging algorithmic layer and a L-shaped method algorithmic layer. Both algorithms are general decomposition techniques to solve large scale stochastic problem. Progressive hedging is a scenario-based decomposition technique. It has the advantage of uniformly distributing the difficulty over the sub-problems [33]. With innovative techniques proposed by J.P. Waston [106],

the progressive hedging algorithm can speed up total computation by fixing decision variables and thus reducing the problem scale significantly. L-shaped method [107] is a stage-based decomposition technique [33]. It has an advantage of refining the optimality and feasibility during the computation process [107].

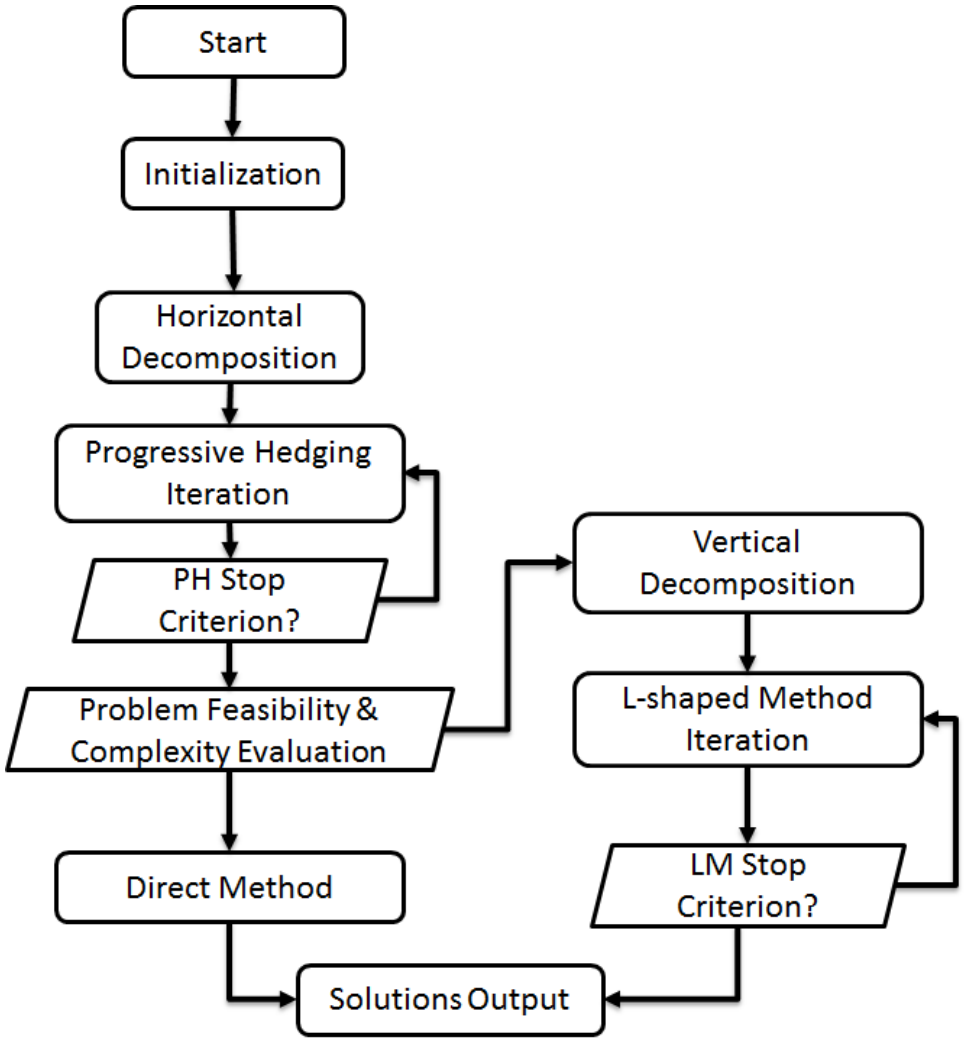

Figure 5.12: The flowchart of the hybrid computation framework

Fig. 5.12 presents the flowchart of the core algorithm to solve a LAED-S problem.

This algorithm is a hybrid computation framework of iterative progressive hedging and L-shaped method steps. It works in the following manner. First, the problem is structured and initialized based on the system and market data feeded in. Second, a horizonal decomposition is conducted to decompose the original stochastic problem by scenarios. Third, Progressive hedging iterations are performed until the progressive hedging stop criterion is met, which indicates either the problem is infeasible or the problem has converged enough. During the progressive hedging process, the original stochastic problem evolves into a much smaller reduced problem by getting rid of significant amount of decision variables and constraints. Fourth, a reduced problem evaluation checks the feasibility and complexity of the reduced problem. If the reduced problem is feasible and small enough, a direct method will be adopted to solve the problem. If the reduced problem is infeasible or still very large, a L-shaped method is employed to solve it. In that case, a vertical decomposition will decompose the reduced problem by stage. L-shaped method then generates feasibility cuts and optimality cuts to find the optimal solution. Finally. the solutions will be feeded to the post-possessing module.

5.5.1 Progressive Hedging Algorithm

Progressive hedging algorithm is able to provide good heuristic to solve a stochastic programming problem based on decomposition by scenarios [106]. By allowing solving the problem by scenario, parallel computing techniques can be used and a optimal solution can be obtained in iterations. The major advantage we utilizes from progressive hedging algorithm is its capability that , within limited iterations, it can provides insightful information to help reduce the stochastic problem size significantly by fixing the decision variables or relaxing constraints. This capability allows our proposed hybrid computation method to speed up the computation effectively.

For the convenience of illustration, the extensive form of the LAED-S model (2)-(11) in Part I [108] can be written using simplified notations as follows:

$$\min : f = c^T x + \sum_{s \in S} P(s) q^T y_s \tag{5.24}$$

subject to

$$Ax \geqslant b, x \geqslant 0, \tag{5.25}$$

$$Tx + Wy_s \geqslant h, y \geqslant 0, \forall s \in S, \tag{5.26}$$

where s is the indicator of each scenario, $P(s)$ is the occurrence probability of scenario s, x is the vector of decision variables for the deterministic portion; y_s is the vector of decision variables for the stochastic portion under scenario s. (5.25) are the constraints only associated with deterministic decision variables x; (5.26) are the constraints associated with stochastic decision variables y_s. A, T, and W are coefficients matrices. c, q, b, and h are parameters vectors.

To solve the problem described in (5.24)-(5.26)via the progressive hedging algorithm, the following steps are taken. First, the initial sub-scenario problem in (5.27)-(5.28) is formulated, where x_s is independently for each scenario. Solving this problem for each scenario, a set of scenario based deterministic optimal solutions are available.

$$\min : f = c^T x_s + q^T y_s \tag{5.27}$$

subject to

$$Ax_s = b, x_s \geqslant 0, \tag{5.28}$$

$$Tx_s + Wy_s = h, y \geqslant 0, \forall s \in S. \tag{5.29}$$

Via (5.30), we can calculate the probabilistic mean of the optimal solutions (for short, mean solution).

$$\bar{x}^k = \sum_{s \in S} P(s) x_s^k. \tag{5.30}$$

A multiplier w_s^k can be calculated based on the distance between the mean solution and the scenario solution,as indicated in (5.31).

$$w_s^k = \rho(x_s^k - \bar{x}^k), \forall s \in S, \tag{5.31}$$

where ρ is a convergence penalty factor. When the initial iteration is completed, a set of optimal solutions are established, which guarantee the optimality of the solution set for each scenario, namely, the total operating cost of the look-ahead operating horizon is minimized under each scenario.

$$g^k = \sum_{s \in S} P(s)(x_s^k - \bar{x}^k). \tag{5.32}$$

Nevertheless, the implementability of this solution may not be guaranteed, if the scenario gap, defined in (5.32), among the optimal solutions exceeds a its predefined threshold ε. This is because we require all the decisions at the same stage over various scenarios agree with each other. The main activity of the progressive hedging algorithm is to converge to the stochastic optimal solution (by iterations) that ensures

both optimality and implementability of the solution. An auxiliary sub-scenario problem (5.33) is solved, for each iteration.

$$\min : f = c^T x_s + q^T y_s + w_s^{k-1} x_s + 0.5\rho \|x_s - \bar{x}^{k-1}\|^2 \tag{5.33}$$

subject to

$$Ax = b, x \geqslant 0, \tag{5.34}$$

$$Tx + Wy_s = h, y \geqslant 0, \forall s \in S. \tag{5.35}$$

In the auxiliary sub-scenario problem (5.33), the scenario decision variables are forced by the multiplier term $w_s^{k-1} x_s$ to change in the direction toward the mean solution. The proximal penalty term $0.5\rho \|x_s - \bar{x}^{k-1}\|^2$ keeps the optimal solution stable within a certain neighbourhood and not deviate too much from the mean solution. This is designed for the sake of convergence stability. The quadratic proximal penalty term can lead to difficulties in practical implementation. Therefore, Watson et. al. proposes to replace this quadratic term with its piece-wise linear approximation [109].

For each iteration, the mean solution are updated by (5.30). Following that, the multiplier w_s is then updated in (5.36) based on the new optimal solutions of all scenarios.

$$w_s^k = \rho(x_s^k - \bar{x}^k) + w_s^{k-1}, \forall s \in S., \tag{5.36}$$

The iteration continues until the scenario gap (5.32) among the optimal solutions of scenarios reaches the predefined threshold ε. In this paper, we do not intend to use the progressive hedging algorithm to converge to the optimal solution, therefore a

large threshold is used to save the iterations and the computation time.

5.5.2 L-shaped method

Extended from Benders' method [110], Slyke and Wets proposed L-shaped method to decompose and solve stochastic programming problem [111]. The L-shaped method is a vertical decomposition approach which decomposes the problem by stages. The advantages of this approach are that it can generate feasibility cuts and optimality cuts to refine the solutions which may be infeasible or sub-optimal.

The L-shaped method is used to make up the disadvantages of the progressive hedging algorithm. After the progressive hedging algorithm completes, we have a stochastic problem with a reduced size.

$$\min : f = c^T x + \sum_{s \in S} P(s) q^T y_s \tag{5.37}$$

subject to

$$Ax \geqslant b, x \geqslant 0, \tag{5.38}$$

$$Tx + Wy_s \geqslant h, y \geqslant 0, \forall s \in S, \tag{5.39}$$

where x is the vector of all remaining deterministic decision variables of the reduced form; y_s is the vector of remaining decision variables for the stochastic portion under scenario s. (5.38) are the remaining constraints only associated with deterministic decision variables x; (5.39) are the remaining constraints associated with stochastic decision variables y_s. A, T, and W are reduced coefficients matrices. c, q, b, and h are corresponding reduced parameter vectors.

Based on the problem setup, we decompose this reduced stochastic problem into a master problem and many sub-problems.

$$\min : f = c^T x + \eta \tag{5.40}$$

subject to

$$Ax \geqslant b, x \geqslant 0, \eta \geqslant 0 \tag{5.41}$$

The master problem is presented as (5.40)-(5.41). Only deterministic decision variables x are considered at this level. All the constraints associated with stochastic decision variables y are relaxed and not considered.

For each scenario s, we have a sub-problem formulated as (5.42)-(5.43):

$$\min : f_s = q^T y_s \tag{5.42}$$

subject to

$$Wy_s \geqslant h - Tx, y \geqslant 0, \forall s \in S, \tag{5.43}$$

Given the determined decision variables x from last iteration, each sub-problem is going to optimize the operating cost for each particular scenario.

For solving each sub-problem, if the solution is optimal, we can then generate an optimality cut as shown in (5.44).

$$\pi_k^T T x + \eta_s \geqslant \pi_k^T h, \eta_s \geqslant 0, \tag{5.44}$$

where π_k^T is the vector of dual variable values at iteration k of the sub-problem (5.42)-(5.43).

If the sub-problem is infeasible, we can then generate a feasibility cut as shown in (5.45).

$$\mu_k^T T x \geqslant \mu_k^T h, \tag{5.45}$$

where μ_k^T is the extreme ray [110] at iteration k for the sub-problem (5.42)-(5.43).

At each iteration, after all the sub-problems are solved. The generated optimality cuts and feasibility cuts are to be introduced to the master problem (5.40)-(5.41) for next iteration.

In the objective function of the master problem, the η term can be represented in terms of η_s as (5.46).

$$\eta = \sum_{s \in S} P(s) q^T \eta_s. \tag{5.46}$$

The upper bound of the reduced stochastic problem can be calculated by (5.47)

$$u^k = c^T x^k + \sum_{s \in S} P(s) f_s^k, \tag{5.47}$$

where x^k is the solution vector of the deterministic decision variables at iteration k; f_s^k is the objective function value of the sub-problem under scenario s at iteration k.

By incorporating the optimality cuts and feasibility cuts into the master problem (5.40)-(5.41), the lower bound of the reduced stochastic problem can be calculated by

$$l^k = c^T x^k + \eta^k, \tag{5.48}$$

where η^k is obtained by the solution of η_s in (5.46) at iteration k.

The termination criterion of this algorithm is given by the gap between the upper bound and the lower bound as in (5.49):

$$u^k - l^k \leqslant \epsilon, \tag{5.49}$$

where ϵ is a pre-defined numerical tolerance.

5.6 Innovative Scale Reduction

In this section, we present our innovative approaches to reducing the LAED-S problem's size: 1) Variable Fixing and 2) Constraints Relaxation. Variable fixing is first proposed by Dr. Waston and Dr. Woodruff[106] that variables can be fixed to speed up the progressive hedging algorithm if they reach a consensus. In this paper, we want elaborate the approach to take advantage of power engineering knowledge and historic system operating data to further improve the effectiveness and safety of variable fixing. Furthermore, we extends our approach to constraints relaxations.

First of all, we would like to check whether it is appropriate to conduct variable fixing and constraints relaxation for power system dispatch. Based on historic data from ERCOT system, we conduct numerical experiments of unit commitment and look-ahead dispatch. The duration curve of decision variables and constraints are presented. In Fig. 5.13, duration curves that decision variables have the same values

for the entire year and for the entire month are depicted. Here, the horizontal axis represents about hundreds of generators' dispatch decisions. The vertical axis represents the percentage of the moments during the whole year (or month) when the particular generator's dispatch decision stays at the same level. Based on our statistical studies, about 86% of the generators are dispatched at a stable level (the dispatch levels stays unchanged for more than 80% of the moments). Only about 14 of the generators frequently change their dispatch levels. This phenomenon suggests if the operational uncertainty is not extremely large, most of the generators' dispatch decisions will remain the same as the decisions under a deterministic programming algorithm.

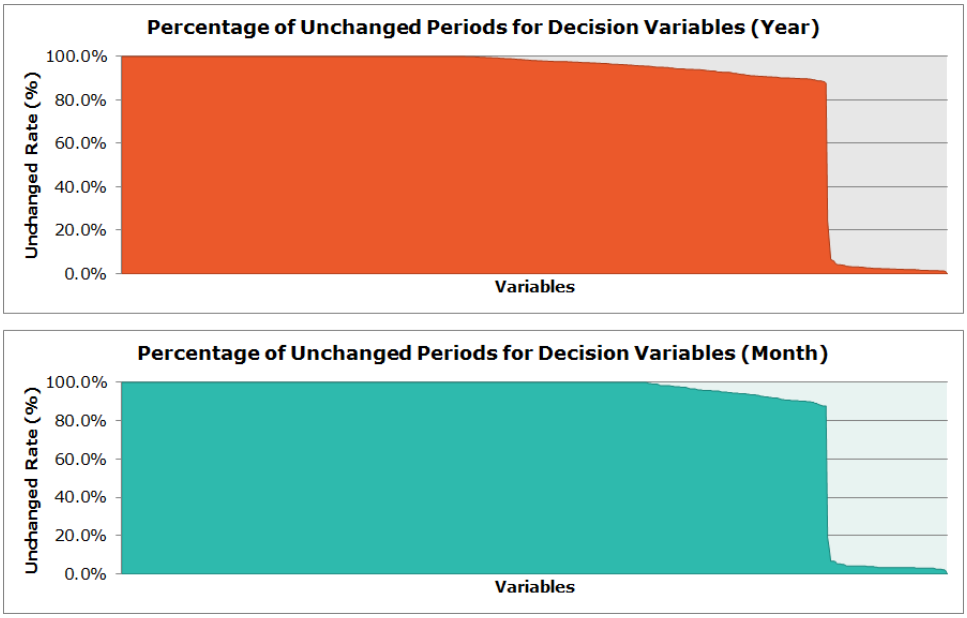

Figure 5.13: Decision variables statistics in a yearly and monthly window

Similarly, we present the duration curves for constraints (un)binding situations in Fig. 5.14, which describes the percentage of the moments when each constraint

is not binding. According to our statistical studies, about 87% of the constraints are not binding over 95% of the moments during the year. Only a small portion of the constraints (13%) are frequently binding. Besides equality constraints (e.g., load balancing equations), these binding constraints include transmission capacity constraints of critical congestion branches, ramping constraints of slow units, STDC requirement constraints and so on. This phenomenon suggests that if the operational uncertainty is not extremely large, most of the unbinding constraints will remain unbinding even given the operational uncertainty.

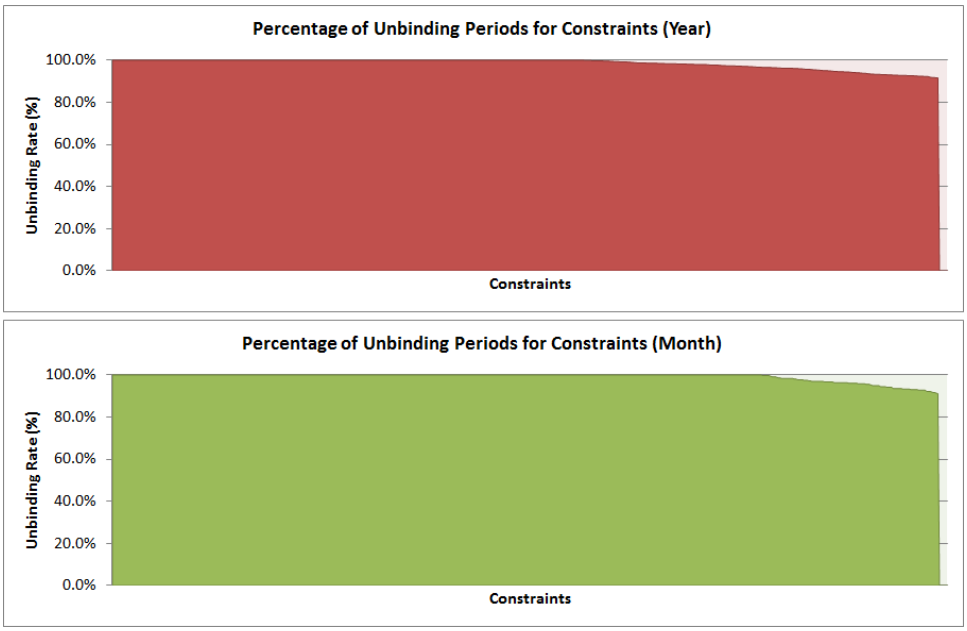

Figure 5.14: Constraints statistics in a yearly and monthly window

For a more scientific way to conduct variable fixing and constraints relaxation, we formulate the optimal size reduction problem (5.50)-(5.54).

$$\min_{x_i, y_j} : f_{CT} = \sum_{i \in I_V} x_i T_{vi} + \sum_{j \in J_C} y_j T_{cj} \tag{5.50}$$

Subject to

$$1 - \prod_{i \in I_V} P_{vi}^{x_i} \leqslant \epsilon_v, \tag{5.51}$$

$$1 - \prod_{j \in J_C} P_{cj}^{y_j} \leqslant \epsilon_c, \tag{5.52}$$

$$x_i \in \{0, 1\}, \tag{5.53}$$

$$y_j \in \{0, 1\}, \tag{5.54}$$

where the objective function (5.50) is to minimize the computation time for next iteration; decision variables x_i and y_i are indicators for variable fixing and constraints relaxation, respectively; if a value of 1 is assigned to x_i and y_i, it indicates to keep the variable (or constraint) otherwise, it indicates to fix or remove the variable (or constraint); probability constraints (5.51) and (5.52) are designed to make sure the probability of inappropriate variable fixing and constraints relaxation is low; (5.53) and (5.54) are the self constraints of decision variables.

In order to implement this formulation (5.50)-(5.54) and enable its efficient computation, we apply the following adjustment to the model.

The probability constraints (5.51) and (5.52) are exponential and nonlinear, which is difficult to be implemented in a real-time application such as economic dispatch. We move the constants to the right hand side and take the log function on both sides, thus yield (5.55) and (5.56) which are linear constraints.

$$\sum_{i \in I_V} x_i \lg P_{vi} \leqslant \lg(1 - \epsilon_v), \tag{5.55}$$

$$\sum_{j \in J_C} y_j \lg P_{cj} \leqslant \lg(1 - \epsilon_c), \tag{5.56}$$

For further improve the computation efficiency, self-integer constraints (5.53) and (5.54) can be relaxed as linear constraints as (5.57) and (5.58). As a robust strategy, for x_i and y_j, any values between 1 and 0 will be treated as 1 and thus be kept in the formulation.

$$0 \leqslant x_i \leqslant 1, \tag{5.57}$$

$$0 \leqslant y_j \leqslant 1, \tag{5.58}$$

For the model (5.50)-(5.54) working appropriately, assessment to the probability of variable fixing P_{vi} and constraints relaxation P_{cj} are very important.

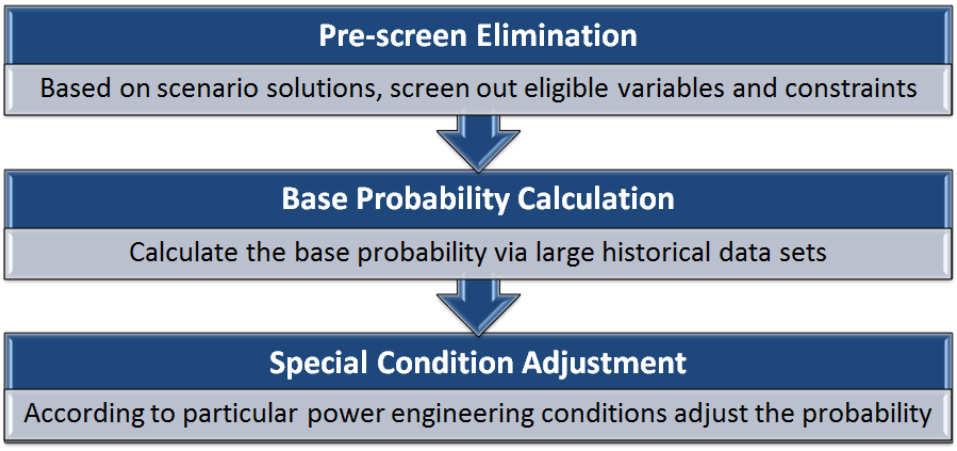

Figure 5.15: Probability assessment for variable fixing and constraints relaxation

We use a 3-layer probability assessment approach to determine the the probability of variable fixing P_{vi} and constraints relaxation P_{cj}. The 3-layer probability assessment approach is presented in Fig. 5.15. The first layer "Pre-screen Elimination" screens out all the decision variables and constraints which are eligible to be considered for fixing or relaxation. In this study, our pre-screen elimination criteria is in order to be eligible, the variables should have the same solution in all of the scenarios and the constraints should not be binding at any scenario. For a different application, this criteria can be relaxed as the variables should have the same solution in most of the scenarios (e.g., 97.5%) and the criteria can be binding under a very small number of scenarios (e.g., 2.5%).

For those eligible variables and constraints being selected, the second layer "Base Probability Calculation" is applied. Via off-line computation via large historical data sets, a estimation of the base probability can be obtained through (5.59) and (5.60).

$$Pb_{base}(i) = \alpha^{v}_{30} Pb^{v}_{30}(i,t) + \alpha^{v}_{365} Pb^{v}_{365}(i), \tag{5.59}$$

$$Pb_{base}(j) = \alpha^{c}_{30} Pb^{c}_{30}(j,t) + \alpha^{c}_{365} Pb^{c}_{365}(j), \tag{5.60}$$

where $Pb_{base}(i)$ and $Pb_{base}(j)$ are base probability for variable fixing and constraints relaxation; α^{v}_{30} and α^{v}_{365} are adjustment weighting factors for variable fixing for a period of past 30 days and past 365 days; Sanitarily,α^{c}_{30} and α^{c}_{365} are adjustment weighting factors for constraints relaxation for a period of past 30 days and past 365 days; $Pb^{v}_{30}(i,t)$ and $Pb^{v}_{365}(i)$ are the estimation of the probability for variable fixing for a period of past 30 days and past 365 days; $Pb^{c}_{30}(j,t)$ and $Pb^{c}_{365}(j)$ are the estimation of the probability for constraints relaxation for a period of past 30 days and past 365 days;

For determining the base probability, our approach considers a combinational inputs of near-history with relevant moments(similar hours in the past 30 days) and of long-history with all moments (a past 365 days' window) historic data. For example, when deciding the base probability for a variable fixing, we consider the moments +/- one hour to the target operating interval in the past 30 days for assessing $Pb^v_{30}(i,t)$ and consider all the moments in the past 365 days for assessing $Pb^v_{365}(i)$. The same way works for the probability assessment of constraints relaxation.

$$Pb^v_{30}(i,t) = \frac{N_{stable}(i,t)\Delta T}{5400}, \tag{5.61}$$

$$Pb^v_{365}(i) = \frac{N_{stable}(i)\Delta T}{525600}, \tag{5.62}$$

The probability for variable fixing for past 30 days and for past 365 days can be estimated through (5.61) and (5.62). N_{stable} is the number of the moments when the decision variable i stays at the same level for past 4 hours, and ΔT is the time duration for each dispatch interval.

$$Pb^c_{30}(j,t) = 1 - \frac{N_{binding}(j,t)\Delta T}{5400}, \tag{5.63}$$

$$Pb^c_{365}(j) = 1 - \frac{N_{binding}(j)\Delta T}{525600}, \tag{5.64}$$

The probability for constraint relaxation for past 30 days and for past 365 days can be estimated through (5.63) and (5.64). $N_{binding}$ is the number of the moments when the constraint j is binding.

After the base probability determined, the third layer "Special Condition Adjustment" applies to some special variables and constraints. This layer allows system operators using power engineering knowledge and operational experiences to further

refine the probability for variable fixing and constraints relaxation. For instance, branch capacity constraints can be handled through (5.65).

$$Pb_{adj} = 2[\frac{\sigma_F(j,t)}{\min(slack_{j-}, slack_{j+})}]^{\gamma} - 1, \gamma \in Z^{+}, \tag{5.65}$$

where Pb_{adj} is the probability adjustment term to the base probability; $\sigma_F(j,t)$ is the standard deviation of the branch flows under all scenarios; γ is the adjustment coefficient; $slack_{j-}$ and $slack_{j+}$ are the slack variables of the branch capacity constraint in negative and positive flow directions, respectively. Formula (5.65) considers the additional impact from the branch flow deviation and the slackness of the branch capacity constraint. The higher the slackness, the higher the probability that the constraint can be removed securely.

As a another instance, the variable fixing adjustment probability can be calculated by differentiating the types of its binding situation. If the the current dispatch point is set at the upper or lower capacity bounds, a positive probability adjustment term can be applied. If the current dispatch point is set by constraints such as ramping constraints or branch capacity constraints, perhaps a negative probability adjustment applies. This is because ramping and branch congestion situations change more easily and frequently while the capacity limits are very much a fixed type of constraints. The dispatch point set by capacity constraints is much more stable and less likely to change under different scenarios.

Finally, the probability of variable fixing P_{vi} or constraints relaxation P_{cj} and can be obtained by the summation of the base probability Pb_{base} and the adjustment term Pb_{adj}.

5.7 Numerical Examples with Stochastic Look-ahead Dispatch

We conduct numerical experiments to justify our proposed LAED-S. The numerical experiments are conducted on a realistic regional transmission network in southwest of United States. The economic dispatch interval is 15 minutes. Load and wind profiles during an entire year are obtained from regional system operator (RTO) for the particular system.

Table 5.7: Computation Environment for Numerical Experiments

Operating System	Windows 7 64-bit
Software Environment	Matlab 7.12 (R2011a)
Solver	CPLEX v12.5
CPU	Intel Core i7 X990 3.47GHz
Memory	18 GB

The numerical experiments are conducted in a computation environment as indicated in TABLE 5.7.

We apply our proposed analytical criteria, which is described in Section V.A of Part I[108], to determine for each interval whether it is necessary to conduct LAED-S. The economic risks are calculated based on the uncertainty levels of load and wind for 10 consecutive days in July, as presented in Fig. 5.17. According to the load patterns and wind generation patterns over the same periods, we find that the economic risk indices goes high during peak load and peak wind periods, especially for those moments when net load is volatile.

We conduct statistical analysis for the results of economic risks. As shown in Fig. 5.17, the four pie charts present the percentage of the dispatch intervals when stochastic look-ahead is needed. During the early morning (before 6 AM) and late

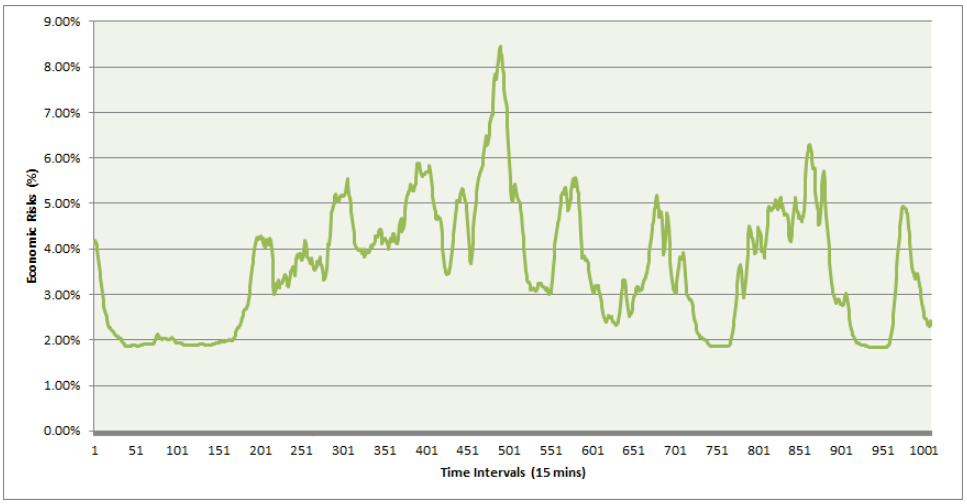

Figure 5.16: Economic risks for ten consecutive days in July

night (after 6 PM), about 20% to 30% of the dispatch intervals require LAED-S for the given 10 days. This is mainly because the active wind generation and frequent ramping events associating with high operational uncertainty. Although the dispatch interval during the day (6 AM to 6 PM) requires much less stochastic programming (less than 10%), the uncertainty of peak load forecasting errors plus wind generations still need to be well managed, namely, by stochastic approach.

Table 5.8: Average Economic Performance for Stochastic Intervals (per Interval)

	EX-Post Cost ($)	Saving (%)
Deterministic Static Dispatch	$207,698.11	-
Deterministic Look-ahead Dispatch	$201,745.01	2.9%
Stochastic Look-ahead Dispatch	$197,500.98	4.9%

For the dispatch intervals which is determined to apply stochastic programming, we present the corresponding economic performance over different dispatch approaches in TABLE 5.8. The results shown in column two "EX-Post Cost ($)" are the

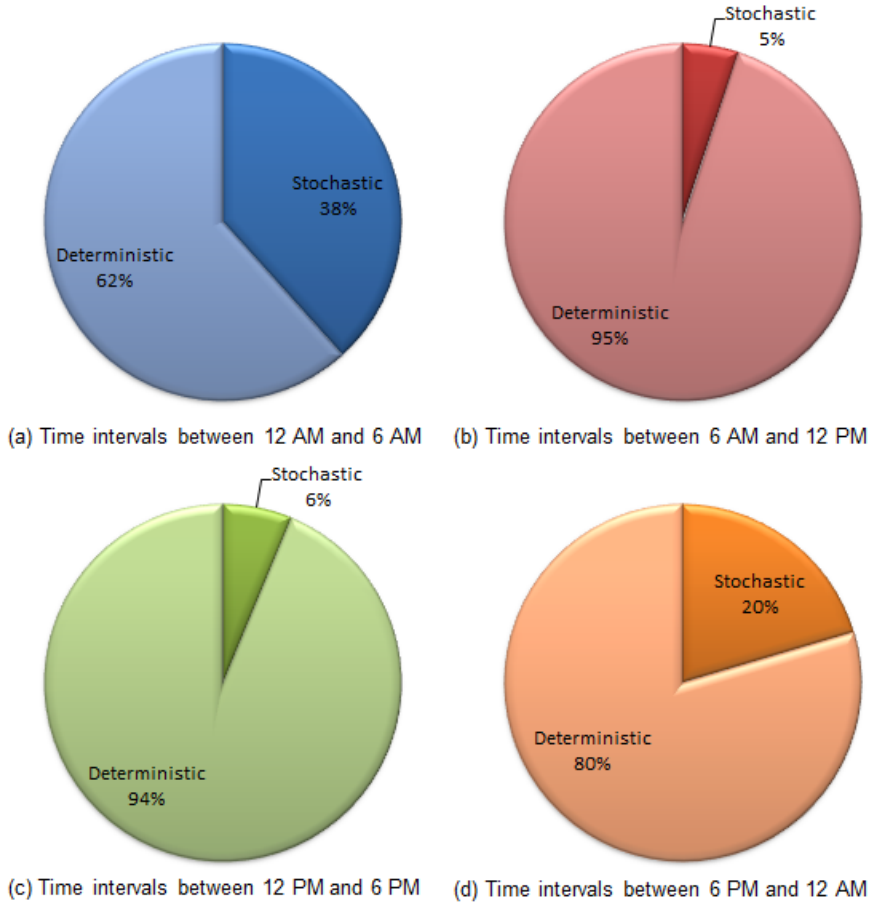

Figure 5.17: Percentages of time intervals when stochastic look-ahead dispatch is needed.

average post-realization costs which includes both the system operating costs and recourse costs. The column three "Saving (%)" provides the percentage-wise cost savings given the benchmark of the deterministic static dispatch (ED-Static). These dispatch intervals covered in TABLE 5.8 are typically associated with high economic risks according to our analytical criteria in Part I of this paper [108]. As we can see, the deterministic look-ahead dispatch (LAED-D) can save about 2.9% from ED-Static while LAED-S can save up to 4.9%.

The results presented in TABLE 5.8 are only for those intervals with high eco-

Table 5.9: Daily Average Economic Performance (post Realization) for Different Types of Dispatch

	EX-Post Cost ($)	Saving (%)
Deterministic Static Dispatch	17,751,015.40	-
Deterministic Look-ahead Dispatch	17,525,386.73	1.27%
Stochastic Look-ahead Dispatch	17,444,422.69	1.73%

Table 5.10: Problem Sizes for Different Types of Dispatch

Look-ahead Horizon	45 mins	90 mins	180 mins
LAED-D	5028 × 25707	10056 × 51414	20169 × 102828
LAED-S (Extensive approach)	36454 × 188468	72908 × 376936	177299 × 753872
LAED-S (Our approach)	3776 × 11472	6504 × 26376	8568 × 44776
% of Original Problem Size (Row 3)	0.63%	0.62%	0.28%

nomic risks. In order to compare the overall economic performance, we conduct a whole month (July) numerical simulations and compare daily average post-realization costs over different dispatch approaches. The simulation results are presented in TABLE 5.9. We compare LAED-S with ED-Static and LAED-D. As we can see, LAED-D is about 1.27% more cost-efficient than ED-Static. LAED-S can further improve the cost-savings to about 1.73%. However, the economic improvement is marginal (no more than 0.5% compared with a deterministic look-ahead disaptch). Given the tremendous computation efforts, we believe it is not reasonable to conduct LAED-S for every interval.

Fig. 5.18 shows the average cost savings (per interval) of LAED-D and LAED-S when the net load uncertainty increases, where ED-Static is the benchmark. As the net load uncertainty increases, both LAED-D and LAED-S have increased economic benefits comparing with ED-Static. LAED-S exhibits an advantages in more cost savings than LAED-D especially under high net load uncertainty level. This sug-

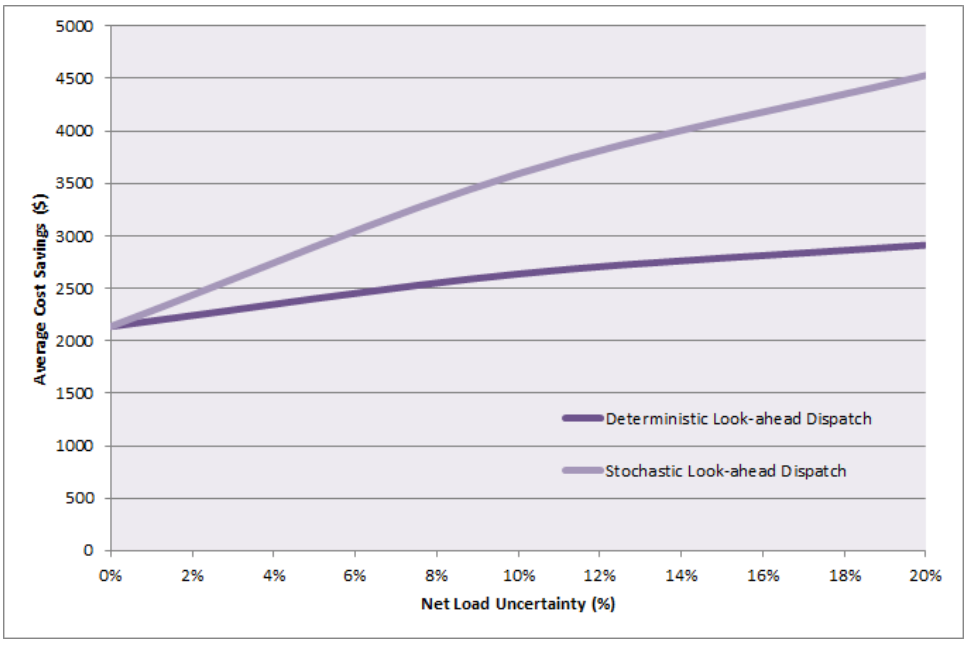

Figure 5.18: Cost savings as the net load uncertainty increases: deterministic approach versus stochastic approach

gests LAED-S is more desired under the scenarios with which high uncertainties are associated.

We also measure the computation time by using different algorithms. The computation time results are presented in Fig. 5.19, where it compares the computation time of LAED-D, LAED-S using extensive approach and LAED-S using the proposed approach. We test the computation on different scales of problems varying from one-step look-ahead horizon up to twelve-step look-ahead horizon. For LAED-S, screening out by scenario generation/reduction process, 100 representative scenarios are considered in the optimization process. As we can observe, the deterministic look-ahead algorithm is still most efficient among the three approaches. Our proposed approach can reduce the computation time by up to 88% comparing with a extensive approach while solving LAED-S. This example reflects the improvement

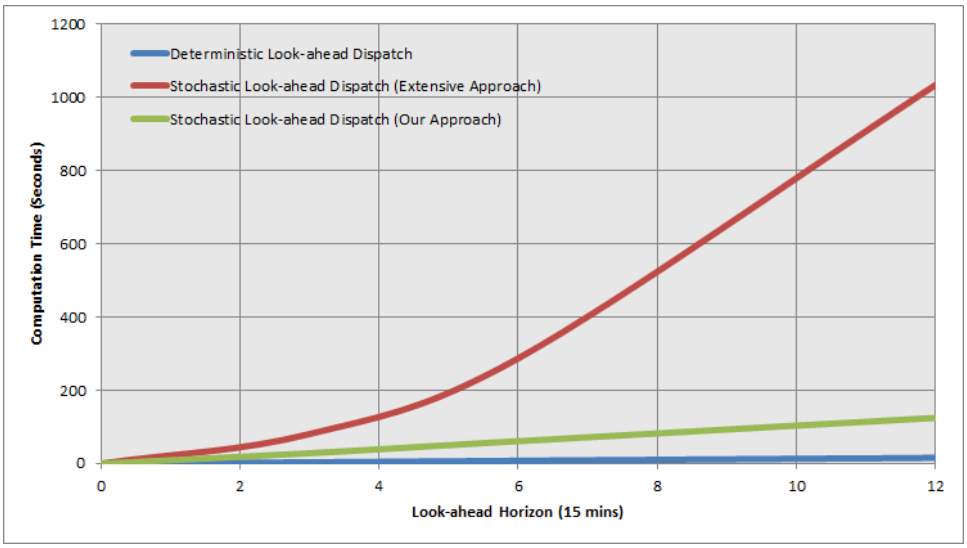

Figure 5.19: Computation time for different economic approaches

in computation efficiency by using our proposed approach but we also acknowledge there is still much work to do to make LAED-S to be as efficient as a LAED-D.

In TABLE 5.10, we compare the problems size of different look-ahead dispatch models (LAED-D, LAED-S with Extensive form and LAED-S with reduced form using our approach. Different look-ahead horizon are considered, including 45 mins, 90 mins and 180 mins. As we can see, our problem size reduction approach can reduce a stochastic problem size by up to 99.72%. With a increase in problem size of the original problem, the scale of problem reduction can be even more effective.

5.8 Summary

In this chapter, we explore the applicability of LAED-S to power system near-real-time operation. We present the LAED-S model and the analytical criterion to determine whether LAED-S is necessary for the target operating interval. A innovative hybrid computation framework is proposed, based on progressive hedging algorithm and L-shaped method, which is able to solve LAED-S more efficiently.

We conduct numerical experiments of a practical 5889 bus system to justify the effectiveness of our approaches.

According to our simulation results, we justify that it is not necessary to apply LAED-S to every dispatch interval because the potential benefits is only 0.5%. However, for dispatch intervals with higher economic risks, the stochastic approach is more cost-effective than a deterministic approach. It is reasonable to screen out these risky intervals and perform stochastic decision-making. Our proposed hybrid computing architecture is proved to be more efficient. However, compared with a deterministic approach, the computation speed for stochastic approach is still low. Therefore, LAED-S may not be able to fit into the existing real-time market setup. It requires more efforts to develop more advanced algorithm for LAED-S and establish innovative market structure to adopt stochastic programming into power system near-real-time operations.

6. CONCLUSIONS AND DIRECTIONS FOR FUTURE RESEARCH

In this chapter, we conclude the dissertation by 1) summarizing our research; and 2) discussing several directions for future research.

6.1 Dissertation Summary

In this dissertation, we recognize the fundamental need for more advanced dispatch algorithms with enhanced capability to manage the security risks and operational uncertainties due to the high penetration of variable resources (e.g., wind and solar) in electric power systems. Extended from the previous work in look-ahead economic dispatch, we propose the security enhanced look-ahead dispatch framework. By introducing the STDC and the contingency constraints, the proposed framework can consider circumstances under both normal operational conditions and contingency conditions. In the security enhanced look-ahead dispatch framework, early detection and optimal corrective measures are implemented. The two functions compose the look-ahead security management (LSM) that can assist system operators to identify and quantify violations of the security constraints and work out an optimal recovery plan at a minimized recovery cost. The proposed enumeration tree approach can help to identify all of the potential factors that can cause system insecurity. The simulation is conducted on a modified IEEE RTS 24 bus system and a practical 5889 bus system. The numerical performance suggests that the security enhanced look-ahead dispatch is implementable in practical systems and has very attractive economic and operational value for power system security.

To support look-ahead dispatch, we also introduce the spatio-temporal wind forecast models. Spatio-temporal wind forecast models (TDD and TDDGW models) are critically evaluated. It shows that by incorporating spatial correlations of neighboring

wind farms, the forecast quality in the near-term (hours-ahead) could be improved. The TDD and TDDGW models are incorporated into a robust look-ahead economic dispatch and a day-ahead reliability unit commitment. Compared with conventional temporal-only statistical wind forecast models, such as the PSS models, the spatio-temporal models consider both the local and geographical wind correlations. By leveraging both temporal and spatial wind historical data, more accurate wind forecasts can be obtained. The potential economic benefits of advanced wind forecast are illustrated using a modified IEEE RTS 24 bus system. It is shown that the spatio-temporal model can increase wind resources utilization, and reduce system operation costs against uncertainty.

In addition, this research explores the applicability of stochastic look-ahead dispatch to power system near-real-time operation. We present the stochastic look-ahead dispatch model and a analytical criterion to determine whether stochastic look-ahead dispatch is necessary for the target operating interval. A hybrid computation framework is proposed, based on the progressive hedging algorithm and L-shaped method, which can solve stochastic look-ahead dispatch more efficiently. We conduct numerical experiments of a practical 5889 bus system to justify the effectiveness of our approaches. According to our simulation results, we justify that it is not necessary to apply stochastic look-ahead dispatch to every dispatch interval since the potential benefit is only 0.5%. However, for dispatch intervals with higher economic risks, the stochastic approach is more cost effective than a deterministic approach. It is reasonable to locate these risky intervals and perform stochastic decision-making. The proposed hybrid computing architecture is shown to be more efficient, but it is still not as fast as a deterministic approach. Therefore, more efforts are required to develop better algorithms for stochastic look-ahead dispatch and establish innovative market structure to adopt stochastic programming into power

system near-real-time operations.

6.2 Future Research

Before it is possible to fully implement advanced look-ahead scheduling algorithms in power system operations, additional research is needed. The following sections outline the future research required for this look-ahead scheduling to be deployed in practical applications.

6.2.1 Trade-offs between Security Enhancement and Computation Burden

In this dissertation, we propose enhanced look-ahead economic dispatch framework with look-ahead security management. The security management consists of early detection and optimal corrective measures. Although the proposed look-ahead security management can detect the potential system risks and provide suggestions of corrective measures, extra computation complexity is introduced into the scheduling models. In examining the potential factors causing system insecurity, the larger the examining domain, the more computation efforts are needed. Therefore, future research should investigate the trade-offs between the security enhancement and computation burden. Designing such trade-off mechanism for look-ahead security management enables an efficient algorithm with the capability of taking necessary actions in a timely fashion.

6.2.2 Security Management under Forecast or Contingency Uncertainties

For power system security management, forecast and contingency uncertainties have substantial impacts on the corrective measures to be adopted. The proposed early detection and optimal corrective measures are still deterministic decision-making. The decision process does not consider the probabilistic outcomes under different scenarios. However, many system circumstances are associated with uncer-

tainties. For example, the uncertainty of a unit outage or the uncertainty of wind generation ramping down may cause security violations of transmission lines and energy balancing. We wish to apply some sophisticated decision-making such as stochastic optimization or robust optimization to look-ahead security management. Adopting such decision-making enables the early detection and optimal corrective measures robust against various system uncertainties.

6.2.3 Theoretical Study in Pricing under Stochastic Near-real-time Market

The stochastic look-ahead dispatch approach has so far justified the economic benefits from the system point of view. In order to implement this stochastic scheduling for power system near-real-time operation, it is important to conduct rigorous theoretical study in electricity market pricing under this new dispatch approach. Using the existing pricing model, transactions in the market may result in low efficiency, price deviation and unfairness among the participants due to some assumed system scenario which may never happen or due to some predictions of the future steps which are subject to change. Therefore, the theoretical study in pricing is highly needed. Such study can help to establish a common protocol for all the market participants and improve the efficiency and fairness for power system near-real-time market.

6.2.4 Probability Methods based Power System Infrastructure Planning

Following the research efforts in power system scheduling, another important area for future research is the applications of probability methods in power system infrastructure planning. Foreseeing extensive development of renewable energy projects globally, significant investment will be required in upgrading electric energy infrastructure to integrate and support these renewable projects. Compared with power system operation, there is much higher uncertainty associated with power system

planning activities such as renewable integration, transmission planning, as well as the deployment of flexible power electronics systems. Owing to the computation complexity of stochastic approaches, most current planning activities are deterministic. This leads to inefficient decisions and unnecessary risks. With cutting-edge programming algorithms (e.g., progressive hedging, column generation), Our future research seeks to design stochastic planning tools that co-optimize the three key factors: (i) investment costs, (ii) system efficiency and (iii) system reliability. Stochastic solutions to those planning problems can effectively improve the cost-effectiveness in managing the risks of large power system planning projects.

REFERENCES

[1] "National renewable energy action plans," tech. rep., European Commission, 2010.

[2] "20% wind energy by 2030 increasing wind energy's contribution to U.S. electricity supply," tech. rep., U.S. Department of Energy, July 2008.

[3] Renewable Energy Policy Network for the 21st Century, *Renewables 2012 Global Status Report*. 2013.

[4] J. E. Price and M. Rothleder, "Recognition of extended dispatch horizons in California's energy markets," in *Power and Energy Society General Meeting, IEEE*, pp. 1–5, 2011.

[5] J. Tong and H. Ni, "Look-ahead multi-time frame generator control and dispatch method in PJM real time operations," in *Power and Energy Society General Meeting, IEEE*, pp. 1–1, 2011.

[6] L. Xie, P. M. S. Carvalho, L. A. F. M. Ferreira, J. Liu, B. H. Krogh, N. Popli, and M. D. Ilić, "Wind integration in power systems: Operational challenges and possible solutions," *Proceedings of the IEEE*, vol. 99, no. 1, pp. 214–232, 2011.

[7] D. W. Ross and K. Sungkook, "Dynamic economic dispatch of generation," *Power Apparatus and Systems, IEEE Transactions on*, vol. PAS-99, no. 6, pp. 2060–2068, 1980.

[8] J. Carpentier, "A link between short term scheduling and dispatching: Separability of dynamic dispatch," in *8th Power System Computation Conference*, (Helsinki), 1984.

[9] R. Raithel, S. Virmani, S. Kim, and D. Ross, "Improved allocation of generation through dynamic economic dispatch," in *Proceedings of the 7th Power Systems Computation Conference*, (Lausanne, Switzerland), 1981.

[10] L. Xie and M. D. Ilić, "Model predictive economic/environmental dispatch of power systems with intermittent resources," in *Power and Energy Society General Meeting, IEEE*, pp. 1–6, 2009.

[11] L. Xie, J.-Y. Joo, and M. D. Ilić, "Integration of intermittent resources with price-responsive loads," in *North American Power Symposium*, pp. 1–6, 2009.

[12] M. D. Ilić, L. Xie, and J. Jhi-Young, "Efficient coordination of wind power and price-responsive demand Part I: Theoretical foundations," *Power Systems, IEEE Transactions on*, vol. 26, no. 4, pp. 1875–1884, 2011.

[13] M. D. Ilić, L. Xie, and J. Jhi-Young, "Efficient coordination of wind power and price-responsive demand Part II: Case studies," *Power Systems, IEEE Transactions on*, vol. 26, no. 4, pp. 1885–1893, 2011.

[14] L. Ma, S. Luan, C. Jiang, H. Liu, and Y. Zhang, "A review on the forecasting of wind speed and generated power," *Renewable and Sustainable Energy Reviews*, vol. 13, no. 4, pp. 915 – 920, 2009.

[15] L. Landberg, "Short-term prediction of the power production from wind farms," *Journal of Wind Engineering and Industrial Aerodynamics*, vol. 80, no. 1C2, pp. 207 – 220, 1999.

[16] M. Negnevitsky, P. Johnson, and S. Santoso, "Short term wind power forecasting using hybrid intelligent systems," in *Power and Energy Society General Meeting, IEEE*, pp. 1–4, June 2007.

[17] G. Giebel, R. Brownsword, G. Kariniotakis, M. Denhard, and C. Draxl, "The state-of-the-art in short-term prediction of wind power : A literature overview, 2nd edition," *ANEMOS.plus*, p. 109, 2011.

[18] G. Kariniotakis, P. Pinson, N. Siebert, G. Giebel, and R. Barthelmie, "The-state-of-the-art in short-term prediction of wind power - from an offshore perspective," in *Symposium ADEME, IFREMER*, 2004.

[19] C. Monteiro, H. Keko, R. Bessa, V. Miranda, A. Botterud, J. Wang, G. Conzelmann, *et al.*, "A quick guide to wind power forecating: state-of-the-art 2009.," tech. rep., Argonne National Laboratory (ANL), 2009.

[20] X. Zhu and M. G. Genton, "Short-term wind speed forecasting for power system operations," *International Statistical Review*, vol. 80, pp. 2–23, 2012.

[21] M. G. Genton and A. S. Hering, "Blowing in the wind," *Significance*, vol. 4, pp. 11–14, 2007.

[22] T. Gneiting, K. Larson, K. Westrick, M. G. Genton, and E. Aldrich, "Calibrated probabilistic forecasting at the stateline wind energy center," *Journal of the American Statistical Association*, vol. 101, no. 475, pp. 968–979, 2006.

[23] A. S. Hering and M. G. Genton, "Powering up with space-time wind forecasting," *Journal of the American Statistical Association*, vol. 105, no. 489, pp. 92–104, 2010.

[24] J. Tastu, P. Pinson, E. Kotwa, H. Nielsen, and H. Madsen, "Spatio-temporal analysis and modeling of wind power forecast errors," *International Statistical Review*, vol. 14, pp. 43–60, 2011.

[25] P. Pinson and H. Madsen, "Adaptive modeling and forecasting of wind power fluctuations with markov-switching autoregressive models," *Journal of Fore-*

casting, vol. 31, pp. 281–313, 2012.

[26] J. Wang, M. Shahidehpour, and Z. Li, "Security-constrained unit commitment with volatile wind power generation," *Power Systems, IEEE Transactions on*, vol. 23, pp. 1319–1327, Aug 2008.

[27] P. Meibom, R. Barth, B. Hasche, H. Brand, C. Weber, and M. O'Malley, "Stochastic optimization model to study the operational impacts of high wind penetrations in ireland," *Power Systems, IEEE Transactions on*, vol. 26, pp. 1367–1379, Aug 2011.

[28] P. Ruiz, C. Philbrick, E. Zak, K. Cheung, and P. Sauer, "Uncertainty management in the unit commitment problem," *Power Systems, IEEE Transactions on*, vol. 24, pp. 642–651, May 2009.

[29] A. Papavasiliou, S. Oren, and R. O'Neill, "Reserve requirements for wind power integration: A scenario-based stochastic programming framework," *Power Systems, IEEE Transactions on*, vol. 26, pp. 2197–2206, Nov 2011.

[30] F. Wang and K. Hedman, "Reserve zone determination based on statistical clustering methods," in *North American Power Symposium (NAPS)*, pp. 1–6, Sept 2012.

[31] D. Bertsimas, E. Litvinov, X. Sun, J. Zhao, and T. Zheng, "Adaptive robust optimization for the security constrained unit commitment problem," *Power Systems, IEEE Transactions on*, vol. 28, pp. 52–63, Feb 2013.

[32] Q. Wang, Y. Guan, and J. Wang, "A chance-constrained two-stage stochastic program for unit commitment with uncertain wind power output," *Power Systems, IEEE Transactions on*, vol. 27, pp. 206–215, Feb 2012.

[33] S. Ryan, R.-B. Wets, D. Woodruff, C. Silva-Monroy, and J.-P. Watson, "Toward scalable, parallel progressive hedging for stochastic unit commitment," in *Power and Energy Society General Meeting, IEEE*, pp. 1–5, July 2013.

[34] R. Jiang, J. Wang, M. Zhang, and Y. Guan, "Two-stage minimax regret robust unit commitment," *Power Systems, IEEE Transactions on*, vol. 28, pp. 2271–2282, Aug 2013.

[35] P. Luh, Y. Yu, B. Zhang, E. Litvinov, T. Zheng, F. Zhao, J. Zhao, and C. Wang, "Grid integration of intermittent wind generation: A markovian approach," *Smart Grid, IEEE Transactions on*, vol. 5, pp. 732–741, March 2014.

[36] B. H. Chowdhury and S. Rahman, "A review of recent advances in economic dispatch," *Power Systems, IEEE Transactions on*, vol. 5, no. 4, pp. 1248–1259, 1990.

[37] X. S. Han, H. B. Gooi, and D. S. Kirschen, "Dynamic economic dispatch: feasible and optimal solutions," *Power Systems, IEEE Transactions on*, vol. 16, no. 1, pp. 22–28, 2001.

[38] L. Xie and M. D. Ilić, "Model predictive dispatch in electric energy systems with intermittent resources," in *IEEE International Conference on Systems, Man and Cybernetics.*, pp. 42–47, 2008.

[39] L. Xie, X. Luo, and O. Obadina, "Look-ahead dispatch in ERCOT: Case study," in *Power and Energy Society General Meeting, IEEE*, pp. 1–3, 2011.

[40] H. B. Gooi, D. P. Mendes, K. R. W. Bell, and D. S. Kirschen, "Optimal scheduling of spinning reserve," *Power Systems, IEEE Transactions on*, vol. 14, no. 4, pp. 1485–1492, 1999.

[41] R. Ah King, H. Rughooputh, and K. Deb, "Evolutionary multi-objective environmental/economic dispatch: Stochastic versus deterministic approaches evolutionary multi-criterion optimization," vol. 3410 of *Lecture Notes in Computer Science*, pp. 677–691, Springer Berlin / Heidelberg, 2005.

[42] F. Bouffard and F. D. Galiana, "Stochastic security for operations planning with significant wind power generation," *Power Systems, IEEE Transactions on*, vol. 23, no. 2, pp. 306–316, 2008.

[43] ERCOT Overview, "ERCOT 2009 Annual Report."

[44] Y. Gu and L. Xie, "Look-ahead coordination of wind energy and electric vehicles: A market-based approach," in *North American Power Symposium*, (The University of Texas at Arlington), 2010.

[45] R. Bohn, M. Caramanis, and F. Schweppe, "Optimal pricing in electrical networks over space and time," *The Rand Journal of Economics*, vol. 15, no. 3, pp. 360–376, 1984.

[46] Y. Gu and L. Xie, "Look-ahead dispatch with forecast uncertainty and infeasibility management," in *Power and Energy Society General Meeting, IEEE*, (San Diego), 2012.

[47] P. Kundur, J. Paserba, V. Ajjarapu, G. Andersson, A. Bose, C. Canizares, N. Hatziargyriou, D. Hill, A. Stankovic, C. Taylor, T. Van Cutsem, and V. Vittal, "Definition and classification of power system stability IEEE/CIGRE joint task force on stability terms and definitions," *Power Systems, IEEE Transactions on*, vol. 19, no. 3, pp. 1387–1401, 2004.

[48] X. Luo and O. Obadina, "Security assessment and enhancement in real-time operations of ERCOT nodal electricity market," in *Power and Energy Society*

General Meeting, IEEE, pp. 1–7, 2010.

[49] T. Konrad, "Drawing the right lessons from the Texas wind emergency," in *http://www.altenergystocks.com*, 2009.

[50] E. Ela and B. Kirby, "ERCOT event on February 26, 2008: Lessons learned," Tech. Rep. NREL/TP-500-43373, National Renewable Energy Laboratory, July.2008.

[51] A. L. Motto, F. D. Galiana, A. J. Conejo, and J. M. Arroyo, "Network-constrained multiperiod auction for a pool-based electricity market," *Power Systems, IEEE Transactions on*, vol. 17, no. 3, pp. 646–653, 2002.

[52] T. E. D. Liacco, "The adaptive reliability control system," *Power Apparatus and Systems, IEEE Transactions on*, vol. PAS-86, no. 5, pp. 517–531, 1967.

[53] C. E. Garcia and A. Morshedi, "Quadratic programming solution of dynamic matrix control (QDMC)," *Chemical Engineering Communications*, vol. 46, pp. 73–87, 1986.

[54] S. J. Qin and T. A. Badgwell, "An overview of industrial model predictive control technology," in *5th International Conference on Chemical Process Control*, pp. 232–256, 1997.

[55] J. B. Rawlings and K. R. Muske, "The stability of constrained receding horizon control," *Automatic Control, IEEE Transactions on*, vol. 38, no. 10, pp. 1512–1516, 1993.

[56] P. O. M. Scokaert and J. B. Rawlings, "Feasibility issues in linear model predictive control," *AIChE Journal*, vol. 45, no. 8, pp. 1649–1659, 1999.

[57] J. Vada, O. Slupphaug, and T. Johansen, "Optimal prioritized infeasibility handling in model predictive control: parametric preemptive multiobjective

linear programming approach," *Journal of Optimization Theory and Applications*, vol. 109, no. 2, pp. 385–413, 2001.

[58] M. L. Tyler and M. Morari, "Propositional logic in control and monitoring problems," *Automatica*, vol. 35, no. 4, pp. 565–582, 1999.

[59] J. Vada, O. Slupphaug, T. Johansen, and B. Foss, "Linear MPC with optimal prioritized infeasibility handling: application, computational issues and stability," *Automatica*, vol. 37, no. 11, pp. 1835–1843, 2001.

[60] J. Vada, O. Slupphaug, and B. Foss, "Infeasibility handling in linear MPC subject to prioritized constraints," in *the 14th IFAC World Congress*, (Beijing), 1999.

[61] A. Zheng and M. Morari, "Stability of model predictive control with mixed constraints," *Automatic Control, IEEE Transactions on*, vol. 40, no. 10, pp. 1818–1823, 1995.

[62] C. Grigg, P. Wong, P. Albrecht, R. Allan, M. Bhavaraju, R. Billinton, Q. Chen, C. Fong, S. Haddad, S. Kuruganty, W. Li, R. Mukerji, D. Patton, N. Rau, D. Reppen, A. Schneider, M. Shahidehpour, and C. Singh, "The IEEE reliability test system-1996. a report prepared by the reliability test system task force of the application of probability methods subcommittee," *Power Systems, IEEE Transactions on*, vol. 14, no. 3, pp. 1010–1020, 1999.

[63] ERCOT Balancing Energy Services Daily Reports Archives, "2008 Balancing Energy Services Daily Reports."

[64] ERCOT Overview, "ERCOT 2009 Annual Report."

[65] C. Raish, "ERCOT emergency interruptible load service," in *AEIC Load Research Workshop*, (San Antonio, Texas), ERCOT, February 26, 2008.

[66] ERCOT Market Information, "Feb.2008 ERCOT Ancillary Services Offer Selected Daily Reports."

[67] L. Xie, Y. Gu, A. Eskandari, and M. Ehsani, "Fast mpc-based coordination of wind power and battery energy storage systems," *Journal of Energy Engineering*, vol. 138, no. 2, pp. 43–53, 2012.

[68] Y. Gu and L. Xie, "Fast sensitivity analysis approach to assessing congestion induced wind curtailment," *Power Systems, IEEE Transactions on*, vol. 29, pp. 101–110, Jan 2014.

[69] Y. Chen, L. Xie, and P. R. Kumar, "Dimensionality reduction and early event detection using online synchrophasor data," in *Power and Energy Society General Meeting, IEEE*, (Vancouver), 2013.

[70] L. Xie, Y. Chen, and H. Liao, "Distributed online monitoring of quasi-static voltage collapse in multi-area power systems," *Power Systems, IEEE Transactions on*, vol. 27, no. 4, pp. 2271–2279, 2012.

[71] Y. Zhang, Y. Chen, and L. Xie, "Multi-scale integration and aggregation of power system modules for dynamic security assessment," in *Power and Energy Society General Meeting, IEEE*, (Vancouver), 2013.

[72] M. Alexiadis, P. Dokopoulos, and H. Sahsamanoglou, "Wind speed and power forecasting based on spatial correlation models," *IEEE Transactions on Energy Conversion*, vol. 14, no. 3, pp. 836–842, 1999.

[73] S. Zhao, L. Xie, and C. Singh, "Cross-correlation study of onshore/offshore wind generation and load in Texas," in *North American Power Symposium*, (Manhattan, KS), 2013.

[74] P. Dehghanian, M. Fotuhi-Firuzabad, S. Bagheri-Shouraki, and A. A. Razi Kazemi, "Critical component identification in reliability centered asset management of power distribution systems via fuzzy AHP," *IEEE Systems Journal*, vol. 6, no. 4, pp. 593–602, 2012.

[75] P. Dehghanian, M. Fotuhi-Firuzabad, F. Aminifar, and R. Billinton, "A comprehensive scheme for reliability centered maintenance in power distribution systems," *IEEE Transactions on Power Delivery*, vol. 28, no. 2, pp. 761–770, 2013.

[76] B. Zhang and M. Kezunovic, "Impact of available electric vehicle battery power capacity on power system reliability," in *Power and Energy Society General Meeting, IEEE*, (Vancouver, Canada), 2013.

[77] G. Gross and F. D. Galiana, "Short-term load forecasting," *Proceedings of the IEEE*, vol. 75, pp. 1558 – 1573, 1987.

[78] J. Black, "Plans for wind integration in ISO-NE: Progress and challenges," in *8th annual Carnegie Mellon Conference on the electricity industry*, (Pittsburgh), 2012.

[79] "Deep Thunder-Precision Forecasting for Weather-Sensitive Business Operations," 2012.

[80] W. P. Mahoney, K. Parks, G. Wiener, L. Yubao, W. L. Myers, S. Juanzhen, L. Delle Monache, T. Hopson, D. Johnson, and S. E. Haupt, "A wind power forecasting system to optimize grid integration," *IEEE Transactions on Sustainable Energy*, vol. 3, no. 4, pp. 670–682, 2012.

[81] E. M. Constantinescu, V. M. Zavala, M. Rocklin, L. Sangmin, and M. Anitescu, "A computational framework for uncertainty quantification and stochastic op-

timization in unit commitment with wind power generation," *Power Systems, IEEE Transactions on*, vol. 26, no. 1, pp. 431–441, 2011.

[82] L. Xie, Y. Gu, X. Zhu, and M. G. Genton, "Power system economic dispatch with spatio-temporal wind forecasts," in *Energytech, IEEE*, pp. 1–6, 2011.

[83] X. Zhu, M. G. Genton, Y. Gu, and L. Xie, "Space-time wind speed forecasting for improved power system dispatch," *Test*, vol. 23, no. 1, pp. 1–25, 2014.

[84] X. Zhu, K. Bowman, and M. G. Genton, "Incorporating geostrophic wind information for improved space-time wind speed forecasting," *Annals of Applied Statistics*, 2013.

[85] Y. Sun and M. G. Genton, "Functional boxplots," *Journal of Computational and Graphical Statistics*, vol. 20, pp. 316–334, 2011.

[86] T. Gneiting and A. E. Raftery, "Strictly proper scoring rules, prediction, and estimation," *Journal of the American Statistical Association*, vol. 102, no. 477, pp. 359–378, 2007.

[87] H. Zhong, Q. Xia, Y. Wang, and C. Kang, "Dynamic economic dispatch considering transmission losses using quadratically constrained quadratic program method," *Power Systems, IEEE Transactions on*, vol. 28, no. 3, pp. 2232–2241, 2013.

[88] H. Zhong, L. Xie, and Q. Xia, "Coupon incentive-based demand response: Theory and case study," *Power Systems, IEEE Transactions on*, vol. 28, no. 2, pp. 1266–1276, 2013.

[89] Y. Gu and L. Xie, "Early detection and optimal corrective measures of power system insecurity in enhanced look-ahead dispatch," *Power Systems, IEEE Transactions on*, vol. 28, pp. 1297–1307, May 2013.

[90] L. Xie, Y. Gu, X. Zhu, and M. Genton, "Short-term spatio-temporal wind power forecast in robust look-ahead power system dispatch," *Smart Grid, IEEE Transactions on*, vol. 5, pp. 511–520, Jan 2014.

[91] Renewable Energy Policy Network for the 21st century, "Renewables 2013 Global Status Report," 2013.

[92] D. Lew, D. Piwko, N. Miller, G. Jordan, K. Clark, and L. Freeman, "How do high levels of wind and solar impact the grid? the western wind and solar integration study," Tech. Rep. NREL/TP-5500-50057, National Renewable Energy Laboratory, December 2010.

[93] Executive Office of the President, The White House, "Economic benefits of increasing electric grid resilience to weather outages," 2013.

[94] G. Giebel, P. Sorensen, and H. Holttinen, "Forecast error of aggregated wind power," Tech. Rep. SI2.442659, RisøNational Laboratory, 2007.

[95] M. Brower, *Wind Energy Forecasting*. Albany, NY: AWS Truepower, 2011.

[96] S. Keshmiri and W. Gao, "Multi-objective stochastic economic dispatch," in *North American Power Symposium (NAPS), 2010*, pp. 1–8, Sept 2010.

[97] R. Jabr, "Adjustable robust opf with renewable energy sources," *Power Systems, IEEE Transactions on*, vol. 28, pp. 4742–4751, Nov 2013.

[98] Y.-Y. Lee and R. Baldick, "A frequency-constrained stochastic economic dispatch model," in *Power and Energy Society General Meeting, IEEE*, pp. 1–1, July 2013.

[99] Y. Makarov, R. Guttromson, Z. Huang, K. Subbarao, P. Etingov, B. Chakrabarti, and J. Ma, "Incorporating wind generation and load forecast

uncertainties into power grid operations," Tech. Rep. PNNL-19189, Pacific Northwest National Laboratory, January 2010.

[100] E. Almeshaiei and H. Soltan, "A methodology for electric power load forecasting," *Alexandria Engineering Journal*, vol. 50, no. 2, pp. 137 – 144, 2011.

[101] K. Binder, "Monte carlo methods," *Quantum Monte Carlo Methods*, p. 241, 1987.

[102] J. M. Morales, S. Pineda, A. J. Conejo, and M. Carrion, "Scenario reduction for futures market trading in electricity markets," *Power Systems, IEEE Transactions on*, vol. 24, no. 2, pp. 878–888, 2009.

[103] J. Dupačová, N. Gröwe-Kuska, and W. Römisch, "Scenario reduction in stochastic programming," *Mathematical Programming*, vol. 95, no. 3, pp. 493–511, 2003.

[104] S. T. Rachev, *Probability metrics and the stability of stochastic models*, vol. 334. Wiley New York, 1991.

[105] H. Heitsch and W. Römisch, "Scenario reduction algorithms in stochastic programming," *Computational optimization and applications*, vol. 24, no. 2-3, pp. 187–206, 2003.

[106] J.-P. Watson and D. Woodruff, "Progressive hedging innovations for a class of stochastic mixed-integer resource allocation problems," *Computational Management Science*, vol. 8, no. 4, pp. 355–370, 2011.

[107] R. Van Slyke and R. Wets, "L-shaped linear programs with applications to optimal control and stochastic programming," *SIAM Journal on Applied Mathematics*, vol. 17, no. 4, pp. 638–663, 1969.

[108] Y. Gu and L. Xie, "Stochastic Look-ahead Economic Dispatch with Intermittent Generation Resources, Part I: To Do or Not To Do," *Power Systems, IEEE Transactions on*, 2015 (submitted).

[109] J.-P. Watson, D. Woodruff, and W. Hart, "PySP: modeling and solving stochastic programs in Python," *Mathematical Programming Computation*, vol. 4, no. 2, pp. 109–149, 2012.

[110] J. Benders, "Partitioning procedures for solving mixed-variables programming problems," *Numerische Mathematik*, vol. 4, no. 1, pp. 238–252, 1962.

[111] R. Van Slyke and R. Wets, "L-shaped linear programs with applications to optimal control and stochastic programming," *SIAM Journal on Applied Mathematics*, vol. 17, no. 4, pp. 638–663, 1969.